COMMUNICATION THEORY (5ETB0)
Course Reader
2024/2025

Frans M.J. Willems and Alex Alvarado
Information and Communication Theory Lab
Signal Processing Systems Group
Electrical Engineering Department
Eindhoven University of Technology
https://www.tue.nl/ictlab

Contents

Part I

INTRODUCTION

Chapter 1

Historical Perspective

SUMMARY: In this chapter we discuss some historical facts related to telegraphy and telephony, wireless communication, electronics, and modulation. Furthermore we shortly discuss some classic fundamental bounds and concepts relevant for digital communication.

1.1 Telegraphy and Telephony

1800 Alessandro Volta (Italy 1745 - 1827) Announcement of the electric battery (Volta's pile). This battery made constant-current electricity possible. Motivated by the "frog-leg" experiments of Luigi Galvani (Italy 1737 - 1798), anatomy professor at the university of Bologna, Volta discovered that it was possible to construct a battery from a plate of silver and a plate of zinc separated by spongy matter impregnated with a saline solution, repeated thirty or forty times.

1819 Hans Christian Oersted (Denmark 1777 - 1851) Discovery of the fact that an electric current generates a magnetic field. This can be regarded as the first electromagnetic result. It took twenty years after Volta's invention to realize and prove that this effect exists although it was known at the time that a stroke of lightning magnetized objects.

1827 Joseph Henry (U.S. 1797 - 1878) Constructed electromagnets using coils of wire.

1838 Samuel Morse (U.S. 1791 - 1872) Demonstration of the electric telegraph in Morristown, New Jersey. The first telegraph line linked Washington with Baltimore. It became operational in May 1844. By 1848 every state east of the Mississippi was linked by telegraph lines. The alphabet that was designed by Morse (a portrait-painter) transforms letters into variable-length sequences (code words) of *dots and dashes* (see table 1.1). A dash should last roughly three times as long as a dot. Frequent letters (e.g., E) get short code words, less frequently occurring letters (e.g., J, Q, and Y) are represented by longer words. The first transcontinental telegraph line

A	. -	G	- - .	M	- -	S	. . .	Y	- . - -
B	- . . .	H	. . . .	N	- .	T	-	Z	- - . .
C	- . - .	I	. .	O	- - -	U	. . -	period	. - . - . -
D	- . .	J	. - - -	P	. - - .	V	. . . -	?	. . - - . .
E	.	K	- . -	Q	- - . -	W	. - -		
F	. . - .	L	. - . .	R	. - .	X	- . . -		

Table 1.1: Morse code.

was completed in 1861. A transatlantic cable became operational in 1866. However already in 1858 a cable was completed but it failed after a few weeks.

It should be mentioned that in 1833 C.F. Gauss and W.E. Weber demonstrated an electromagnetic telegraph in Göttingen, Germany.

1875 Alexander Graham Bell (Scotland 1847 - 1922 U.S.) Invention of the telephone. Bell was a teacher of the deaf. His invention was patented in 1876 (electromagnetic telephone). In 1877 Bell established the Bell Telephone Company. Early versions provided service over several hundred miles. Advances in quality resulted, e.g., from the invention of the carbon microphone.

1900 Michael Pupin (Yugoslavia 1858 - 1935 U.S.) Obtained a patent on loading coils for the improvement of telephone communications. Adding these Pupin-coils at specified intervals along a telephone line reduced attenuation significantly. The same invention was disclosed by Campbell two days later than Pupin. Pupin sold his patent for $455000 to AT&T Co. Pupin (and Campbell) were the first to set up a theory of transmission lines. The implications of this theory were not obvious at all for "experimentalists".

1.2 Wireless Communications

1831 Michael Faraday (England 1791 - 1867) Discovery of the fact that a changing magnetic field induces an electric current in a conducting circuit. This is the famous law of induction.

1873 James Clerk Maxwell (Scotland 1831 - 1879, England) The publication of "Treatise on Electricity and Magnetism". Maxwell combined the results obtained by Oersted and Faraday into a single theory. From this theory he could predict the existence of electromagnetic waves.

1886 Heinrich Hertz (Germany 1857 - 1894) Demonstration of the existence of electromagnetic waves. In his laboratory at the university of Karlsruhe, Hertz used a spark-transmitter to generate the waves and a resonator to detect them.

1890 Edouard Branly (France 1844 - 1940) Origination of the coherer. This is a receiving device for electromagnetic waves based on the principle that, while most powdered metals are poor direct current conductors, metallic powder becomes conductive when high-frequency current is applied. The coherer was further refined by Augusto Righi (Italy 1850 - 1920) at the University of Bologna and by Oliver Lodge (England 1851 - 1940) .

1896 Aleksander Popov (Russia 1859 - 1906) Wireless telegraph transmission between two buildings (200 meters) was shown to be possible. Marconi did similar experiments at roughly the same time.

1901 Guglielmo Marconi (Italy 1874 - 1937) attended the lectures of Righi in Bologna and built a first radio telegraph in 1895. He used Hertz's spark transmitter, and Lodge's coherer and added antennas to improve performance. In 1898 he developed a tuning device and was now able to use two radio circuits simultaneously. The first cross-Atlantic radio link was operated by Marconi in 1901. A radio signal was received at St. John's, Newfoundland while being originated from Cornwall, England, 1700 miles away. Important was that Marconi applied directional antennas.

1955 John R. Pierce (U.S. 1910 - 2002) Pierce (Bell Laboratories) proposed the use of satellites for communications and did pioneering work in this area. Originally this idea came from Arthur C. Clarke who suggested already in 1945 the idea to use earth-orbiting satellites as relay points between earth stations. The first satellite, Telstar I, built by Bell Laboratories, was launched in 1962. It served as a relay station for TV programs across the Atlantic. Pierce also headed the Bell-Labs team that developed the transistor and suggested the name for it.

1.3 Electronics

1874 Karl Ferdinand Braun (Germany 1850 - 1918) Observation of rectification at metal contacts to galena (lead sulfide). These semiconductor devices were the forerunners of the "cat's whisker" diodes used for detection of radio channels (crystal detectors).

1904 John Ambrose Fleming (England 1849 - 1945) Invention of the thermionic diode, "the valve", that could be used as rectifier. A rectifier can convert trains of high-frequency oscillations into trains of intermittent but unidirectional current. A telephone can then be used to produce a sound with the frequency of the trains of the sparks.

1906 Lee DeForest (U.S. 1873 - 1961) Invention of the vacuum triode, a diode with grid control. This invention made practical the cascade amplifier, the triode oscillator and the regenerative feedback circuit. As a result transcontinental telephone transmission became operational in 1915. A transatlantic cable was laid not earlier than 1953.

1948 John Bardeen, Walter Brattain and William Shockley Development of the theory of the junction transistor. This transistor was first fabricated in 1950. The point contact transistor was invented in December 1947 at Bell Telephone Labs.

1958 Jack Kilby and Robert Noyce (U.S.) Invention of the integrated circuit.

1.4 Classical Modulation Methods

Beginning of the 20th century Carrier-frequency currents were generated by electric arcs or by high-frequency alternators. These currents were modulated by carbon transmitters and demodulated (or converted to audio) by a crystal detector or an other kind of rectifier.

1909 George A. Campbell (U.S. 1870 - 1954) Internal AT&T memorandum on the "Electric Wave Filter". Campbell there discussed band-pass filters that would reject frequencies other than those in a narrow band. A patent application filed in 1915 was awarded [1].

1915 Edwin Howard Armstrong (U.S. 1890 - 1954) Invention of regenerative amplifiers and oscillators. Regenerative amplification (using positive feedback to obtain a nearly oscillating circuit) considerably increased the sensitivity of the receiver. DeForest claimed the same invention.

1915 Hendrik van der Bijl, Ralph V.L. Hartley, and Raymond A. Heising In a patent that was filed in 1915 van der Bijl showed how the non-linear portion of a vacuum tube could be utilized to modulate and demodulate. Heising participated in a project (in Arlinton, VA) in which a vacuum-tube transmitter based on the van der Bijl modulator was designed. Heising invented the constant-current modulator. Hartley also participated in the Arlington project and designed the receiver. He invented an oscillator that was named after him. In a paper published in 1923 Hartley explained how suppression of the carrier signal and using only one of the sidebands could economize transmitter power and reduce interference.

1915 John R. Carson Publication of a mathematical analysis of the modulation and demodulation process. Description of single-sideband and suppressed carrier methods.

1918 Edwin Howard Armstrong Invention of the superheterodyne radio receiver. The combination of the received signal with a local oscillation resulted in an audio beatnote.

1922 John R. Carson "Notes on the Theory of Modulation [2]". Carson compares amplitude modulation (AM) and frequency modulation (FM) . He came to the conclusion that FM was inferior to AM from the perspective of bandwidth requirement. He overlooked the possibility that wideband FM might offer some advantages over AM as was later demonstrated by Armstrong.

1933 Edwin Howard Armstrong Demonstration of an FM system to the Radio Corporation of America (RCA). A patent was granted to Armstrong. Despite of the larger bandwidth that is needed, FM gives a considerable better performance than AM.

1.5 Fundamental Bounds and Concepts

1924 Harry Nyquist (Sweden 1889 - 1976 U.S.) Shows that the number of resolvable (non-interfering) pulses that can be transmitted per second over a bandlimited channel is proportional to the channel bandwidth [9]. If the bandwidth is W Hz the number of pulses per second cannot exceed $2W$. This is strongly related to the sampling theorem which says that time is essentially discrete. If a time-continuous signal has bandwidth not larger than W Hz then it is completely specified by samples taken from it at discrete time instants $1/2W$ seconds apart.

1928 Ralph V.L. Hartley (U.S. 1888 - 1970) Determined the number of distinguishable pulse amplitudes [5]. Suppose that the amplitudes are confined to the interval $[-A, +A]$, and that the receiver can estimate an amplitude reliably only to an accuracy of $\pm\Delta$. Then the number of distinguishable pulses is roughly $\frac{2(A+\Delta)}{2\Delta} = \frac{A}{\Delta} + 1$. Clearly Hartley was concerned with digital communication. He realized that inaccuracy (due to noise) limited the amount of information that could be transmitted.

1938 Alec Reeves Invention of Pulse Code Modulation (PCM) for digital encoding of speech signals. In World War II PCM-encoding allowed transmission of encrypted speech (Bell Laboratories). In [10] Oliver, Pierce and Shannon compared PCM to classical modulation systems.

1939 Homer Dudley Description of a vocoder. This system did overthrow the idea that communication requires a bandwidth at least as wide as that of the signal to be communicated.

1942 Norbert Wiener (U.S. 1894 - 1964) Investigated the problem shown in Fig. 1.1. The linear filter is to be chosen such that its output $\hat{s}(t)$ is the best mean-square approximation to $s(t)$ given the statistical properties of the processes $S(t)$ and $N(t)$. A drawback of the result of Wiener was that that carrier modulation did not fit into his model and could not be analyzed.

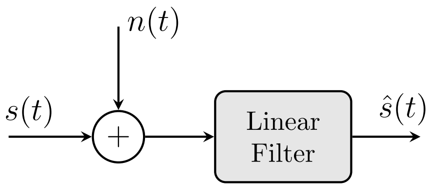

Figure 1.1: The communication problem considered by Wiener.

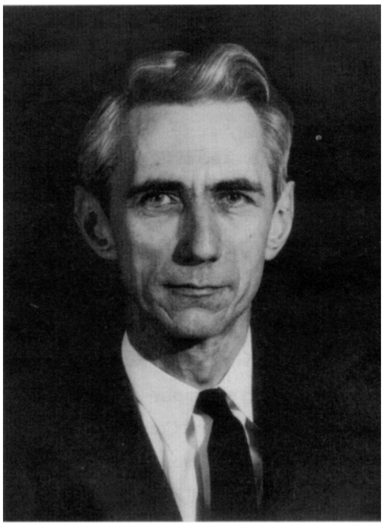

Figure 1.2: Claude E. Shannon, founder of Information Theory. Photo IEEE-IT Soc. Newsl., Summer 1998.

1943 Dwight O. North Discovery of the matched filter. This filter was shown to be the optimum detector of a known signal in additive white noise.

1947 Vladimir A. Kotelnikov (Russia 1908 - 2005) Analysis of several modulation systems. His noise immunity work [6] dealt with how to design receivers (but not how to choose the transmitted signals) to minimize error probability in the case of digital signals or mean square error in the case of analog signals. Kotelnikov discovered independently of Nyquist, the sampling theorem in 1933.

1948 Claude E. Shannon (U.S. 1916 - 2001) Publication of "A Mathematical Theory of Communication [12]." Shannon (see Fig. 1.2) showed that noise does not place an inescapable restriction on the accuracy of communication. He showed that noise properties, channel bandwidth, and restricted signal magnitude can be incorporated into a single parameter C which he called the *channel capacity*. If the cardinality $|\mathcal{M}|$ of the message $\mathcal{M}$ grows as a function of the signal duration T such that

$$\frac{1}{T}\log_2|\mathcal{M}| \approx C - \epsilon,$$

for some small $\epsilon > 0$, then arbitrarily high communication accuracy is possible by increasing T, i.e., by taking longer and longer signals (code words). Conversely Shannon showed that reliable communication is not possible when

$$\frac{1}{T}\log_2|\mathcal{M}| \approx C + \epsilon,$$

for any $\epsilon > 0$. Therefore a channel can be considered as a pipe through which which bits can reliably be transmitted up to rate C.

Shannon also developed a theory dealing with efficient processing of the outcome of information sources. Quite an interesting idea is that the processing for source outputs and the processing for transmission over channels can be separated. This is one of the foundations of digital communications.

Other results of Shannon include the application of Boole's algebra to switching circuits (M.S. thesis, MIT, 1938). It was also Shannon who introduced the sampling theorem to the engineering community in 1949.

Chapter 2

Analog versus Digital Communication

SUMMARY: In this chapter we first briefly review analog communication with a focus on noise behavior. Then we discuss the advantages and disadvantages of analog systems. We subsequently move to digital communication and we argue that digital communication is successful mainly because source and channel processing can be separated by an interface based on binary sequences (packets), without loss of performance. This view leads to a generic and flexible architecture of a communication system, allows for separate optimization of source and channel processing methods, and matches perfectly to today's digital technology.

2.1 Communication System, White Noise, Waveform Channels, Waveform Source

2.1.1 Our Communication System

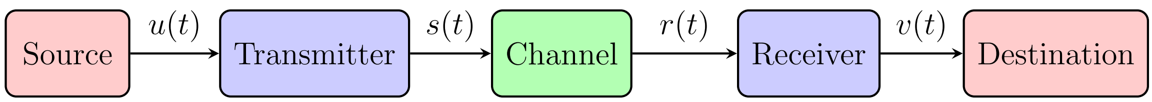

Figure 2.1: Elements in a communications system.

In a communication system, see Fig. 2.1, there is a **source** that generates a real-valued source waveform $u(t)$. As examples of a source consider a microphone that picks up an acoustic signal (e.g., speech or music) or a temperature sensor, or a sensor that monitors seismic vibrations.

The source waveform $u(t)$ is observed by a **transmitter** that transforms the waveform $u(t)$ into a transmitted waveform $s(t)$. It is the task of the transmitter to represent the relevant parts of the source waveform in such a way that they will be conveyed reliably and efficiently over the channel. e.g., not all spectral components need to be transmitted to the receiver and maybe some distortion is acceptable.

The **channel** converts the transmitted waveform $s(t)$ into a received waveform $r(t)$. Typically noise is added to the transmitted waveform but other deformations (deterministic and/or statistical) are also possible. As examples of a channel we can think of a wireless channel, an optical channel, channels that perform communication over a *distance*, but also of a storage medium that allows for communication over *time*.

It is the task of the **receiver** to reconstruct from the received waveform $r(t)$ an estimate-waveform $v(t)$ of the source waveform, and to hand it over to the **destination**. It is obvious that we want the estimated waveform $v(t)$ to be as close as possible to the source waveform in some sense.

It should be noted that the source does not always produce a waveform. It is also quite common that a source produces a stream of discrete symbols. Think of e-mail messages or computer programs. Also the channel can accept discrete inputs and produce discrete outputs (as we shall see later).

2.1.2 White Noise

Both the source waveform $u(t)$ and channel can be defined in terms of *white noise*. A white-noise waveform $n_w(t)$ is supposed to be generated by the random process $N_w(t)$ which is assumed to be zero-mean (i.e., $E[N_w(t)] = 0$), stationary, white, and Gaussian. The *autocorrelation function* of the noise is

$$R_{N_w}(t,s) \triangleq E[N_w(t)N_w(s)] = \frac{N_0}{2}\delta(t-s), \tag{2.1}$$

and depends only on the time difference $t-s$ (by the stationarity). The noise has *power spectral density* (in W/Hz)

$$S_{N_w}(f) = \frac{N_0}{2}\left[\frac{W}{Hz}\right], \text{ for } -\infty < f < \infty, \tag{2.2}$$

i.e., it is white, see Appendix B. Note that f is the frequency in Hz.

White noise is inevitable if we use electronic equipment. It is the result of adding together many small voltages or currents. It is a consequence of the central limit theorem that the noise is Gaussian. Note that white noise is only a model of reality, not reality itself. Why?

We will now describe three waveform channels corrupted by additive white Gaussian noise (AWGN): the wideband AWGN channel, the baseband AWGN channel, and the passband AWGN channel. A (baseband) waveform source will also be described in terms of filters and white noise.

2.1.3 Waveform Channels

Here we discuss three waveform channels. The first one is a wideband channel where all frequencies are allowed. The second one is a baseband channel where only certain frequencies around zero are allowed. The third channel is a passband channel, typically needed to describe channels that only allow frequencies around certain carrier frequency f_0.

Wideband AWGN Channel

A (wideband) waveform AWGN channel accepts an input waveform $s(t)$ and adds white Gaussian noise $n_w(t)$ to it, i.e., for the received waveform $r(t)$ we have that

$$r(t) = s(t) + n_w(t). \tag{2.3}$$

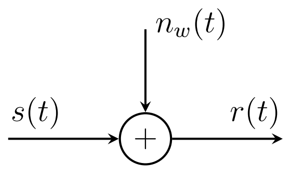

Figure 2.2: Wideband AWGN channel.

The noise $n_w(t)$ comes from the random process $N_w(t)$ as described in Sec. 2.1.2. The basic version of this AWGN channel, see Fig. 2.2, does not block any input frequencies.

Baseband AWGN Channel

The baseband version of the AWGN channel shown in Fig. 2.3 does not block input waveforms in the baseband, i.e., in the frequency-band $[-W, +W]$. All other frequencies are blocked. We write the channel output as

$$r(t) = s(t) * w_b(t) + n_w(t), \tag{2.4}$$

where $w_b(t)$ is the impulse response of the corresponding ideal low-pass filter. The baseband AWGN channel is a good model for transmission over, e.g., twisted copper pair cables.

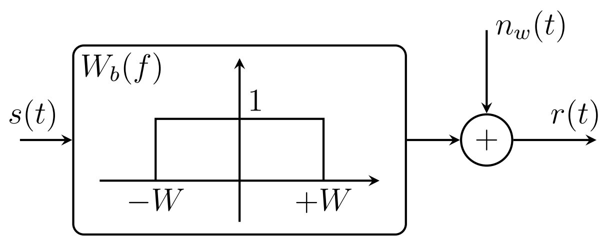

Figure 2.3: AWGN channel for baseband waveforms.

Pass-band AWGN channel

The passband version of the wideband AWGN channel in Fig. 2.2 is shown in Fig. 2.4. This channel does not block input frequencies in the frequency-bands $[-f_0 - W, -f_0 + W]$ and $[f_0 - W, f_0 + W]$. It is assumed that the center frequency f_0 of the bandpass filter satisfies $f_0 > W$. All other frequencies are blocked. We write the output of the channel as

$$r(t) = s(t) * w_p(t) + n_w(t), \tag{2.5}$$

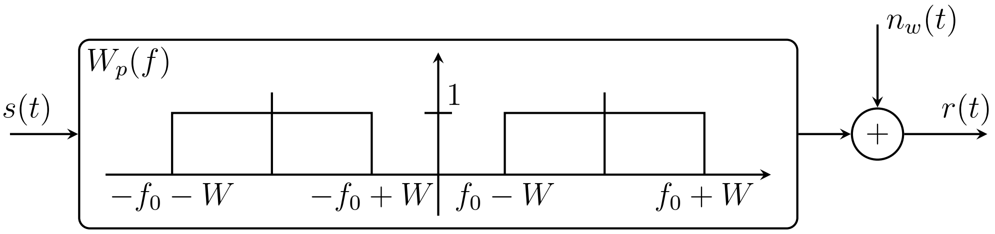

Figure 2.4: AWGN channel for passband waveforms.

where $w_p(t)$ is the impulse response of the corresponding ideal bandpass filter. Wireless transmission channels can be modeled using the passband AWGN channel, where f_0 corresponds to the carrier frequency. Moreover note that passband transmission can be used for multiplexing of several streams (usually known as frequency division multiplexing).

Definition 2.1 *The transmitter delivers the signal $s(t)$ to the channel. We assume that the average transmit power P is limited. The* instantaneous *power is $s^2(t)$, and thus, the average power is $E[S^2(t)]$, where the expectation is over time.*[1] *Because of the average power constraint, we require $E[S^2(t)] \leq P$.*

2.1.4 Baseband Waveform Source

We conclude this section by introducing the baseband Gaussian waveform source depicted in Fig. 2.5. The source outputs a low-pass filtered version of a white Gaussian noise waveform $u_w(t)$ with power spectral density $S_{U_w}(f) = U_0/2$. We write

$$u(t) = u_w(t) * w_b(t), \tag{2.6}$$

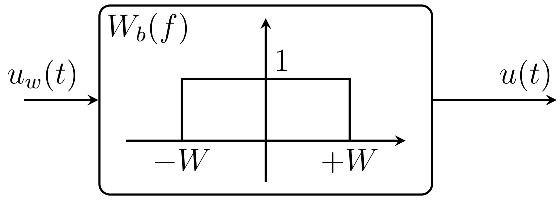

Figure 2.5: A baseband Gaussian waveform source.

where $w_b(t)$ is the impulse response of the corresponding low-pass filter. Note that $u(t)$ contains only baseband frequencies, i.e., frequencies in the baseband $[-W, +W]$.

This model of a source is also not always valid. In practice analog sources are not always white, also not ideally baseband, and not Gaussian. However, the model that we use here will allow us to analyze and understand the basic properties of communication systems. The white waveform source is also the worst source that we can have. For other sources there is more to gain.

[1] An instantaneous power constraint could also be imposed, i.e., $s^2(t) \leq \hat{P}$ for all time instants t.

2.2 Analog Communication

For reviewing analog communication, we distinguish between two cases. First we consider transmission of the source waveform $u(t)$ through the baseband AWGN channel, as described in (2.4). Then we consider transmission of $u(t)$ in the passband as given by (2.5).

2.2.1 Baseband Transmission

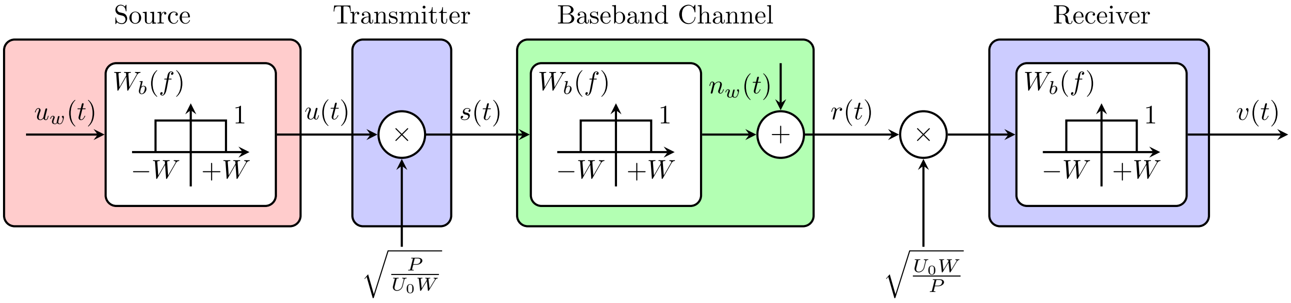

Figure 2.6: Transmitting a baseband source waveform over a baseband channel.

We can now be more specific about the source waveform $u(t)$. We know that its bandwidth is W, that it is white over $[-W, +W]$, and therefore it has power[2]

$$E[U^2(t)] = \int_{-\infty}^{\infty} S_U(f)df = \int_{-W}^{W} \frac{U_0}{2}df = \frac{U_0}{2}2W = U_0W \tag{2.7}$$

Fig. 2.7 contains a part of such a waveform. Here $W = 1$ Hz.

As shown in Fig. 2.6, the transmitter now observes $u(t)$ and transmits a scaled version of $u(t)$

$$s(t) = \sqrt{\frac{P}{U_0W}}u(t), \tag{2.8}$$

where P is the transmit power. This results in transmit-signal power $E[S^2(t)] = \frac{P}{U_0W}E[U^2(t)] = P$. The channel output is

$$r(t) = s(t) * w_b(t) + n_w(t) = \sqrt{\frac{P}{U_0W}}u(t) + n_w(t), \tag{2.9}$$

where we note that the low-pass filter $w_b(t)$ has no effect since $u(t)$ and $s(t)$ are baseband. The receiver low-pass filters the received waveform, scales it, and obtains

$$v(t) = \sqrt{\frac{U_0W}{P}}r(t) * w_b(t) = u(t) + \sqrt{\frac{U_0W}{P}}n_w(t) * w_b(t). \tag{2.10}$$

[2] Or equivalently, its variance.

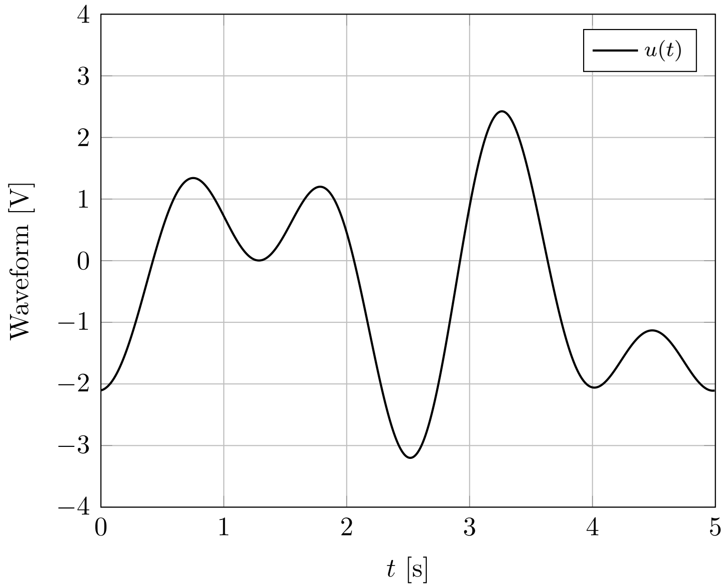

Figure 2.7: A part of an example source waveform $u(t)$.

Again we see that the filter $w_b(t)$ has no effect on the signal $u(t)$ and only affects the noise.

The power of the distortion waveform $d(t) = v(t) - u(t) = \sqrt{U_0 W/P} n_w(t) * w_b(t)$ is

$$E[D^2(t)] = \frac{U_0 W}{P} \frac{N_0}{2} 2W = U_0 W \frac{N_0 W}{P}, \tag{2.11}$$

and therefore the **source signal-to-distortion ratio** SDR in the estimate $v(t)$ is

$$\mathrm{SDR} \triangleq \frac{E[U^2(t)]}{E[D^2(t)]} = \frac{P}{N_0 W} = \mathrm{SNR}_b, \tag{2.12}$$

where SNR_b is the **baseband channel signal-to-noise ratio**. We call $D = E[D^2(t)]$ the **mean squared error distortion**.

2.2.2 Pass-band transmission

Here we focus on passband transmission of the source waveform $u(t)$ based on **double sideband suppressed carrier (DSB-SC) modulation**. The receiver performs **coherent demodulation**.

The transmitter in this system observes $u(t)$ and transmits a scaled and amplitude-modulated version of $u(t)$, i.e.,

$$s(t) = \sqrt{\frac{P}{U_0 W}} u(t) \sqrt{2} \cos(2\pi f_0 t), \tag{2.13}$$

where P is the transmit power, and f_0 the carrier-frequency ($f_0 > W$). Note the waveform $s(t)$ is a passband waveform, i.e., it fits in frequency band $\pm[f_0 - W, f_0 + W]$, see Fig. 2.8.

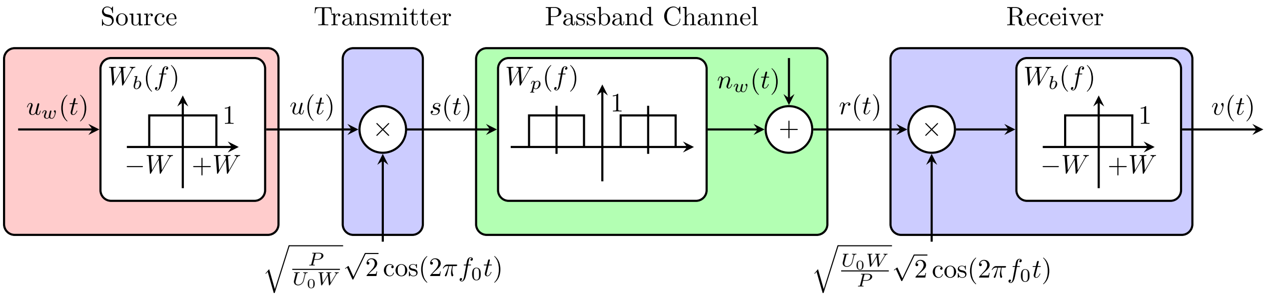

Figure 2.8: Transmitting a baseband source waveform over a passband channel.

This kind of modulation results in

$$E[S^2(t)] = \frac{P}{U_0W}E[U^2(t)] \cdot 2\cos^2(2\pi f_0 t) \tag{2.14}$$

$$= \frac{P}{U_0W}E[U^2(t)] \cdot [1 + \cos(4\pi f_0 t)] \tag{2.15}$$

$$= P \cdot [1 + \cos(4\pi f_0 t)] \tag{2.16}$$

The instantaneous power in (2.16) is a periodic function with period $T = 1/(2f_0)$. The average power over one period is then given by as

$$\frac{1}{T}\int_0^T E[S^2(t)]dt = \frac{P}{T}\int_0^T [1 + \cos(4\pi f_0 t)]dt \tag{2.17}$$

$$= P. \tag{2.18}$$

The output waveform of the channel

$$r(t) = s(t) * w_p(t) + n_w(t) = \sqrt{\frac{P}{U_0W}}u(t)\sqrt{2}\cos(2\pi f_0 t) * w_p(t) + n_w(t),$$

$$= \sqrt{\frac{P}{U_0W}}u(t)\sqrt{2}\cos(2\pi f_0 t) + n_w(t), \tag{2.19}$$

where we have used the fact that the bandpass filter $w_p(t)$ has no effect since $s(t)$ is passband.

The receiver multiplies the received waveform by $\sqrt{2}\cos(2\pi f_0 t)$, low-pass filters the

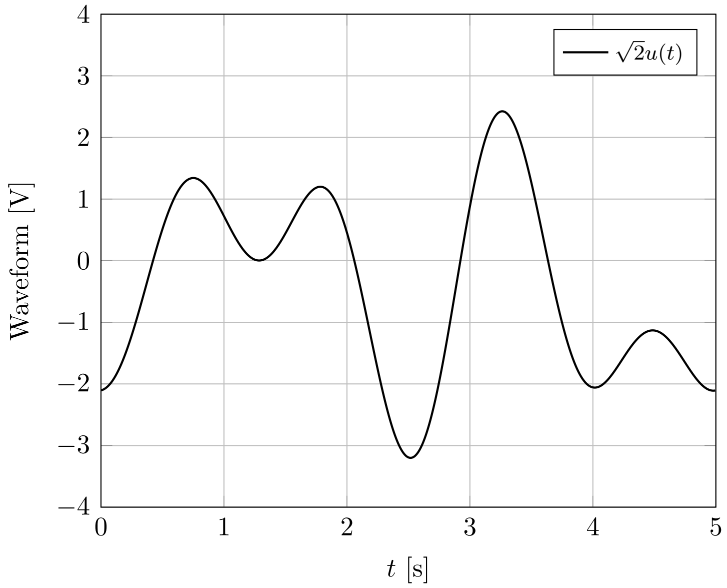

Figure 2.9: Part of the modulated waveform $u(t)\sqrt{2}\cos(10\pi t)$, carrier frequency 5 Hz.

result, and scales it, and obtains

$$\begin{aligned} v(t) &= \sqrt{\frac{U_0 W}{P}} r(t)\sqrt{2}\cos(2\pi f_0 t) * w_b(t) \\ &= \sqrt{\frac{U_0 W}{P}} \left(\sqrt{\frac{P}{U_0 W}} u(t)\sqrt{2}\cos(2\pi f_0 t) + n_w(t) \right) \sqrt{2}\cos(2\pi f_0 t) * w_b(t) \\ &= u(t) 2\cos^2(2\pi f_0 t) * w_b(t) + \sqrt{\frac{U_0 W}{P}} n_w(t)\sqrt{2}\cos(2\pi f_0 t) * w_b(t) \\ &= u(t) + \sqrt{\frac{U_0 W}{P}} n_w(t)\sqrt{2}\cos(2\pi f_0 t) * w_b(t) \end{aligned} \tag{2.20}$$

where the filter $w_b(t)$ filters out the term at twice the frequency $u(t)\cos(4\pi f_0 t)$.

The power of the distortion waveform $d(t) = \sqrt{U_0 W/P} n_w(t)\sqrt{2}\cos(2\pi f_0 t) * w_b(t)$, i.e., the mean squared error distortion D, can be shown to be:

$$D = E[D^2(t)] = \frac{U_0 W}{P}\frac{N_0}{2}2W = U_0 W \frac{N_0 W}{P}, \tag{2.21}$$

again and therefore the **source signal-to-distortion ratio** in the estimate $v(t)$ is

$$\mathrm{SDR} \triangleq \frac{E[U^2(t)]}{E[D^2(t)]} = \frac{P}{N_0 W} = \mathrm{SNR}_b, \tag{2.22}$$

where again SNR_b is the **baseband channel signal-to-noise ratio**, the same result as in the baseband case (see (2.12)). Note however that the bandwidth for DSB-SC is twice as large as that of baseband transmission.

We have considered DSB-SC modulation here, with coherent demodulation, i.e., the receiver is assumed to be synchronized perfectly with the transmitter. It should be noted that this type of modulation is more easy to analyze than other analog modulation methods. These include conventional AM (amplitude modulation), where we transmit $u'(t) = K + u(t)$ instead of $u(t)$, for some constant K such that $K + u(t) > 0$ for all t. AM makes it possible to use envelope detection for demodulating the received waveform, i.e., the receiver does not need to be synchronized with the transmitter. However, adding the constant K, i.e., adding carrier to the transmit signal, also decreases the power efficiency of the system.

Another alternative to DSB-SC is single side-band (SSB) transmission, which requires only half of the bandwidth of DSB. The same signal-to-noise behavior as with DSB-SC can be obtained however. Finally, it is also important to note that instead of modulating the amplitude of the carrier, we can modulate the phase (PM) or the frequency (FM) of the carrier. These methods potentially increase the (output) signal-to-noise ratio, however at the expense of expanding the bandwidth of the transmitted signal.

2.2.3 Pros and Cons of Analog Transmission

Analog systems have a number of advantages:

- Analog transmission systems are **easy to implement, using analog electronics**. They fitted perfectly with the electronics that were available in the previous century.
- AM systems have a **graceful degradation** effect. If the quality of the received signal decreases gradually the signal-to-noise ratio also decreases gradually. This also holds for PM and FM systems as long as the received signal is not too bad (is below the threshold). Graceful degradation is a nice property of radio broadcasting systems.
- **Multiplexing of several services is easy** using frequency division multiple-access (FDMA) techniques. In telephony and radio broadcasting FDMA is an essential technique.

but also some disadvantages:

- AM systems are **inflexible with respect to the bandwidth requirements**. For efficient communication the channel bandwidth should be matched to the source bandwidth. If the channel bandwidth is smaller than the source bandwidth we have a problem.
- Transmission of a waveform based on analog modulation over multiple hops (channels) causes the **signal-to-noise ratio to decrease after each hop**, even if repeaters are used.
- **Advanced encryption and compression methods typically cannot be not be applied** in analog systems.

The disadvantages mentioned above makes massive networking based on analog transmission practically impossible. Since also the supporting technology (electronics) changed from analog to digital in the last decades of the previous century, the emphasis in communication gradually changed from analog to digital.

2.3 Digital Communication

(Based on Chapter 1, Gallager [4]).

2.3.1 Separating Source and Channel Processing, Binary Interface

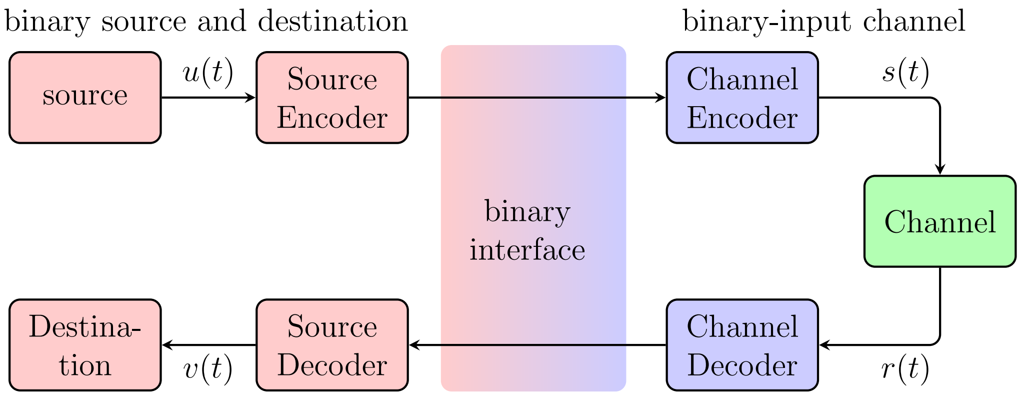

Figure 2.10: Separation of source and channel processing by placing a binary interface in between.

Modern communication started at the beginning of the previous century. First telegraphy, then telephony, radio, later television, and more recently computer communication (e-mail, web-browsing), became available for many people. First there was a special technology and there were separate networks for all these services, however today "simple" devices as smart-phones, can process all such services more or less simultaneously. AT& T (American Telephone and Telegraph) was the first company to realize that all such services should obey the same underlying principles and theory. To sustain innovation and system evolution, an architectural understanding of communication systems would be necessary. Such an understanding would allow many kinds of services to be integrated and guarantees inter-operability.

Claude E. Shannon, a researcher at Bell Laboratories, created Information Theory in 1948. Two ideas, that came from his paper "A Mathematical Theory of Communication," [12] were essential for the development of communication systems.

- The first idea is that the **output of all communication sources, e.g., speech waveforms, image waveforms, and text files, can be represented by binary**

sequences.

- The second idea is that **source processing and channel processing should be separated**. The source output should be converted into a binary sequence. Channel processing would then focus on transforming sequences of binary digits into signals (typically waveforms) that could be transmitted over physical media (cable, optical fibre, or radio links).

In Fig. 2.10 Shannon's view on communication is expressed. There is a clear separation between source and channel processing. The **interface between these two "tasks" is binary (digital)**. The ideas of Shannon lead to a digital approach to communication. The success of digital communication can be explained as follows.

- **Digital hardware** has become cheap, reliable, and can be miniaturized. Therefore now digital communication is practical.
- The **notion of the binary interface** simplifies the development of systems. Source processing can be done independently of channel processing and vice versa.
- A standardized binary interface that connects the source and channel processing parts **simplifies networking**. Networking reduces to sending binary sequences (packets) through the network.
- Shannon not only proposed the source/channel separation idea, but he also proved that **we do not have to loose performance by separation**.

In the next subsections we will shortly discuss what specific procedures are carried out in source and channel processing.

2.3.2 Source Processing

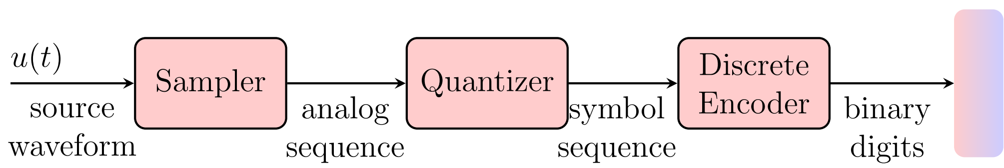

Figure 2.11: Dividing source processing at the transmit side into sampling, quantizing, and discrete encoding.

In Fig. 2.11 we have broken up source processing for waveforms in three different tasks. The first task is sampling, i.e., converting a waveform into a sequence of (analog) samples. We have seen before that the amount of samples per second is related to bandwidth of the waveform. Next these samples are transformed into (discrete) symbols. Such symbols can be represented in a digital form. The transition from analog to digital induces a performance loss since many analog values are approximated by the same quantization point. A last third step is focusing on removing redundancy from the sequence of symbols. This is a crucial step, a step that can dramatically decrease the number of binary digits that need to be transmitted over the channel.

Source processing at the decoder includes the inverse tasks of the three tasks mentioned above, i.e., discrete decoding, table lookup, and analog filtering.

2.3.3 Channel Processing

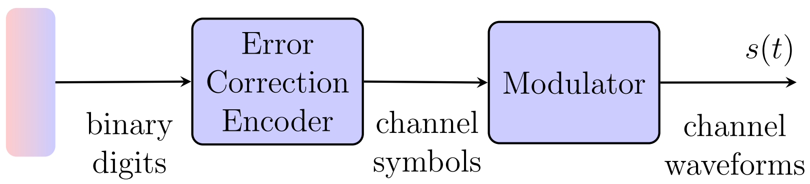

Figure 2.12: Dividing channel processing at the transmit side into error correction encoding, and modulation.

Fig. 2.12 shows that channel processing consists of two tasks. The first task is to add redundancy to the sequences of binary digits to make recovery from channel errors possible, the second task is to modulate the binary (digital) information onto carefully chosen waveforms, waveforms that fit to the specific channel. At the receiver side noisy versions of those waveforms are demodulated, and subsequently a decoder corrects errors that may have occurred during transmission of the waveforms. The outcomes of this decoder are binary sequences again.

2.3.4 Binary Interface

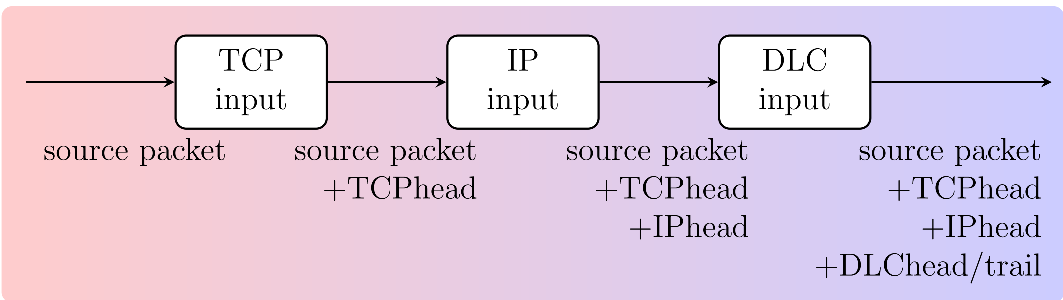

Figure 2.13: Breaking up the binary interface into three layers for internet communication.

The binary interface performs a number of tasks that relate to recovering from remaining errors, matching of channel transmission rates to source rates, and to networking. In Fig. 2.13 we see how the interface looks like for Internet communication. The TCP (transport control protocol) layer is responsible for end-to-end error recovery and for slowing down the source when the network gets congested. There is a TCP module for each source/destination pair. The IP (internet protocol) layer handles routing decisions, and sometimes drops packets when at the corresponding node the queues are too long. There is an IP module for every node in the network. A DLC (data link control) module is associated with each channel. The DLC layer performs rate-matching and error recovery on the channel, the so-called physical layer.

2.4 Additional Advantages of Digital Systems

So far we have more or less assumed that the waveform source is white and also that the channel noise is white. Source processing gains can be quite large when the waveform source is not white. The same holds for channel processing when the channel noise is not white.

The techniques that we rely on to achieve these gains are source and channel coding techniques, typically in the discrete domain. Modern source processing standards (e.g., JPEG, MPEG, H.264, MP3, and AAC) and channel transmission standards (e.g., IEEE 802.11x and 3G/4G) are based on advanced source and channel coding techniques. These standards have an essentially better performance than what could be achieved with the conventional analog communication methods. They offer reliable high-quality content delivery, at low bandwidth requirements.

Part II

CHANNEL PROCESSING: RECEIVERS

Chapter 3

Decision Rules for DIDO Channels

SUMMARY: In this chapter we investigate communication over a discrete-input discrete-output (DIDO) channel, i.e., a channel with discrete input and output alphabets. For this discrete channel we determine the optimum receiver, i.e., the receiver that minimizes the error probability. The so-called maximum a-posteriori (MAP) receiver turns out to be optimum. When all messages are equally likely the optimum receiver reduces to a maximum-likelihood (ML) receiver. In the last section of this chapter we distinguish between discrete scalar channels and discrete vector channels.

3.1 Optimum Receiver Definition

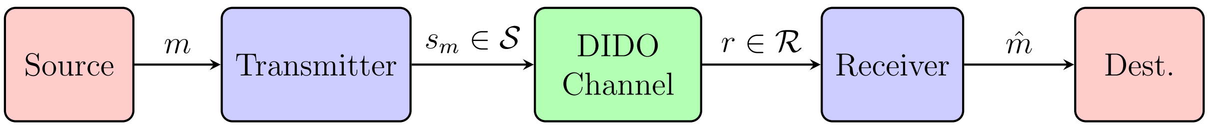

Figure 3.1: Elements in a communication system based on a DIDO channel.

We are focusing on channel processing, and, as discussed before in Sec. 2.3.1, we consider transmission of **digital information** over the channel. This information is contained in **discrete messages** as we shall see next. We start by considering a very simple communication system based on a *discrete-input discrete-output (DIDO)*. It consists of the following elements (see Fig. 3.1):

SOURCE An *information source* produces a *message* $m \in \mathcal{M} \stackrel{\Delta}{=} \{1, 2, \dots, |\mathcal{M}|\}$, one out of $|\mathcal{M}|$ alternatives. Message m occurs with probability $\Pr\{M = m\}$ for $m \in \mathcal{M}$. This probability is called the *a-priori message probability* and M is the name of the random variable associated with this mechanism. **Think of the messages as coming from the binary interface in Fig. 2.10**.

TRANSMITTER The *transmitter* sends a *signal* s_m if message m is to be transmitted. This signal is input to the channel. It takes values from the discrete channel input alphabet $\mathcal{S}$. The random variable corresponding to the signal is denoted by S. The collection of used signals is $\mathcal{S} \stackrel{\Delta}{=} \{s_1, s_2, \ldots, s_{|\mathcal{M}|}\}$.

DIDO CHANNEL The channel produces an output r that takes a value from a discrete alphabet $\mathcal{R}$ (in general different than $\mathcal{S}$). If the channel input is signal $s \in \mathcal{S}$ the output $r \in \mathcal{R}$ occurs with conditional probability $\Pr\{R = r|S = s\}$. This channel output is directed to the receiver. The random variable associated with the channel output is denoted by R.

When message $m \in \mathcal{M}$ occurs, the transmitter chooses s_m as channel input. Therefore

$$\Pr\{R = r|M = m\} = \Pr\{R = r|S = s_m\} \text{ for all } r \in \mathcal{R}. \tag{3.1}$$

These conditional probabilities describe the behavior of the transmitter followed by the channel.[1]

RECEIVER The *receiver* forms an *estimate* $\hat{m}$ of the transmitted message (or signal) by observing the received channel output $r \in \mathcal{R}$, hence $\hat{m} = f(r)$, where $f(\cdot)$ is a properly chosen mapping. The random variable corresponding to this estimate is called $\hat{M}$. We assume here that $\hat{m} \in \mathcal{M} = \{1, 2, \ldots, |\mathcal{M}|\}$, and thus, the receiver has to choose one of the possible messages (i.e., it cannot declare an error).

DESTINATION The *destination* accepts the estimate $\hat{m}$. **Think of the destination as the binary interface in Fig. 2.10.**

Note that we call our system *discrete* because the channel is discrete. It has discrete input and output alphabets.

For a given channel, the performance of our communication system is evaluated by considering the probability of error. This performance depends on the receiver, i.e., on the mapping function $f(\cdot)$.

Definition 3.1 *The mapping $f(\cdot)$ is called the* **decision rule**.

Definition 3.2 *The* **probability of error** *is defined as*

$$P_\mathrm{e} \stackrel{\Delta}{=} \Pr\{\hat{M} \neq M\}. \tag{3.2}$$

We are interested in choosing a decision rule $f(\cdot)$ that minimizes P_e. A decision rule that minimizes the error probability P_e is called **optimum**. The corresponding receiver is called an **optimum receiver**.

The probability of correct decision is denoted as P_c and defined below. The probability of error and the probability of correct decision satisfy $P_\mathrm{e} + P_\mathrm{c} = 1$.

[1] Note also that the channel we consider here is also *memoryless*, i.e., the channel outcome $R = r$ depends only on the the signal $S = s$, and not on previous or future transmitted signals.

Definition 3.3 *The* **probability of correct decision** *is defined as*

$$P_{\mathrm{c}} \stackrel{\Delta}{=} \Pr\{\hat{M} = M\}. \tag{3.3}$$

To get more familiar with the properties of our system we study an example first.

Example 3.1 We assume that $|\mathcal{M}| = 2$, i.e., there are two possible messages. Their a-priori probabilities can be found in the following table.

m	$\Pr\{M = m\}$
1	0.4
2	0.6

The two signals corresponding to the messages are s_1 and s_2 and the conditional probabilities $\Pr\{R = r|S = s_m\}$ are given in the table below for the values of r and m that can occur. There are three values that r can assume, i.e., $\mathcal{R} = \{a, b, c\}$.

m	$\Pr\{R = a\|S = s_m\}$	$\Pr\{R = b\|S = s_m\}$	$\Pr\{R = c\|S = s_m\}$
1	0.5	0.4	0.1
2	0.1	0.3	0.6

Note that the row sums are equal to one.

Now suppose that we use the decision rule $f(\cdot)$ that is given below.

r	a	b	c
$f(r)$	1	1	2

This means that the receiver outputs the estimate $\hat{m} = 1$ if the channel output is a or b and $\hat{m} = 2$ if the channel output is c. To determine the probability of error P_{e} that is achieved by this rule we first compute the joint probabilities

$$\begin{aligned}
\Pr\{M = m, R = r\} &= \Pr\{M = m\} \Pr\{R = r|M = m\} \\
&= \Pr\{M = m\} \Pr\{R = r|S = s_m\},
\end{aligned} \tag{3.4}$$

where we used (3.1). We list these joint probabilities in the following table.

m	$\Pr\{M = m, R = a\}$	$\Pr\{M = m, R = b\}$	$\Pr\{M = m, R = c\}$
1	0.20	0.16	0.04
2	0.06	0.18	0.36

Now we can determine the probability of correct decision $P_{\mathrm{c}} = 1 - P_{\mathrm{e}}$ which is:

$$\begin{aligned}
P_{\mathrm{c}} &= \Pr\{M = 1, R = a\} + \Pr\{M = 1, R = b\} + \Pr\{M = 2, R = c\} \\
&= 0.20 + 0.16 + 0.36 = 0.72.
\end{aligned} \tag{3.5}$$

This decision rule is not optimum. To see why, note that for every $r \in \mathcal{R}$ a certain message $\hat{m} \in \mathcal{M}$ is chosen. In other words the decision rule selects in each column exactly one joint probability. These selected probabilities are added together to form P_{c}. Our decision rule selects the joint probability $\Pr\{M = 1, R = b\} = 0.16$ in the column that corresponds to $R = b$. A larger P_c is obtained if for output $R = b$ instead of message 1 the message 2 is chosen. In that case the larger joint probability $\Pr\{M = 2, R = b\} = 0.18$ will be selected. Now, the probability of correct decision becomes

$$\begin{aligned} P_c &= \Pr\{M = 1, R = a\} + \Pr\{M = 2, R = b\} + \Pr\{M = 2, R = c\} \\ &= 0.20 + 0.18 + 0.36 = 0.74. \end{aligned} \tag{3.6}$$

Note that the probability of error can be expressed as

$$P_e = \Pr\{\hat{M} \neq M\} = \sum_{m \in \mathcal{M}} \Pr\{\hat{M} \neq M | M = m\} \Pr\{M = m\}, \tag{3.7}$$

which allows us to interpret the results obtained above in a different way. This interpretation is shown in Fig. 3.2, where the error probability calculation in (3.7) results in

$$P_e = 0.4 \cdot 0.1 + 0.6 \cdot (0.1 + 0.3) = 0.28, \tag{3.8}$$

and therefore, $P_c = 0.72$. The interpretation here is that for every transmitted message m, we should find all paths in the figure that lead us to the wrong estimate $\hat{m}$. When $M = 1$, only one path exits (with probability 0.1), while when $M = 2$, two paths exist (with probabilities 0.1 and 0.3).

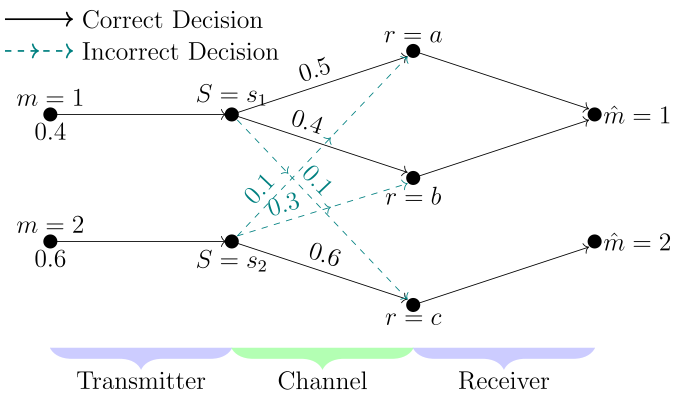

Figure 3.2: Graphical interpretation of the probability of error in (3.7).

We may conclude from this example that, in general, to maximize P_c, we have to choose the m that achieves the largest $\Pr\{M = m, R = r\}$ for the r that was received. This will be made more precise in the following section.

3.2 The Maximum A-Posteriori Decision Rule

We can upper bound the probability of correct decision as follows:

$$\begin{aligned} P_c &= \sum_{r \in \mathcal{R}} \Pr\{M = f(r), R = r\} \\ &\leq \sum_{r \in \mathcal{R}} \max_{m \in \mathcal{M}} \Pr\{M = m, R = r\}. \end{aligned} \tag{3.9}$$

This upper bound is achieved if for all r the estimate $f(r)$ corresponds to the message m that achieves the maximum in $\max_{m\in\mathcal{M}} \Pr\{M = m, R = r\}$, hence an optimum decision rule for the DIDO channel satisfies

$$\Pr\{M = f(r), R = r\} \geq \Pr\{M = m, R = r\}, \text{ for all } m \in \mathcal{M}, \tag{3.10}$$

for all $r \in \mathcal{R}$ that can be received, i.e., that have $\Pr\{R = r\} > 0$. Note that it is possible that for some channel outputs $r \in \mathcal{R}$ more than one decision $f(r)$ is optimum.

Definition 3.4 *For a communication system based on a DIDO channel the joint probabilities*

$$\begin{aligned}\Pr\{M = m, R = r\} &= \Pr\{M = m\} \Pr\{R = r|M = m\}\\ &= \Pr\{M = m\} \Pr\{R = r|S = s_m\}.\end{aligned} \tag{3.11}$$

which are, given the received output value r, indexed by $m \in \mathcal{M}$, are called the **decision variables**.

An optimum decision rule $f(\cdot)$ is based on these variables.

RESULT 3.1 (MAP decision rule) *To minimize the probability of error P_e, the decision rule $f(\cdot)$ should produce for each received r a message m having the largest decision variable. Hence for $r \in \mathcal{R}$ that actually can occur, i.e., that have* $\Pr\{R = r\} > 0$,

$$f(r) = \operatorname*{argmax}_{m\in\mathcal{M}} \Pr\{M = m\} \Pr\{R = r|S = s_m\}. \tag{3.12}$$

For such r we can divide all decision variables by the positive channel output probability $\Pr\{R = r\}$*. This results in the a-posteriori probabilities of the message $m \in \mathcal{M}$ given the channel output r. By Bayes rule*

$$\frac{\Pr\{M = m\} \Pr\{R = r|S = s_m\}}{\Pr\{R = r\}} = \Pr\{M = m|R = r\}, \textit{ for all } m \in \mathcal{M}, \tag{3.13}$$

therefore the optimum receiver chooses as $\hat{m}$ a message that has **maximum a-posteriori probability (MAP)**. *This decision rule is called the MAP-decision rule, the receiver is called a MAP-receiver.*

Example 3.2 Below are the a-posteriori probabilities that correspond to the example in the previous section (obtained from $\Pr\{R = a\} = 0.26, \Pr\{R = b\} = 0.34$, and $\Pr\{R = c\} = 0.4$). Note that the probabilities in a column add up to one now.

m	$\Pr\{M = m\|R = a\}$	$\Pr\{M = m\|R = b\}$	$\Pr\{M = m\|R = c\}$
1	20/26	16/34	4/40
2	6/26	18/34	36/40

From this table it is clear that the optimum decision rule is as given below.

r	a	b	c
$f(r)$	1	2	2

This leads to an error probability

$$P_{\mathrm{e}} = \sum_{m \in \mathcal{M}} \Pr\{M = m\} \Pr\{\hat{M} \neq m | M = m\} = 0.4(0.4 + 0.1) + 0.6 \cdot 0.1 = 0.26, \tag{3.14}$$

where $\Pr\{\hat{M} \neq m | M = m\} = \sum_{r: f(r) \neq m} \Pr\{R = r | S = s_m\}$ is the probability of error conditional on the fact that message m was sent.

3.3 The Maximum Likelihood Decision Rule

When all messages are *equally likely*, i.e., when

$$\Pr\{M = m\} = \frac{1}{|\mathcal{M}|} \text{ for all } m \in \mathcal{M} = \{1, 2, \ldots, |\mathcal{M}|\}, \tag{3.15}$$

we get for the joint probabilities

$$\Pr\{M = m, R = r\} = \Pr\{M = m\} \Pr\{R = r | M = m\} = \frac{1}{|\mathcal{M}|} \Pr\{R = r | S = s_m\}. \tag{3.16}$$

Considering (3.10) we obtain:

RESULT 3.2 (ML decision rule) *If the a-priori message probabilities are all equal, in order to minimize the error probability P_{e}, a decision rule $f(\cdot)$ has to be applied that satisfies*

$$f(r) = \operatorname*{argmax}_{m \in \mathcal{M}} \Pr\{R = r | S = s_m\}, \tag{3.17}$$

for $r \in \mathcal{R}$ that can occur i.e., for r with $\Pr\{R = r\} > 0$. Such a decision rule is called a **maximum likelihood (ML)** *decision rule, the resulting receiver is a maximum likelihood receiver.*

Given the received channel output $r \in \mathcal{R}$ the receiver chooses a message $\hat{m} \in \mathcal{M}$ for which the received r has maximum likelihood. The transition probabilities $\Pr\{R = r | S = s_m\}$ for $r \in \mathcal{R}$ and $m \in \mathcal{M}$ are called likelihoods. A receiver that operates like this (no matter whether or not the messages are indeed equally likely) is called a maximum likelihood receiver. It should be noted that such a receiver is less complex than a maximum a-posteriori receiver since it does not have to multiply the transition probabilities (likelihoods) $\Pr\{R = r | S = s_m\}$ by the a-priori probabilities $\Pr\{M = m\}$.

Example 3.3 Consider again the transition probabilities in Example 3.1.

m	$\Pr\{R = a \| S = s_m\}$	$\Pr\{R = b \| S = s_m\}$	$\Pr\{R = c \| S = s_m\}$
1	0.5	0.4	0.1
2	0.1	0.3	0.6

From this table follows the maximum-likelihood decision rule which is given below.

r	a	b	c
$f(r)$	1	1	2

When the messages 1 and 2 both have a-priori probability 1/2 the probability of correct decision is

$$P_{\mathrm{c}} = \sum_{m \in \mathcal{M}} \Pr\{M = m\} \Pr\{\hat{M} = m | M = m\} = \frac{1}{2}(0.5 + 0.4) + \frac{1}{2} 0.6 = 0.75. \tag{3.18}$$

Here $\Pr\{\hat{M} = m|M = m\} = \sum_{r \in \mathcal{R}: f(r)=m} \Pr\{R = r|S = s_m\}$ is the correct-probability conditioned on the fact that message m was sent. Note that the maximum likelihood decision rule is optimum here since both messages have the same a-priori probability.

3.4 Scalar and Vector Channels

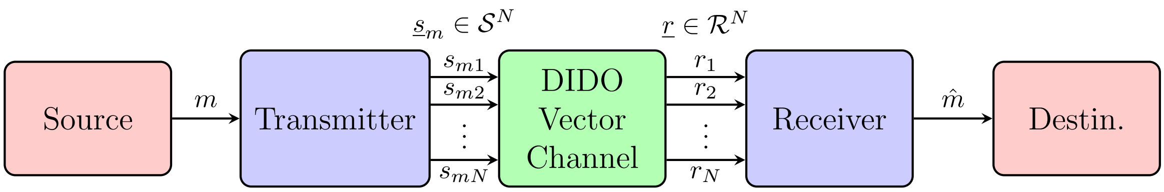

Figure 3.3: Elements in a communication system based on a discrete vector channel.

So far we have considered in this chapter a discrete channel that accepts a single input $s \in \mathcal{S}$ and produces a single output $r \in \mathcal{R}$. This channel could be called a discrete *scalar* channel. There is also a *vector* variant of this channel in Fig. 3.3. The components of a discrete vector system are described below.

TRANSMITTER Let N be a positive integer. Then the *vector transmitter* sends a *signal vector* $\underline{s}_m = (s_{m1}, s_{m2}, \ldots, s_{mN})$ of N components from the discrete alphabet $\mathcal{S}$ if message m is to be conveyed. This signal vector is input to the discrete vector channel. The random variable corresponding to the signal signal vector is denoted by $\underline{S}$. The collection of used signal vectors is $\underline{s}_1, \underline{s}_2, \ldots, \underline{s}_{|\mathcal{M}|}$.

DIDO VECTOR CHANNEL This channel produces an output vector $\underline{r} = (r_1, r_2, \ldots, r_N)$ with N components all assuming a value from a discrete alphabet $\mathcal{R}$. If the channel input was signal $\underline{s} \in \mathcal{S}^N$ the output $\underline{r} \in \mathcal{R}^N$ occurs with conditional probability $\Pr\{\underline{R} = \underline{r}|\underline{S} = \underline{s}\}$. This channel output vector is directed to the vector receiver. The random variable associated with the channel output is denoted by $\underline{R}$.

When message $m \in \mathcal{M}$ occurs, $\underline{s}_m$ is chosen by the transmitter as channel input vector. Then the conditional probabilities

$$\Pr\{\underline{R} = \underline{r}|M = m\} = \Pr\{\underline{R} = \underline{r}|\underline{S} = \underline{s}_m\} \text{ for all } \underline{r} \in \mathcal{R}^N, \tag{3.19}$$

describe the behavior of the vector transmitter followed by the discrete vector channel.

RECEIVER The *vector receiver* forms an *estimate* $\hat{m}$ of the transmitted message (or signal) by observing the received channel output vector $\underline{r} \in \mathcal{R}^N$, hence $\hat{m} = f(\underline{r})$. The mapping $f(\cdot)$ is again called the decision rule.

It will not be a big surprise that we define the decision variables for the discrete vector channel as follows:

Definition 3.5 *For a communication system based on a discrete vector channel the decision variables are again the joint probabilities*

$$\begin{aligned} \Pr\{M = m, \underline{R} = \underline{r}\} &= \Pr\{M = m\} \Pr\{\underline{R} = \underline{r} | M = m\} \\ &= \Pr\{M = m\} \Pr\{\underline{R} = \underline{r} | \underline{S} = \underline{s}_m\}. \end{aligned} \tag{3.20}$$

which are, given the received output vector $\underline{r}$*, indexed by* $m \in \mathcal{M}$*.*

The following result tells us what the optimum decision rule should be for the discrete vector channel:

RESULT 3.3 (MAP decision rule for the discrete vector channel) *To minimize the probability of error* P_e*, the decision rule* $f(\cdot)$ *should produce for each received vector* $\underline{r}$ *a message* m *having the largest decision variable. Hence for vectors* $\underline{r} \in \mathcal{R}^N$ *that actually can occur, i.e., that have* $\Pr\{\underline{R} = \underline{r}\} > 0$,

$$f(\underline{r}) = \operatorname*{argmax}_{m \in \mathcal{M}} \Pr\{M = m\} \Pr\{\underline{R} = \underline{r} | \underline{S} = \underline{s}_m\}. \tag{3.21}$$

This decision rule is the MAP-decision rule.

There is obviously also a "maximum likelihood version" of this result.

Chapter 4

Decision Rules for DICO Channels

SUMMARY: Here we will first consider transmission of information over discrete-input continuous-output (DICO) channels, i.e., channels with single real-valued outputs. Again the optimum receiver is determined. As an example we investigate the additive Gaussian noise channel, i.e., the channel that adds Gaussian noise to the input signal.

Then we discuss the channel whose input and output are vectors of real-valued components. An important example of such a vector channel is the additive Gaussian noise (AGN) vector channel. This channel adds zero-mean Gaussian noise to each input signal component. All noise samples are assumed to be independent of each other and have the same variance. For the AGN vector channel we determine the optimum receiver. If all messages are equally likely this receiver chooses the input vector that is closest to the received vector in terms of Euclidean distance. For the error probability in this case we derive an upper bound based on the union bound. We conclude by investigating the multi-vector channel here, i.e., a channel with more than one output vector. We discuss a sufficient condition under which one of the output vectors is irrelevant and can be discarded without changing the average error probability.

4.1 The Q-function

To compute error probabilities, the so-called Q-function is very useful.

Definition 4.1 (Q-function) *This function of $x \in (-\infty, \infty)$ is defined as*

$$Q(x) \stackrel{\Delta}{=} \int_x^\infty \frac{1}{\sqrt{2\pi}} \exp\left(-\frac{\alpha^2}{2}\right) d\alpha. \tag{4.1}$$

It is the probability that a Gaussian random variable with mean 0 *and variance* 1 *takes a value larger than x.*

x	$Q(x)$	x	$Q(x)$	x	$Q(x)$
0.00	0.50000	1.5	$6.6681 \cdot 10^{-2}$	5.0	$2.8665 \cdot 10^{-7}$
0.25	0.40129	2.0	$2.2750 \cdot 10^{-2}$	6.0	$9.8659 \cdot 10^{-10}$
0.50	0.30854	2.5	$6.2097 \cdot 10^{-3}$	7.0	$1.2798 \cdot 10^{-12}$
0.75	0.22663	3.0	$1.3499 \cdot 10^{-3}$	8.0	$6.2210 \cdot 10^{-16}$
1.00	0.15866	4.0	$3.1671 \cdot 10^{-5}$	10.0	$7.6200 \cdot 10^{-24}$

Table 4.1: Table of $Q(x)$ for some values of x.

In Table 4.1 we tabulated the function $Q(x)$ for several values of x. Fig. 4.1 shows $Q(1)$ as a tail integral of the Gaussian probability density function (as a shaded region).

A useful property of the Q-function is

$$Q(x) + Q(-x) = 1. \tag{4.2}$$

This property can be understood based on the symmetry of the Gaussian probability density function in Fig. 4.1 and can also be expressed as

$$Q(x) = 1 - Q(-x). \tag{4.3}$$

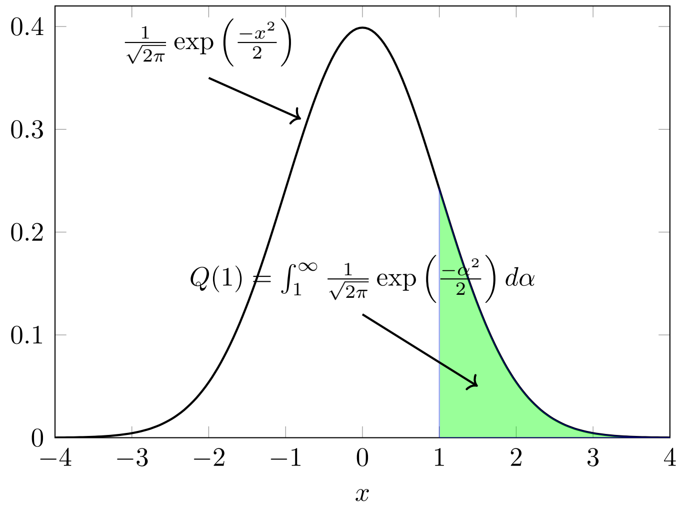

Figure 4.1: Gaussian probability density function for mean 0 and variance 1.

4.2 DICO Channels

Again we focus on channel processing, and, as discussed in Sec. 2.3.1, we consider transmission of **digital information**, in the form of discrete messages, over the channel. In Sec. 3.1 (see Fig. 3.1), we considered a very simple communication system based on a *discrete-input discrete-output channel*. Here we consider a communication system based on a *a discrete-input continuous-output* (DICO) channel. As we will see below, this *real scalar channel* does not differ very much from a system based on a DIDO channel.

The system under consideration is shown in Fig. 4.2 and it consists of the following elements:

SOURCE An information source produces the *message* $m \in \mathcal{M} = \{1, 2, \dots, |\mathcal{M}|\}$ with a-priori probability $\Pr\{M = m\}$ for $m \in \mathcal{M}$. Again, M is the name of the random variable associated with this mechanism.

TRANSMITTER The transmitter sends a real-valued scalar signal $s_m \in \mathcal{S} \subset \mathbb{R}$ if message m is to be transmitted. The scalar signal is input to the channel. The random variable corresponding to the signal is denoted by S. The collection of used signals is $\mathcal{S} = \{s_1, s_2, \dots, s_{|\mathcal{M}|}\}$.

DICO CHANNEL The channel now produces an output r in the range $(-\infty, \infty)$, i.e., $r \in \mathbb{R}$. In other words, the output alphabet can be considered to be $\mathcal{R} = \mathbb{R}$. When the input signal is the real-valued scalar s, the channel output is generated according to the conditional *probability density function* (PDF) $p_R(r|S = s)$ and thus R is a real-valued scalar random variable. The probability of receiving a channel output $r \leq R < r + dr$ is equal to $p_R(r|S = s)dr$ for an infinitely small interval dr.

When message $m \in \mathcal{M}$ is to be transmitted, signal s_m is chosen by the transmitter as channel input. Then, the conditional PDF

$$p_R(r|M = m) = p_R(r|S = s_m) \text{ for all } r \in (-\infty, \infty), \tag{4.4}$$

describes the behavior of the transmitter followed by the DICO channel.

RECEIVER The receiver forms an estimate $\hat{m}$ of the transmitted message (or signal) based on the received real-valued scalar channel output r, hence $\hat{m} = f(r)$. The mapping $f(\cdot)$ is again called the *decision rule*.

DESTINATION The destination accepts the estimate $\hat{m}$.

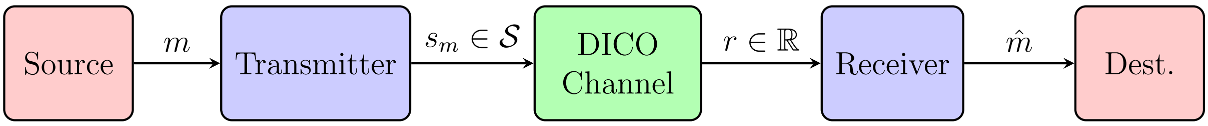

Figure 4.2: Elements in a communication system based on a DICO channel.

4.3 MAP and ML Decision Rules

For a DICO channel, we can write the probability of correct decision (see Definition 3.3) as

$$P_c = \Pr\{M = f(R)\} \tag{4.5}$$

$$= \int_{-\infty}^{\infty} p_{R,M}(r, f(r)\}dr \tag{4.6}$$

$$= \int_{-\infty}^{\infty} \Pr\{M = f(r)\} p_R(r|M = f(r))dr. \tag{4.7}$$

An optimum decision rule is obtained if, after receiving the scalar $R = r$, the decision $f(r)$ is taken in such a way that

$$\Pr\{M = f(r)\} p_R(r|M = f(r)) \geq \Pr\{M = m\} p_R(r|M = m) \text{ for all } m \in \mathcal{M}. \tag{4.8}$$

This leads to the definition of the decision variables given below.

Alternatively we can assume that a value $r \leq R < r + dr$ was received. Then the decision variables would be

$$\begin{aligned}\Pr\{M = m, r \leq R < r + dr\} &= \Pr\{M = m\} \Pr\{r \leq R < r + dr | S = s_m\} \\ &= \Pr\{M = m\} p_R(r|S = s_m) dr. \qquad (4.9)\end{aligned}$$

Also this reasoning leads to the definition of the decision variables below.

Definition 4.2 *For a system based on a DICO channels the products*

$$\Pr\{M = m\} p_R(r|M = m) = \Pr\{M = m\} p_R(r|S = s_m) \qquad (4.10)$$

which are, given the received output r, indexed by $m \in \mathcal{M}$, are called the **decision variables**.

The optimum decision rule $f(\cdot)$ is again based on these variables. It is possible that for certain channel outputs r more decisions $f(r)$ are optimum.

RESULT 4.1 (MAP) *To minimize the error probability P_e, the decision rule $f(\cdot)$ should be such that for each received r a message m is chosen with the largest decision variable. Hence for r that can be received, an optimum decision rule $f(\cdot)$ should satisfy*

$$f(r) = \operatorname*{argmax}_{m \in \mathcal{M}} \Pr\{M = m\} p_R(r|S = s_m). \qquad (4.11)$$

Both sides of the inequality (4.8) can be divided by $p_R(r) = \sum_{m \in \mathcal{M}} \Pr\{M = m\} p_R(r|S = s_m)$, i.e., de density for the value of r that actually did occur. Then we obtain an equivalent formulation of this optimum decision rule

$$f(r) = \operatorname*{argmax}_{m \in \mathcal{M}} \Pr\{M = m | R = r\}, \qquad (4.12)$$

for r for which $p_R(r) > 0$. Therefore this rule is again called maximum a-posteriori (MAP) decision rule.

RESULT 4.2 (ML) *When all messages have equal a-priori probabilities, i.e., when $\Pr\{M = m\} = 1/|\mathcal{M}|$ for all $m \in \mathcal{M}$, we observe from (4.11), that the optimum receiver has to choose*

$$f(r) = \operatorname*{argmax}_{m \in \mathcal{M}} p_R(r|S = s_m), \qquad (4.13)$$

for all r with $p_R(r) > 0$. This rule is referred to as the maximum likelihood (ML) decision rule.

4.4 The Scalar Additive Gaussian Noise Channel

4.4.1 Introduction

Gaussian noise is probably the most important kind of impairment. Therefore we will investigate a simple communication situation based on a channel that adds a Gaussian noise sample n to the input signal s. This is shown in Fig. 4.3 and we call it the scalar additive Gaussian noise (AGN) channel.

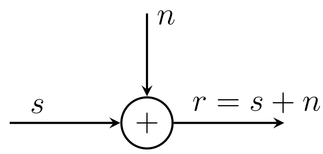

Figure 4.3: Scalar AGN channel. The PDF of the noise is in (4.14).

Definition 4.3 *The* **AGN channel** *adds Gaussian noise N to the input signal S. This Gaussian noise N has variance σ^2 and mean 0. The PDF of the noise is defined to be*

$$p_N(n) \triangleq \frac{1}{\sqrt{2\pi\sigma^2}} \exp\left(-\frac{n^2}{2\sigma^2}\right). \tag{4.14}$$

The noise variable N is assumed to be independent of the signal S.

4.4.2 The MAP decision rule

We assume that $|\mathcal{M}| = 2$, i.e., there are two messages and M can be either 1 or 2. The corresponding two signals s_1 and s_2 are the inputs of our channel. We will refer to this channel as the binary-input AGN (bi-AGN) channel.

The conditional PDF of receiving $R = r$ given the message m depends only on the value n that the noise variable N gets. In order to receive $R = r$ when the signal is $S = s_m$, the noise variable N should have value $r - s_m$. The noise N is independent of the signal S (and thus, also from the message M). Assuming that dr is infinitely small, we have

$$\begin{aligned} p_R(r|S = s_m) &= \Pr\{r \le R < r + dr|S = s_m\}/dr \\ &= \Pr\{r - s_m \le N < r - s_m + dr\}/dr \\ &= p_N(r - s_m) \\ &= \frac{1}{\sqrt{2\pi\sigma^2}} \exp\left(-\frac{(r - s_m)^2}{2\sigma^2}\right), \text{ for } m = 1, 2. \end{aligned} \tag{4.15}$$

In view of (4.7) (see also (4.11)), we obtain an optimum (MAP) receiver for $\hat{m} = f(r) = 1$ if

$$\Pr\{M = 1\}\frac{1}{\sqrt{2\pi\sigma^2}} \exp\left(-\frac{(r - s_1)^2}{2\sigma^2}\right) \ge \Pr\{M = 2\}\frac{1}{\sqrt{2\pi\sigma^2}} \exp\left(-\frac{(r - s_2)^2}{2\sigma^2}\right). \tag{4.16}$$

and $\hat{m} = 2$ otherwise. The following inequalities are all equivalent to (4.16):

$$\begin{aligned}
\ln(\Pr\{M=1\}) - \frac{(r-s_1)^2}{2\sigma^2} &\geq \ln(\Pr\{M=2\}) - \frac{(r-s_2)^2}{2\sigma^2},\\
2\sigma^2 \ln(\Pr\{M=1\}) - (r-s_1)^2 &\geq 2\sigma^2 \ln(\Pr\{M=2\}) - (r-s_2)^2,\\
2\sigma^2 \ln(\Pr\{M=1\}) + 2rs_1 - s_1^2 &\geq 2\sigma^2 \ln(\Pr\{M=2\}) + 2rs_2 - s_2^2,\\
2rs_1 - 2rs_2 &\geq 2\sigma^2 \ln\left(\frac{\Pr\{M=2\}}{\Pr\{M=1\}}\right) + s_1^2 - s_2^2 \qquad (4.17)\\
r &\geq \frac{\sigma^2}{s_1 - s_2} \ln\left(\frac{\Pr\{M=2\}}{\Pr\{M=1\}}\right) + \frac{s_1+s_2}{2}. \qquad (4.18)
\end{aligned}$$

RESULT 4.3 (Optimum receiver for the scalar bi-AGN channel) *A receiver that decides $\hat{m} = 1$ if*

$$r \geq r^* \triangleq \frac{\sigma^2}{s_1 - s_2} \ln\left(\frac{\Pr\{M=2\}}{\Pr\{M=1\}}\right) + \frac{s_1+s_2}{2}, \qquad (4.19)$$

and $\hat{m} = 2$ otherwise, is optimum. When the a-priori probabilities $\Pr\{M=1\}$ and $\Pr\{M=2\}$ are equal the optimum threshold is

$$r^* = \frac{s_1+s_2}{2}. \qquad (4.20)$$

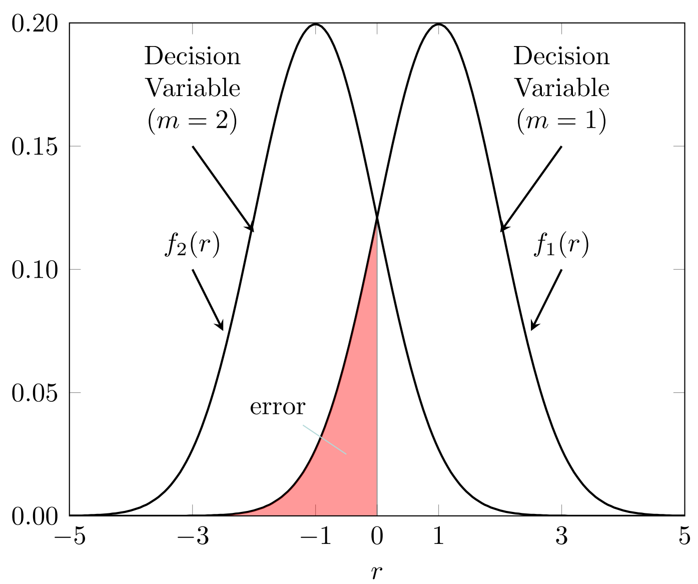

Figure 4.4: Decision variables for equal a-priori probabilities as a function of r for the AGN channel and input alphabet $\mathcal{S}\{s_1, s_2\}$. Here, $f_1(r) = \frac{1}{2}\frac{1}{\sqrt{2\pi}}\exp\left(\frac{(r-(+1))^2}{2}\right)$ and $f_2(r) = \frac{1}{2}\frac{1}{\sqrt{2\pi}}\exp\left(\frac{(r-(-1))^2}{2}\right)$

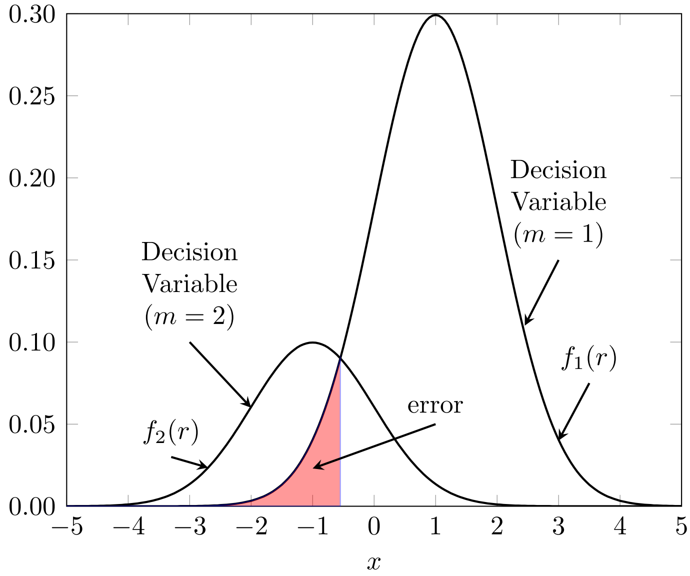

Figure 4.5: Decision variables as a function of r for a-priori probabilities 1/4 and 3/4 and with $f_1(r) = \frac{3}{4}\frac{1}{\sqrt{2\pi}}\exp\left(\frac{(r-(+1))^2}{2}\right)$ and $f_2(r) = \frac{1}{4}\frac{1}{\sqrt{2\pi}}\exp\left(\frac{(r-(-1))^2}{2}\right)$.

Example 4.1 Assume that $\sigma^2 = 1$ and $s_1 = +1$ and $s_2 = -1$. If the a-priori message probabilities are equal, i.e., $\Pr\{M = 1\} = \Pr\{M = 2\} = 1/2$, we obtain an optimum receiver if for $r \geq r^* = \frac{s_1+s_2}{2}$ we decide for $\hat{m} = 1$. The decision changes exactly halfway between s_1 and s_2. The intervals $(-\infty, r^*)$ and (r^*, ∞) are called *decision intervals*. In our case, since $s_2 = -s_1$, the threshold $r^* = 0$. The decision variables are

$$\Pr\{M = 1\}\frac{1}{\sqrt{2\pi\sigma^2}}\exp\left(-\frac{(r-s_1)^2}{2\sigma^2}\right) \tag{4.21}$$

and

$$\Pr\{M = 2\}\frac{1}{\sqrt{2\pi\sigma^2}}\exp\left(-\frac{(r-s_2)^2}{2\sigma^2}\right), \tag{4.22}$$

which are plotted in Fig. 4.4 as a function of r assuming that $\Pr\{M = 1\} = \Pr\{M = 2\} = 1/2$.

Assume now that the a-priori probabilities are not equal and let $\Pr\{M = 1\} = 3/4$ and $\Pr\{M = 2\} = 1/4$. Now the decision variables change (see Fig. 4.5) and we must also change the decision rule. It turns out that for $r \geq r^* = -\frac{\ln 3}{2} \approx -0.5493$ the optimum receiver should choose $\hat{m} = 1$ (see again Fig. 4.5). The threshold r^* has moved away from the more probable signal s_1.

Note that, no matter how much the a-priori probabilities differ, there is always a value of r, which we call r^*, the threshold, before, for which (4.16) is satisfied with equality. For $r > r^*$ the left side in (4.16) is larger than the right side, and for $r < r^*$ the right side is the largest.

4.4.3 Error Probability

We now want to find an expression for the error probability of our scalar system (bi-AGN channel) with two messages. We write

$$P_{\mathrm{e}} = \Pr\{M=1\}\Pr\{R<r^*|M=1\} + \Pr\{M=2\}\Pr\{R\geq r^*|M=2\}, \tag{4.23}$$

where

$$\begin{aligned}\Pr\{R\geq r^*|M=2\} &= \int_{r=r^*}^{\infty}\frac{1}{\sqrt{2\pi\sigma^2}}\exp\left(-\frac{(r-s_2)^2}{2\sigma^2}\right)dr\\ &= \int_{r=r^*}^{\infty}\frac{1}{\sqrt{2\pi}}\exp\left(-\frac{((r/\sigma)-s_2/\sigma)^2}{2}\right)d(r/\sigma)\\ &= \int_{\mu=r^*/\sigma-s_2/\sigma}^{\infty}\frac{1}{\sqrt{2\pi}}\exp\left(-\frac{\mu^2}{2}\right)d\mu = Q(r^*/\sigma - s_2/\sigma),\end{aligned} \tag{4.24}$$

and similarly

$$\begin{aligned}\Pr\{R<r^*|M=1\} &= \int_{-\infty}^{r=r^*}\frac{1}{\sqrt{2\pi\sigma^2}}\exp\left(-\frac{(r-s_1)^2}{2\sigma^2}\right)dr\\ &= \int_{-\infty}^{r=r^*}\frac{1}{\sqrt{2\pi}}\exp\left(-\frac{((r/\sigma)-s_1/\sigma)^2}{2}\right)d(r/\sigma)\\ &= \int_{-\infty}^{\mu=r^*/\sigma-s_1/\sigma}\frac{1}{\sqrt{2\pi}}\exp\left(-\frac{\mu^2}{2}\right)d\mu\\ &= 1-Q\left(\frac{r^*}{\sigma}-\frac{s_1}{\sigma}\right)\overset{(*)}{=} Q\left(\frac{s_1}{\sigma}-\frac{r^*}{\sigma}\right) = Q\left(\frac{s_1-r^*}{\sigma}\right).\end{aligned} \tag{4.25}$$

Note that the last equality (*) follows from (4.2).

If we combine (4.23), (4.24), and (4.25), we obtain

$$P_{\mathrm{e}} = \Pr\{M=1\}Q\left(\frac{s_1-r^*}{\sigma}\right) + \Pr\{M=2\}Q\left(\frac{r^*-s_2}{\sigma}\right). \tag{4.26}$$

If the a-priori message probabilities $\Pr\{M=1\}$ and $\Pr\{M=2\}$ are equal then, according to (4.20), we get $r^* = \frac{s_1+s_2}{2}$ and

$$\begin{aligned}\frac{s_1-r^*}{\sigma} &= \frac{s_1-\frac{s_1+s_2}{2}}{\sigma} = \frac{s_1-s_2}{2\sigma}\\ \frac{r^*-s_2}{\sigma} &= \frac{\frac{s_1+s_2}{2}-s_2}{\sigma} = \frac{s_1-s_2}{2\sigma}.\end{aligned} \tag{4.27}$$

Hence, for equally likely messages, the minimum error probability is

$$P_{\mathrm{e}} = Q\left(\frac{s_1-s_2}{2\sigma}\right). \tag{4.28}$$

Example 4.2 For $s_1 = +1$, $s_2 = -1$, and $\sigma^2 = 1$, we obtain if $\Pr\{M = 1\} = \Pr\{M = 2\}$ that

$$P_e = Q(1) \approx 0.1587. \tag{4.29}$$

For $\Pr\{M = 1\} = 3/4$ and $\Pr\{M = 2\} = 1/4$ we get that $r^* = -\frac{\ln 3}{2} \approx -0.5493$ and

$$\begin{aligned} P_e &= \frac{3}{4} Q\left(1 + \frac{\ln 3}{2}\right) + \frac{1}{4} Q\left(-\frac{\ln 3}{2} + 1\right) \\ &\approx 0.75 \cdot Q(1.5493) + 0.25 \cdot Q(0.4507) \\ &\approx 0.75 \cdot 0.0607 + 0.25 \cdot 0.3261 \approx 0.1270. \end{aligned} \tag{4.30}$$

Note that this is smaller than $Q(1) \approx 0.1587$ which would be the error probability after ML-detection (which is suboptimum here).

4.5 Vector Channels

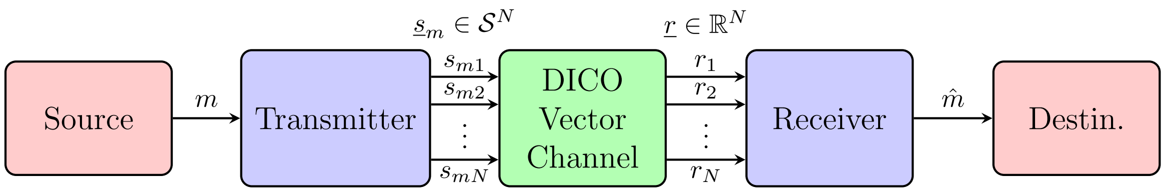

Figure 4.6: A communication system based on a vector channel.

In a communication system based on a vector channel (see Fig. 4.6) the channel input and output are vectors with real-valued components.

SOURCE The information source generates the *message* $m \in \mathcal{M} = \{1, 2, \ldots, |\mathcal{M}|\}$ with a-priori probability $\Pr\{M = m\}$ for $m \in \mathcal{M}$. M is the random variable associated with this mechanism.

TRANSMITTER The transmitter sends a vector signal $\underline{s}_m = (s_{m1}, s_{m2}, \ldots, s_{mN})$ consisting of N components if message m is to be transmitted. Each component takes a value from the discrete set $\mathcal{S} \subset \mathbb{R}$. The random vector corresponding to the signal vector is denoted by $\underline{S}$. The vector signal is input of the channel. The set of used signals is $\{\underline{s}_1, \underline{s}_2, \ldots, \underline{s}_{|\mathcal{M}|}\}$.

VECTOR CHANNEL The channel produces an output vector $\underline{r} = (r_1, r_2, \ldots, r_N)$ consisting of N components. We assume here that each of these components take values from the set $\mathbb{R}$. The conditional PDF of the channel output $\underline{r}$ when the message $M = m$ is $p_{\underline{R}}(\underline{r}|M = m) = p_{\underline{R}}(\underline{r}|\underline{S} = \underline{s}_m)$. Thus, when $M = m$, the probability of receiving an N-dimensional channel output vector $\underline{R}$ with components R_n for $n = 1, 2, \ldots, N$ satisfying $r_n \le R_n < r_n + dr_n$ is equal to $p_{\underline{R}}(\underline{r}|M = m)d\underline{r}$ for an infinitely small $d\underline{r} = dr_1 dr_2 \ldots dr_N$.

RECEIVER The receiver forms $\hat{m}$ based on the received real-valued channel output vector $\underline{r}$, hence $\hat{m} = f(\underline{r})$. The mapping function $f(\cdot)$ is the *decision rule*.

DESTINATION The destination accepts $\hat{m}$.

4.6 Decision Variables, MAP Decoding

The optimum receiver upon receiving $\underline{r}$ determines which one of the possible messages has maximum a-posteriori probability. It therefore chooses the decision rule $f(\underline{r})$ such that for all $\underline{r}$ that can be received

$$\Pr\{M = f(\underline{r})\}p_{\underline{R}}(\underline{r}|M = f(\underline{r})) \geq \Pr\{M = m\}p_{\underline{R}}(\underline{r}|M = m), \text{ for all } m \in \mathcal{M}. \tag{4.31}$$

In other words, upon receiving $\underline{r}$, the optimum receiver produces an estimate $\hat{m}$ that corresponds to a largest *decision variable*. The decision variables for the vector channel are

$$\Pr\{M = m\}p_{\underline{R}}(\underline{r}|M = m) \text{ for all } m \in \mathcal{M}. \tag{4.32}$$

That (4.31) is the MAP decoding rule follows from Bayes rule:

$$\Pr\{M = m|\underline{R} = \underline{r}\} = \frac{\Pr\{M = m\}p_{\underline{R}}(\underline{r}|M = m)}{p_{\underline{R}}(\underline{r})} \tag{4.33}$$

for $\underline{r}$ with $p_{\underline{R}}(\underline{r}) > 0$. Note that $p_{\underline{R}}(\underline{r}) > 0$ for any output vector $\underline{r}$ that has actually been received.

4.7 Decision Regions

The optimum receiver, upon receiving $\underline{r}$, determines the maximum of all decision variables which are given in (4.32). To compute these decision variables the a-priori probabilities $\Pr\{M = m\}$ must be known to the receiver and also the conditional density functions $p_{\underline{R}}(\underline{r}|M = m)$ for all $m \in \mathcal{M}$. This calculation can be carried out for every $\underline{r}$ in the *observation space*, i.e., the set of all possible output vectors $\underline{r}$. Each point $\underline{r}$ in the observation space is therefore assigned to one of the possible messages $m \in \mathcal{M}$. This results in a *partitioning* of the observation space in (at most) $|\mathcal{M}|$ regions.

Definition 4.4 *Given the decision rule $f(\cdot)$ we can write*

$$\mathcal{I}_m \stackrel{\Delta}{=} \{\underline{r} \in \mathbb{R}^N : f(\underline{r}) = m\}. \tag{4.34}$$

where $\mathcal{I}_m$ is called the **decision region** *that corresponds to message $m \in \mathcal{M}$.*

Note that in Example 4.2, we considered decision intervals. A decision region is an N-dimensional generalization of a (one-dimensional) decision interval.

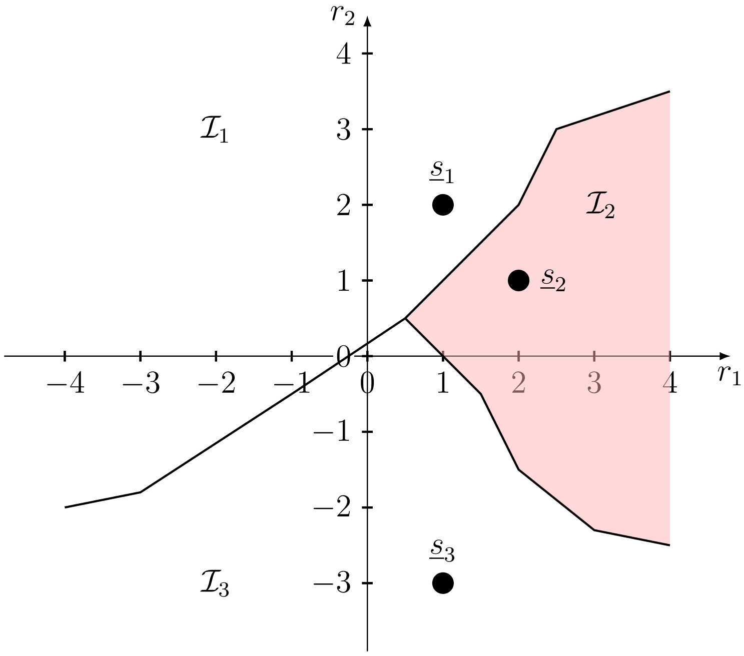

Figure 4.7: Three two-dimensional signal vectors and their decision regions.

Example 4.3 Suppose that we have three messages i.e., $\mathcal{M} = \{1, 2, 3\}$, and the corresponding signal vectors are two-dimensional, i.e., $\underline{s}_1 = (1, 2), \underline{s}_2 = (2, 1)$, and $\underline{s}_3 = (1, -3)$. A possible partitioning of the observation space into the three decision regions $\mathcal{I}_1, \mathcal{I}_2$, and $\mathcal{I}_3$ is shown in the Fig. 4.7. In this figure, we highlight $\mathcal{I}_2$ to show that any $\underline{r} \in \mathcal{I}_2$, the receiver will return $\hat{m} = 2$.

4.8 Additive Gaussian Noise

The actual shape of the decision regions is determined by the a-priori message probabilities $\Pr\{M = m\}$, the signals $\underline{s}_m$, and the conditional density functions $p_{\underline{R}}(\underline{r}|\underline{S} = \underline{s}_m)$ for all $m \in \mathcal{M}$. A relatively simple but again quite important situation is the case where the channel adds Gaussian noise to the signal components. This is shown in Fig. 4.8, which generalizes Fig. 4.3 to multiple dimensions.

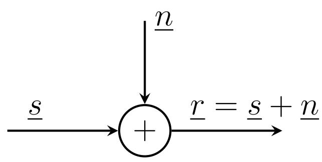

Figure 4.8: Additive Gaussian noise vector channel.

Definition 4.5 *The AGN vector channel is*

$$\underline{r} = \underline{s} + \underline{n}, \tag{4.35}$$

where $\underline{n} \stackrel{\Delta}{=} (n_1, n_2, \ldots, n_N)$ is an N-dimensional noise vector. We denote this random noise vector by $\underline{N}$. The noise vector $\underline{N}$ is assumed to be independent of the signal vector $\underline{S}$.

The N components of the noise vector are also assumed to be independent of each other. Moreover all noise components have mean 0 and the same variance σ^2. Therefore the joint density function of the noise vector is given by

$$p_{\underline{N}}(\underline{n}) = \prod_{i=1}^{N} \frac{1}{\sqrt{2\pi\sigma^2}} \exp\left(-\frac{n_i^2}{2\sigma^2}\right) = \frac{1}{(2\pi\sigma^2)^{N/2}} \exp\left(-\frac{1}{2\sigma^2}\sum_{i=1}^{N} n_i^2\right). \tag{4.36}$$

This notation in the definition can be contracted by noting that

$$\sum_{i=1}^{N} n_i^2 = (\underline{n} \cdot \underline{n}) = \|\underline{n}\|^2, \tag{4.37}$$

where $\|\underline{n}\|$ is the norm of the vector $\underline{n}$, $(\underline{a} \cdot \underline{b}) \triangleq \sum_{i=1}^{N} a_i b_i$ is the dot product of the vectors $\underline{a} = (a_1, a_2, \ldots, a_N)$ and $\underline{b} = (b_1, b_2, \ldots, b_N)$. Thus

$$p_{\underline{N}}(\underline{n}) = \frac{1}{(2\pi\sigma^2)^{N/2}} \exp\left(-\frac{\|\underline{n}\|^2}{2\sigma^2}\right). \tag{4.38}$$

If the channel output is $\underline{r}$ and its input was $\underline{s}_m$ then the noise vector must have been $\underline{n} = \underline{r} - \underline{s}_m$. This and the independence of the noise vector and the signal vector yields that

$$p_{\underline{R}}(\underline{r}|M = m) = p_{\underline{R}}(\underline{r}|\underline{S} = \underline{s}_m) = p_{\underline{N}}(\underline{r} - \underline{s}_m|\underline{S} = \underline{s}_m) = p_{\underline{N}}(\underline{r} - \underline{s}_m). \tag{4.39}$$

Now we can easily determine the decision variables, one for each $m \in \mathcal{M}$:

$$\begin{aligned} \Pr\{M = m\} p_{\underline{R}}(\underline{r}|M = m) &= \Pr\{M = m\} p_{\underline{N}}(\underline{r} - \underline{s}_m) \\ &= \Pr\{M = m\} \frac{1}{(2\pi\sigma^2)^{N/2}} \exp\left(-\frac{\|\underline{r} - \underline{s}_m\|^2}{2\sigma^2}\right). \end{aligned} \tag{4.40}$$

Note that the factor $(2\pi\sigma^2)^{N/2}$ is independent of m. Hence maximizing over the decision variables in (4.40) is equivalent to *minimizing*

$$\|\underline{r} - \underline{s}_m\|^2 - 2\sigma^2 \ln \Pr\{M = m\} \tag{4.41}$$

over all $m \in \mathcal{M}$. We get a very simple decision rule if all messages are equally likely.

RESULT 4.4 (Minimum Euclidean distance decision rule) *If the a-priori message probabilities are all equal, the optimum receiver has to minimize the* **squared Euclidean distance**

$$\|\underline{r} - \underline{s}_m\|^2, \text{ for all } m \in \mathcal{M}. \tag{4.42}$$

In other words the receiver has to choose the message $\hat{m}$ with corresponding signal vector $\underline{s}_{\hat{m}}$ that is closest in Euclidean sense to the received vector $\underline{r}$.

Example 4.4 Consider again the three two dimensional signal vectors $\underline{s}_1 = (1, 2), \underline{s}_2 = (2, 1)$, and $\underline{s}_3 = (1, -3)$ in (see Example 4.3. The optimum decision regions can be found by drawing the perpendicular bisectors of the sides of the triangle generated by the signals, as shown in Fig. 4.9. These are the boundaries of the decision regions $\mathcal{I}_1, \mathcal{I}_2$, and $\mathcal{I}_3$ (see figure). Note that the three bisectors have a single point in common.

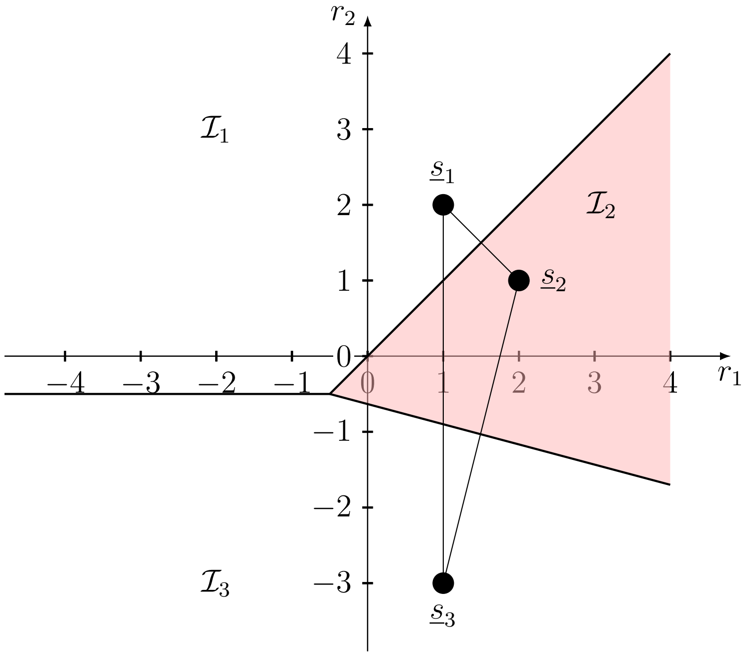

Figure 4.9: Three two-dimensional signal vectors and the corresponding optimum decision regions for the AGN channel and equally likely messages.

4.8.1 Error probabilities

The error probability for the AGN vector channel is determined by the location of the signals $\{\underline{s}_1, \underline{s}_2, \ldots, \underline{s}_{|\mathcal{M}|}\}$, and, more importantly, the hyperplanes that separate these signal-vectors. An error occurs if the noise "pushes" a signal-point to the wrong side of a hyperplane. In general it is quite difficult to determine the exact error probability, however it is easy to compute the probability that the received signal is on the wrong side of a hyperplane.

To study this behavior we investigate a simple example in two dimensions. i.e., $N = 2$. Consider a signal vector $\underline{s} = (a, b)$, see Fig. 4.10. This signal vector is corrupted by the AGN vector $\underline{n} = (n_1, n_2)$ with independent components that both have mean zero and variance σ^2. What is now the probability $P_{\mathcal{I}}$ that the received vector $\underline{r} = (r_1, r_2) = (a, b) + (n_1, n_2)$ is in the region $\mathcal{I}$, i.e., in the region above the line (see Fig. 4.10).

To solve this problem we have to change the coordinate system. Let

$$r_1 = a + u_1 \cos\theta - u_2 \sin\theta \quad (4.43)$$

$$r_2 = b + u_1 \sin\theta + u_2 \cos\theta, \quad (4.44)$$

where (a, b) is the center of a Cartesian system with coordinates u_1 and u_2, and θ the rotation-angle. Coordinate u_1 is perpendicular to and coordinate u_2 is parallel to the line in Fig. 4.10 Note that $P_{\mathcal{I}}$ can be expressed as

$$P_{\mathcal{I}} = \int_{\mathcal{I}} \frac{1}{2\pi\sigma^2} \exp\left(-\frac{(r_1 - a)^2 + (r_2 - b)^2}{2\sigma^2} \right) dr_1 dr_2. \quad (4.45)$$

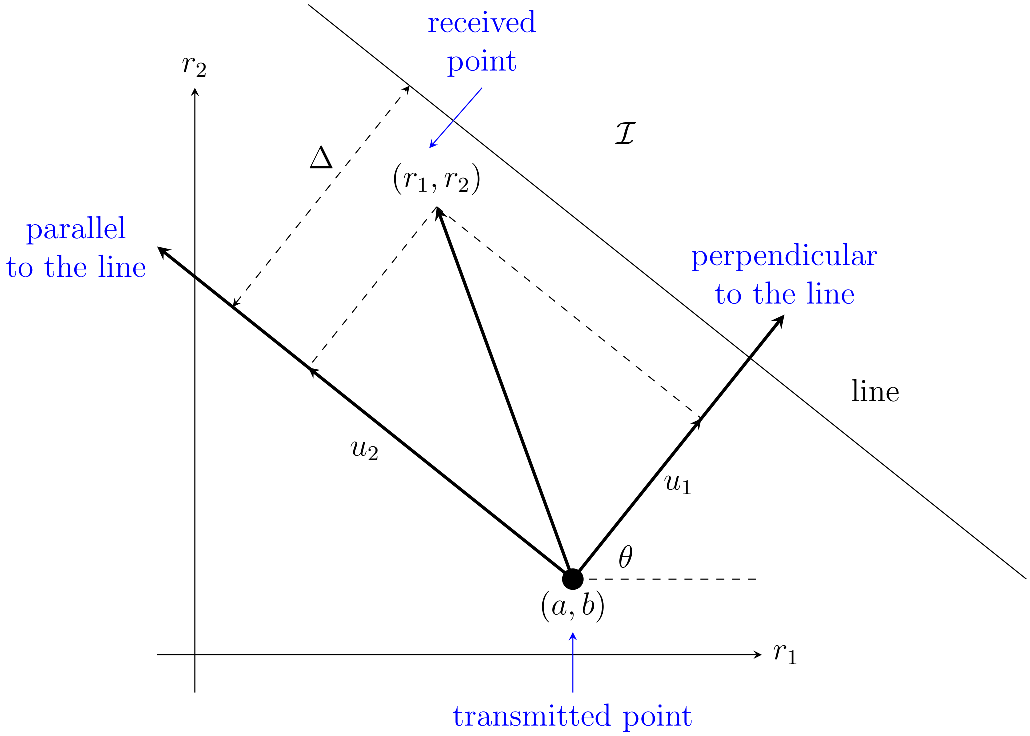

Figure 4.10: A signal point (a, b) and a line at distance Δ.

Elementary calculus (see, e.g., Theorem 7.7.13 of [16, p. 386] tells us that

$$\int_{\mathcal{I}} f(r_1, r_2) dr_1 dr_2 = \int_{\mathcal{I}} f(r_1(u_1, u_2), r_2(u_1, u_2)) |J| du_1 du_2, \tag{4.46}$$

where $|J|$ is the determinant of the Jacobian J which is in this case (see (4.43)–(4.44))

$$J = \begin{pmatrix} \frac{\partial r_1}{\partial u_1} & \frac{\partial r_1}{\partial u_2} \\ \frac{\partial r_2}{\partial u_1} & \frac{\partial r_2}{\partial u_2} \end{pmatrix} = \begin{pmatrix} \cos\theta & -\sin\theta \\ \sin\theta & \cos\theta \end{pmatrix}. \tag{4.47}$$

Note that $|J| = \cos^2\theta + \sin^2\theta = 1$ and $(r_1 - a)^2 + (r_2 - b)^2 = u_1^2 + u_2^2$. Therefore

$$\begin{aligned} P_{\mathcal{I}} &= \int_{\mathcal{I}} \frac{1}{2\pi\sigma^2} \exp\left(-\frac{u_1^2 + u_2^2}{2\sigma^2}\right) du_1 du_2 \\ &= \int_{u_1=\Delta}^{\infty} \int_{u_2=-\infty}^{\infty} \frac{1}{2\pi\sigma^2} \exp\left(-\frac{u_1^2 + u_2^2}{2\sigma^2}\right) du_1 du_2 \\ &= \int_{u_1=\Delta}^{\infty} \frac{1}{\sqrt{2\pi\sigma^2}} \exp\left(-\frac{u_1^2}{2\sigma^2}\right) du_1 \int_{u_2=-\infty}^{\infty} \frac{1}{\sqrt{2\pi\sigma^2}} \exp\left(-\frac{u_2^2}{2\sigma^2}\right) du_2 \\ &= Q\left(\frac{\Delta}{\sigma}\right) \cdot 1 = Q\left(\frac{\Delta}{\sigma}\right). \end{aligned} \tag{4.48}$$

Conclusion is that the probability depends only on the distance Δ from the signal point (a, b) to the line. This result carries over to more than two dimensions:

RESULT 4.5 *For the AGN vector channel, the probability that the noise pushes a signal to the wrong side of a hyperplane is*

$$P_{\mathcal{I}} = Q\left(\frac{\Delta}{\sigma}\right), \tag{4.49}$$

where Δ is the distance from the signal-point to the hyperplane and σ^2 is the variance of each noise component.

4.9 Upper bound on the error probability

For the AGN channel (and also for most other channels), the probability of error P_{e} of an optimum receiver cannot be computed easily. However we can use the "union bound" to obtain an upper bound for it. To see how this works we assume that the a priori message probabilities are all equal. Then for the error probability P_{e}^1 when message 1 is sent, we can write

$$\begin{aligned} P_{\mathrm{e}}^1 &= \Pr\left\{\bigcup_{m\in\mathcal{M},m\neq 1}(\|\underline{R}-\underline{s}_m\| \leq \|\underline{R}-\underline{s}_1\|)|M=1\right\} \\ &\leq \sum_{m\in\mathcal{M},m\neq 1}\Pr\{\|\underline{R}-\underline{s}_m\| \leq \|\underline{R}-\underline{s}_1\||M=1\}. \end{aligned} \tag{4.50}$$

Note that in the last step we used the union bound $\Pr\{\cup_i E_i\} \leq \sum_i \Pr\{E_i\}$, where E_i is an event indexed by i.

Now the total error probability can be upper bounded by

$$\begin{aligned} P_{\mathrm{e}} &= \sum_{m\in\mathcal{M}}\Pr\{M=m\}P_{\mathrm{e}}^m \\ &\leq \sum_{m\in\mathcal{M}}\frac{1}{|\mathcal{M}|}\sum_{m'\in\mathcal{M},m'\neq m}\Pr\{\|\underline{R}-\underline{s}_{m'}\| \leq \|\underline{R}-\underline{s}_m\||M=m\}. \end{aligned} \tag{4.51}$$

By recognizing the last term in (4.50) as the probability that the received signal is pushed across the hyperplane between signals s_m and $s_{m'}$, we obtain for the AWG vector channel with per-dimension noise variance σ^2

$$P_{\mathrm{e}} \leq \sum_{m\in\mathcal{M}}\frac{1}{|\mathcal{M}|}\sum_{m'\in\mathcal{M},m'\neq m}Q\left(\frac{\Delta_{m'm}}{\sigma}\right), \tag{4.52}$$

where $\Delta_{m'm} = \|\underline{s}_{m'} - \underline{s}_m\|/2$ is half the distance between $\underline{s}_{m'}$ and $\underline{s}_m$, i.e., the distance between the signal points and the hyperplane separating them (see Result 4.5). Note that when the a priori probabilities are not all equal, we can also use the union bound to upper bound the error probability.

4.10 Multi-Vector Channels

4.10.1 System description

The output of a multi-vector channel consists of a pair $(\underline{r}_1, \underline{r}_2)$ of vectors, often but not necessarily of the same dimension as the input vector $\underline{s}$. This is shown in Fig. 4.53, where the input vectors $\underline{s}_m = (s_{m1}, s_{m2}, \ldots, s_{mN})$ are N-dimensional, and the output vectors are K- and L-dimensional, i.e., $\underline{r}_1 = (r_{11}, r_{12}, \ldots, r_{1K})$ and $\underline{r}_2 = (r_{21}, r_{22}, \ldots, r_{2L})$.

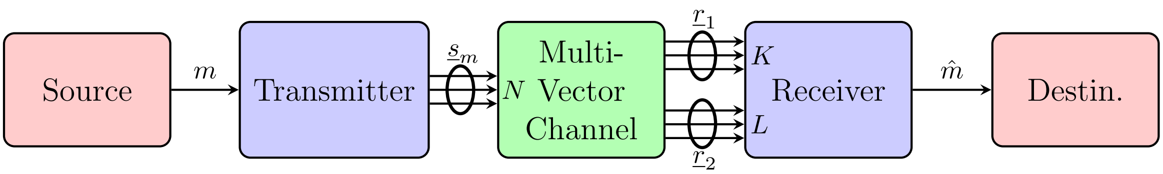

Figure 4.11: A multi-vector communication system.

We sometimes call our system one with "diversity". The decision variables for a multi-vector channel are

$$\Pr\{M = m\} p_{\underline{R}_1, \underline{R}_2}(\underline{r}_1, \underline{r}_2 | \underline{S} = \underline{s}_m) \text{ for all } m \in \mathcal{M}, \tag{4.53}$$

and the optimum receiver chooses an $\hat{m}$ that maximizes (4.53).

4.10.2 Theorem of irrelevance

An important question is whether for a multi-vector channel one of the output vectors, say $\underline{r}_2$, may be disregarded by the receiver without affecting the average error probability P_{e}. If that is the case, we call the output $\underline{r}_2$ *irrelevant*.

To investigate this problem we rewrite the decision variables (4.53) as follows

$$\Pr\{M = m\} p_{\underline{R}_1}(\underline{r}_1 | \underline{S} = \underline{s}_m) p_{\underline{R}_2}(\underline{r}_2 | \underline{S} = \underline{s}_m, \underline{R}_1 = \underline{r}_1) \text{ for all } m \in \mathcal{M}. \tag{4.54}$$

If the factor $p_{\underline{R}_2}(\underline{r}_2 | \underline{S} = \underline{s}_m, \underline{R}_1 = \underline{r}_1)$ does not depend on the message m, it can be ignored. From this observation we immediately get the following result.

THEOREM 4.6 (Theorem of irrelevance) *The output $\underline{r}_2$ of a multi-vector channel is irrelevant if, for all $\underline{r}_1$ and $\underline{r}_2$, the value of $p_{\underline{R}_2}(\underline{r}_2 | \underline{S} = \underline{s}_m, \underline{R}_1 = \underline{r}_1)$ does not depend on the message m.*

To understand this theorem we study three examples. These examples all involve two additive noise signals $\underline{n}_1$ and $\underline{n}_2$ that are independent of each other and the signal vector $\underline{s}$.

Example 4.5 In the first example (see Fig. 4.12) clearly

$$p_{\underline{R}_2}(\underline{r}_2 | \underline{S} = \underline{s}_m, \underline{R}_1 = \underline{r}_1) = p_{\underline{N}_2}(\underline{r}_2) \tag{4.55}$$

which does not depend on m. Therefore $\underline{r}_2$ is irrelevant.

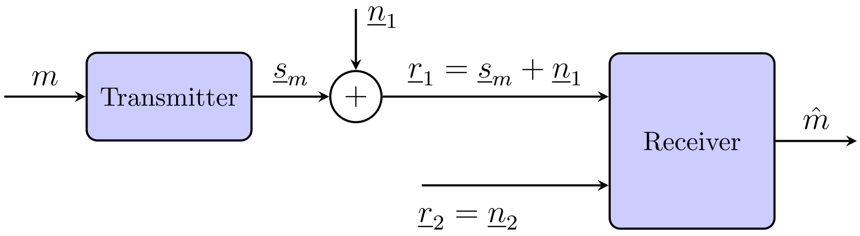

Figure 4.12: The vector $\underline{r}_2$ is irrelevant.

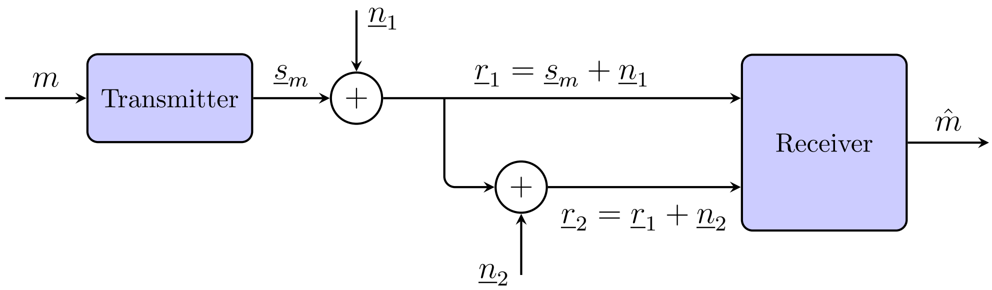

Figure 4.13: The vector $\underline{r}_2$ is irrelevant.

Example 4.6 In the second example (see Fig. 4.13) we get that

$$p_{\underline{R}_2}(\underline{r}_2|\underline{S} = \underline{s}_m, \underline{R}_1 = \underline{r}_1) = p_{\underline{N}_2}(\underline{r}_2 - \underline{r}_1). \tag{4.56}$$

Since this does not depend on m again $\underline{r}_2$ is irrelevant.

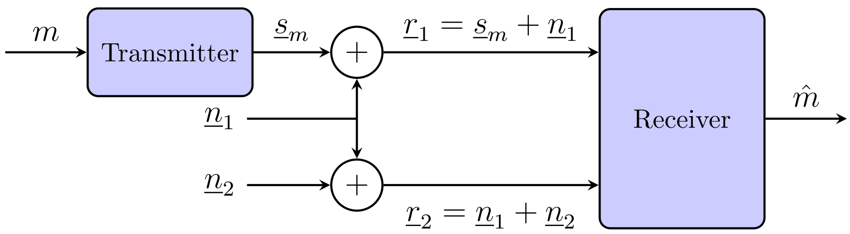

Figure 4.14: Now the vector $\underline{r}_2$ need not be irrelevant.

Example 4.7 In the last example (see Fig. 4.14) clearly

$$p_{\underline{R}_2}(\underline{r}_2|\underline{S} = \underline{s}_m, \underline{R}_1 = \underline{r}_1) = p_{\underline{N}_2}(\underline{r}_2 - \underline{r}_1 + \underline{s}_m) \tag{4.57}$$

and therefore $\underline{r}_2$ need not be irrelevant.

We will now analyze a simple but yet more specific case to see that $\underline{r}_2$ in general is not irrelevant in our last example. Assume that all the vectors are actually one-dimensional. There are two messages each having a-priori probability $1/2$. The corresponding signals are $s_1 = +1$ and $s_2 = -1$. For the noise variables, that are assumed to be Gaussian, the variances are

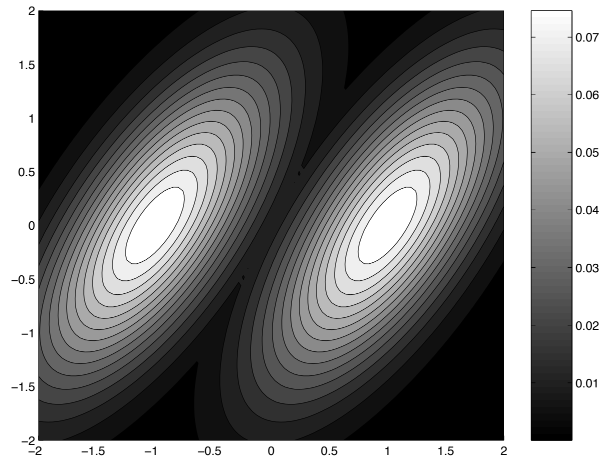

Figure 4.15: Contour plot of $\max_m \Pr\{M = m\} p_{R_1,R_2}(r_1, r_2|S = s_m)$.

$\sigma^2_{n_1} = \sigma^2_{n_2} = 1$. The mean values of the noise variables are both 0. Now we can consider for $-2 \leq r_1, r_2 \leq 2$ the decision variables

$$\Pr\{M = m\} p_{R_1,R_2}(r_1, r_2|S = s_m) \text{ for } m = 1, 2. \tag{4.58}$$

In Fig. 4.15 a contour plot is presented, which shows for each coordinate pair (r_1, r_2), the value $\max_m \Pr\{M = m\} p_{R_1,R_2}(r_1, r_2|S = s_m)$. Simple calculus shows that the optimum boundary of the decision regions is given by the straight line $r_2 = 2r_1$. Hence this boundary is not a *vertical* line and r_2 is not irrelevant.

Note that the condition in the theorem of irrelevance is sufficient but not always necessary. One can think of situations where the channel output $\underline{r}_2$ is irrelevant but still $p_{\underline{R}_2}(\underline{r}_2|\underline{S} = \underline{s}_m, \underline{R}_1 = \underline{r}_1)$ does depend on m. One such example is given in the table below. For the sake of simplicity we consider a discrete system. The possible channel output values are a and b for both outputs.

	$m = 1$	$m = 2$
$\Pr\{M = m, \underline{R} = (a, a)\}$	$2/16$	$1/16$
$\Pr\{M = m, \underline{R} = (a, b)\}$	$3/16$	$2/16$
$\Pr\{M = m, \underline{R} = (b, a)\}$	$1/16$	$2/16$
$\Pr\{M = m, \underline{R} = (b, b)\}$	$2/16$	$3/16$

The optimum receiver decides that $\hat{m} = 1$ if $R_1 = a$ and $\hat{m} = 2$ if $R_1 = b$ no matter what R_2 was. It can be checked on the other hand that, e.g., $2/5 = \Pr\{R_2 = a|M = 1, R_1 = a\} \neq \Pr\{R_2 = a|M = 2, R_1 = a\} = 1/3$, hence depends on M.

4.10.3 Theorem of reversibility

An important consequence of the theorem of irrelevance is the following result.

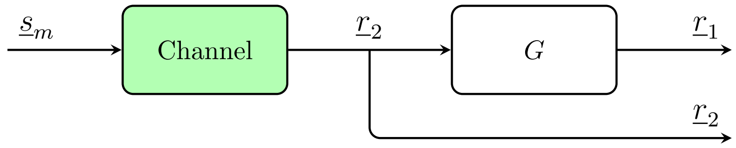

Figure 4.16: If G is reversible then $\underline{r}_2$ is irrelevant.

THEOREM 4.7 (Theorem of reversibility) *The minimum attainable probability of error is not affected by the introduction of a reversible operation at the output of a channel.*

Proof: Consider the system in Fig. 4.16. Assume that G is a reversible function. The idea of the proof is to show that, to make the optimum decision in (4.53), it is sufficient to use only $G(\underline{r}_2) = \underline{r}_1$. The theorem will be proven via the theorem of irrelevance, i.e., by showing that $p_{\underline{R}_2}(\underline{r}_2|\underline{S} = \underline{s}_m, \underline{R}_1 = \underline{r}_1)$ is independent of m.

Consider a certain $\underline{r}_2^*$ such that $\underline{r}_2^* \neq G^{-1}(\underline{r}_1)$. In this case, the probability $p_{\underline{R}_2}(\underline{r}_2^*|\underline{S} = \underline{s}_m, \underline{R}_1 = \underline{r}_1)$ is zero: given that $\underline{R}_1 = \underline{r}_1$, the only possible value for the random variable $\underline{R}_2$ is $G^{-1}(\underline{r}_1)$ (because of the reversibility of the function G). On the other hand, if $\underline{r}_2^* = G^{-1}(\underline{r}_1)$, $p_{\underline{R}_2}(\underline{r}_2^*|\underline{S} = \underline{s}_m, \underline{R}_1 = \underline{r}_1)$is one. This follows from the fact that $\underline{R}_1 = \underline{r}_1$ implies certainty on that $\underline{R}_2 = G^{-1}(\underline{r}_1) = \underline{r}_2$. Therefore, $p_{\underline{R}_2}(\underline{r}_2|\underline{S} = \underline{s}_m, \underline{R}_1 = \underline{r}_1)$ is solely determined by the values $\underline{r}_1$ and $\underline{r}_2$, i.e.,

$$p_{\underline{R}_2}(\underline{r}_2|\underline{S} = \underline{s}_m, \underline{R}_1 = \underline{r}_1) = p_{\underline{R}_2}(\underline{r}_2|\underline{R}_1 = \underline{r}_1), \tag{4.59}$$

which is equivalent to say that $p_{\underline{R}_2}(\underline{r}_2^*|\underline{S} = \underline{s}_m, \underline{R}_1 = \underline{r}_1)$ is independent of the message m. Thus, an optimum decision can be made from $\underline{r}_1$ only.

An alternative proof of the theorem of reversibility follows from observing that a receiver for $\underline{r}_1$ can be built by first recovering $\underline{r}_2$ from $\underline{r}_1$ (see Fig. 4.17). This is possible since the mapping G from $\underline{r}_2$ to $\underline{r}_1$ is reversible. Then an optimum receiver for $\underline{r}_2$ is used to determine $\hat{m}$. The receiver constructed in this way for $\underline{r}_1$ is optimum, thus a reversible operation does not (necessarily) lead to an increase of P_{e}.

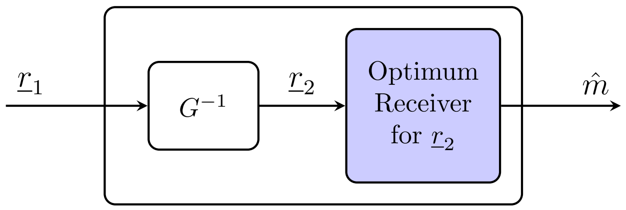

Figure 4.17: An optimum receiver for $\underline{r}_1$

□

Chapter 5

Waveform Channels

SUMMARY: All the topics discussed so far are necessary to analyse the AWGN waveform channel. In a waveform channel continuous-time waveforms are transmitted over a channel that adds continuous-time white Gaussian noise. We show in this chapter that such a waveform channel can be transformed into an Additive Gaussian Noise vector channel without loss of optimality. To each input waveform there corresponds a vector in what is called the signal space. It is possible to make an optimum decision based on the projection of the channel output waveform onto this signal space. The difference between this projection and the transmitted vector is a Gaussian noise vector which is spherically distributed.

5.1 System Description, Additive White Gaussian Noise

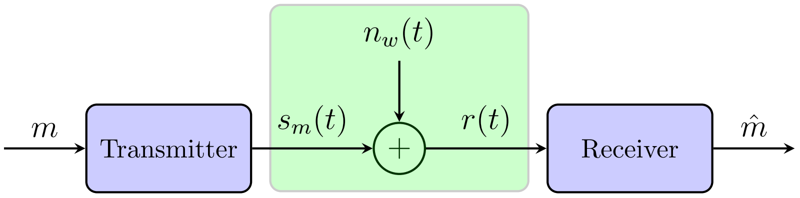

Figure 5.1: Communication of discrete messages over an AWGN channel.

The problem of optimal detection of waveforms in white noise is studied in this chapter. We will see that a waveform transmission problem can be transformed into a vector transmission problem. But we know already how to solve the vector transmission problem! Note that we are focusing on channel processing, and, as discussed before in Sec. 2.3.1, we consider transmission of **discrete messages**.

In a communication system based on a waveform channel (see Fig. 5.1) the channel input and output signals are waveforms.

TRANSMITTER The transmitter chooses a waveform $s_m(t)$ when message m is to be transmitted. The set of used waveforms is therefore $\{s_1(t), s_2(t), \ldots, s_{|\mathcal{M}|}(t)\}$. This waveform is input to the channel.

WAVEFORM CHANNEL The channel accepts the input waveform $s_m(t)$ and adds Gaussian noise $n_w(t)$ to it, i.e., for the received waveform $r(t)$ we get

$$r(t) = s_m(t) + n_w(t). \tag{5.1}$$

Note that this is the wideband additive Gaussian noise waveform channel as defined in Sec. 2.1.3. The noise $n_w(t)$ coming from the random process $N_w(t)$ is assumed to be stationary, Gaussian, zero-mean, and white. The autocorrelation function of the noise process is

$$R_{N_w}(t,s) \triangleq E[N_w(t)N_w(s)] = \frac{N_0}{2}\delta(t-s), \tag{5.2}$$

and consequently (see also Sec. 2.1.2), the noise power spectral density $S_{N_w}(f) = N_0/2$ for all f.

RECEIVER The receiver forms the estimate $\hat{m}$ based on the received waveform $r(t)$.

The waveform-channel system is what we actually want to study in the first part of this course reader. It is the basic model for digital communication. In the next sections we will show that a waveform channel is equivalent to a vector channel for which each component channel is an additive Gaussian noise channel. Since the noise process $N_w(t)$ is white, the component channels are independent and identical. We start by showing that the signal process can be represented in an equivalent vector form. Then we prove that the *relevant* noise can also be represented by a random vector.

5.2 Waveform Synthesis

We start by defining two important properties of waveforms: energy and orthogonality.

Definition 5.1 *The* energy *of a real waveform $x(t)$ is defined as*

$$E_x \triangleq \int_{-\infty}^{\infty} x^2(t)dt. \tag{5.3}$$

To get convinced that this is a reasonable definition assume that $x(t)$ is the voltage across (or the current through) a resistor of 1Ω. The total energy that is dissipated in this resistor is then equal to E_x.

Definition 5.2 *The waveforms $\varphi_i(t), i = 1, \ldots, N$ are said to be* ***orthogonal*** *if*

$$\int_{-\infty}^{\infty} \varphi_i(t)\varphi_j(t)dt \triangleq \begin{cases} E_i & \text{if } i = j \\ 0 & \text{if } i \neq j \end{cases}. \tag{5.4}$$

If $E_i = 1, \forall i$, the waveforms are said to be ***orthonormal***.

Now we will describe how to generate the waveforms $s_m(t)$ for $m = 1, 2, \ldots, |\mathcal{M}|$. This will be done based on Fig. 5.2. Signal vectors $s_m(t)$ can be synthesized at the transmitter by using an impulse generator and a bank of filters. When the message m is to be transmitted, the impulse generator produces the N impulses $s_{m1}\delta(t), s_{m2}\delta(t), \ldots, s_{mN}\delta(t)) =$ that are the inputs of N filters with impulse responses $\varphi_1(t), \varphi_2(t), \ldots, \varphi_N(t)$. The i-th filter is excited by an impulse $s_{mi}\delta(t)$. Therefore the output of this filter is $s_{mi}\varphi_i(t)$ for $i = 1, \ldots, N$. The filter outputs are finally added together to yield the waveform $s_m(t)$. We can write

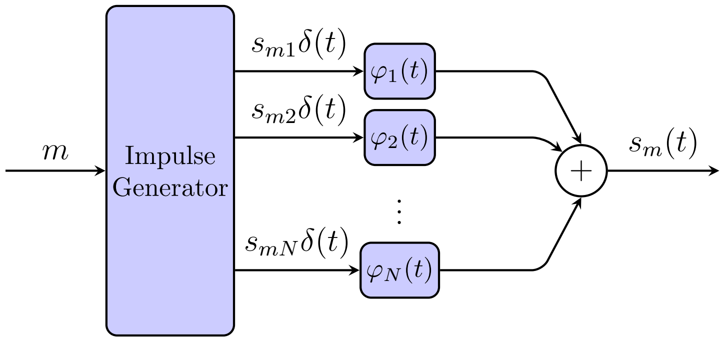

Figure 5.2: Waveform synthesis with a canonical transmitter.

$$s_m(t) = \sum_{i=1}^{N} s_{mi}\varphi_i(t), \text{ for } m \in \mathcal{M} = \{1, 2, \ldots, |\mathcal{M}|\}. \tag{5.5}$$

For reasons that will become clear later, we assume that the N *building-block waveforms* $\{\varphi_i(t), i = 1, \ldots, N\}$ are *orthonormal*. A transmitter that builds up the signals $s_m(t)$ by forming linear combinations of orthonormal functions is called *canonical*.

Example 5.1 In Fig. 5.3 four building-block waveforms are shown that are time-translated orthogonal pulses. Note that the energy in each pulse is $\int_{-\infty}^{\infty} \varphi_i^2(t)dt = 1$, and thus, the pulses are orthonormal.

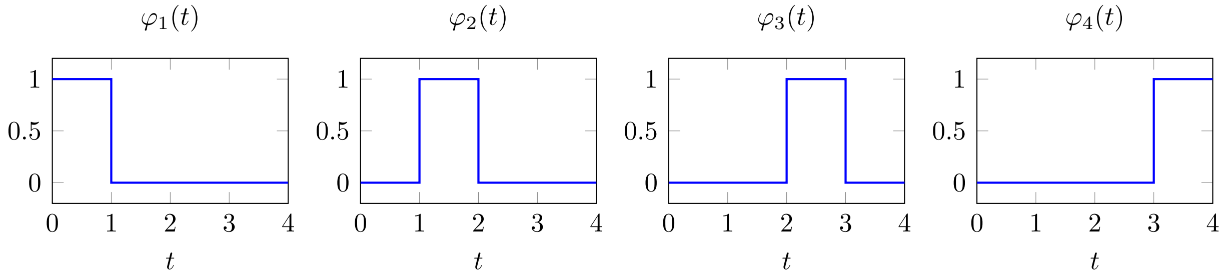

Figure 5.3: Example of orthonormal waveforms: time-translated pulses.

Example 5.2 In Fig. 5.4 five building-block waveforms are shown on a one-second time interval: a pulse with amplitude 1 and four sine and cosine waves whose amplitude is $\sqrt{2}$. the waveforms are zero outside this time interval. Note that all these waveforms are again mutually orthogonal and have unit energy. Therefore, these waveforms are orthonormal.

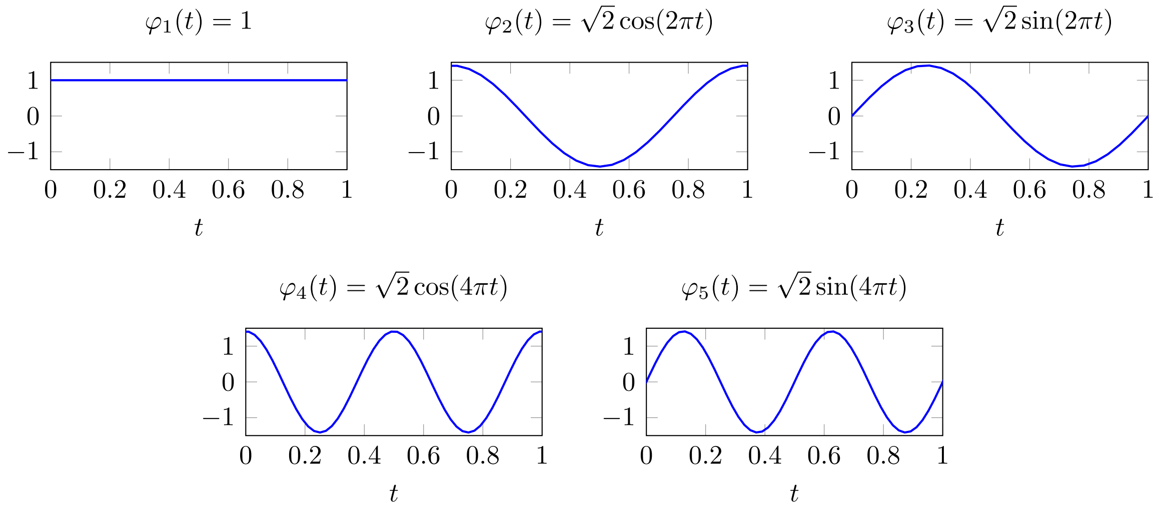

Figure 5.4: Example of orthonormal waveforms: a DC-pulse and four sine and cosine waves.

5.3 The Gram-Schmidt Orthogonalization Procedure

As we will show below, it is not so difficult to construct an orthonormal basis (i.e., a set of building-block waveforms) for a given set of *finite-energy* signaling waveforms. Therefore, without loss of generality, we can consider the canonical transmitter shown in Fig. 5.2. We shall soon see that the number of building blocks (N) used to generate the waveforms $s_m(t)$ is always smaller than the number of signals ($|\mathcal{M}|$).

THEOREM 5.1 (Gram-Schmidt) *For an arbitrary signal set, i.e., a set of waveforms* $\{s_1(t),\, s_2(t),\, \dots, s_{|\mathcal{M}|}(t)\}$*, we can construct a set of* $N \le |\mathcal{M}|$ *building-block waveforms* $\{\varphi_1(t),\, \varphi_2(t),\, \dots, \varphi_N(t)\}$ *and find coefficients* s_{mi} *such that for* $m = 1, 2, \dots, |\mathcal{M}|$ *the signals can be synthesized as* $s_m(t) = \sum_{i=1}^{N} s_{mi}\varphi_i(t)$.

We will only prove the result for signal sets with signals $s_m(t) \not\equiv 0$ for all $m \in \mathcal{M}$. The statement then also should hold for sets that do contain at least one all-zero signal.
Proof: The proof is based on induction.

1. First we will show that the induction hypothesis holds for one signal, i.e., for $|\mathcal{M}| = 1$. Therefore consider $s_1(t)$ and take

$$\varphi_1(t) = \frac{s_1(t)}{\sqrt{E_1}} \text{ with } E_1 = \int_{-\infty}^{\infty} s_1^2(t)dt. \tag{5.6}$$

   Note that by doing so

$$\int_{-\infty}^{\infty} \varphi_1^2(t)dt = \int_{-\infty}^{\infty} \frac{1}{E_1} s_1^2(t)dt = 1, \tag{5.7}$$

i.e., $\varphi_1(t)$ has unit energy (is normal). Since $s_1(t) = \sqrt{E_1}\varphi_1(t)$ the coefficient $s_{11} = \sqrt{E_1}$.

2. Now suppose that induction hypothesis holds for $m-1 \geq 1$ signals. Thus there exists an orthonormal basis $\varphi_1(t), \varphi_2(t), \ldots, \varphi_{n-1}(t)$ for the signals $s_1(t), s_2(t), \ldots, s_{m-1}(t)$ with $n-1 \leq m-1$. Now consider the next signal $s_m(t)$ and an auxiliary signal $\theta_m(t)$ which is defined as follows:

$$\theta_m(t) \triangleq s_m(t) - \sum_{i=1}^{n-1} s_{mi}\varphi_i(t) \tag{5.8}$$

with

$$s_{mi} = \int_{-\infty}^{\infty} s_m(t)\varphi_i(t)dt \text{ for } i = 1, 2, \ldots, n-1. \tag{5.9}$$

We can distinguish between two cases now:

(a) If $\theta_m(t) \equiv 0$ then $s_m(t) = \sum_{i=1}^{n-1} s_{mi}\varphi_i(t)$ and the induction hypothesis also holds for m signals.

(b) If on the other hand $\theta_m(t) \not\equiv 0$ then take a new building-block waveform

$$\varphi_n(t) = \frac{\theta_m(t)}{\sqrt{E_{\theta_m}}} \text{ with } E_{\theta_m} = \int_{-\infty}^{\infty} \theta_m^2(t)dt. \tag{5.10}$$

By doing so

$$\int_{-\infty}^{\infty} \varphi_n^2(t)dt = \int_{-\infty}^{\infty} \frac{1}{E_{\theta_m}}\theta_m^2(t)dt = 1, \tag{5.11}$$

i.e., also $\varphi_n(t)$ has unit energy.
Moreover for all $i = 1, 2, \ldots, n-1$

$$\begin{aligned}
\int_{-\infty}^{\infty} \varphi_n(t)\varphi_i(t)dt &= \int_{-\infty}^{\infty} \frac{1}{\sqrt{E_{\theta_m}}}\theta_m(t)\varphi_i(t)dt \\
&= \frac{1}{\sqrt{E_{\theta_m}}}\left(\int_{-\infty}^{\infty} s_m(t)\varphi_i(t)dt - \int_{-\infty}^{\infty}\sum_{j=1}^{n-1} s_{mj}\varphi_j(t)\varphi_i(t)dt\right) \\
&= \frac{1}{\sqrt{E_{\theta_m}}}\left(s_{mi} - \sum_{j=1}^{n-1} s_{mj}\int_{-\infty}^{\infty}\varphi_j(t)\varphi_i(t)dt\right) \\
&= \frac{1}{\sqrt{E_{\theta_m}}}(s_{mi} - s_{mi}) = 0,
\end{aligned} \tag{5.12}$$

and therefore $\varphi_n(t)$ is orthogonal to all $\varphi_i(t)$.
Note that now

$$\begin{aligned} s_m(t) &= \theta_m(t) + \sum_{i=1}^{n-1} s_{mi}\varphi_i(t) \\ &= \sqrt{E_{\theta_m}}\varphi_n(t) + \sum_{i=1}^{n-1} s_{mi}\varphi_i(t) = \sum_{i=1}^{N} s_{mi}\varphi_i(t) \end{aligned} \tag{5.13}$$

with $s_{mn} = \sqrt{E_{\theta_m}}$. Thus also for m signals there exists an orthonormal basis with $n \leq m$ building-block waveforms. Therefore the induction hypothesis also holds for m signals.

$\square$

It should be noted that, when using the Gram-Schmidt procedure, any ordering of the signals other than $s_1(t), s_2(t), \ldots, s_{|\mathcal{M}|}(t)$ will yield a basis, i.e., a set of building-block waveforms, of the same dimensionality, however in general with different building-block waveforms.

We will next discuss an example in which we actually carry out the Gram-Schmidt procedure for a given set of waveforms.

Example 5.3 Consider the three waveforms $s_m(t), m = 1, 2, 3$, shown in Fig. 5.5. We first

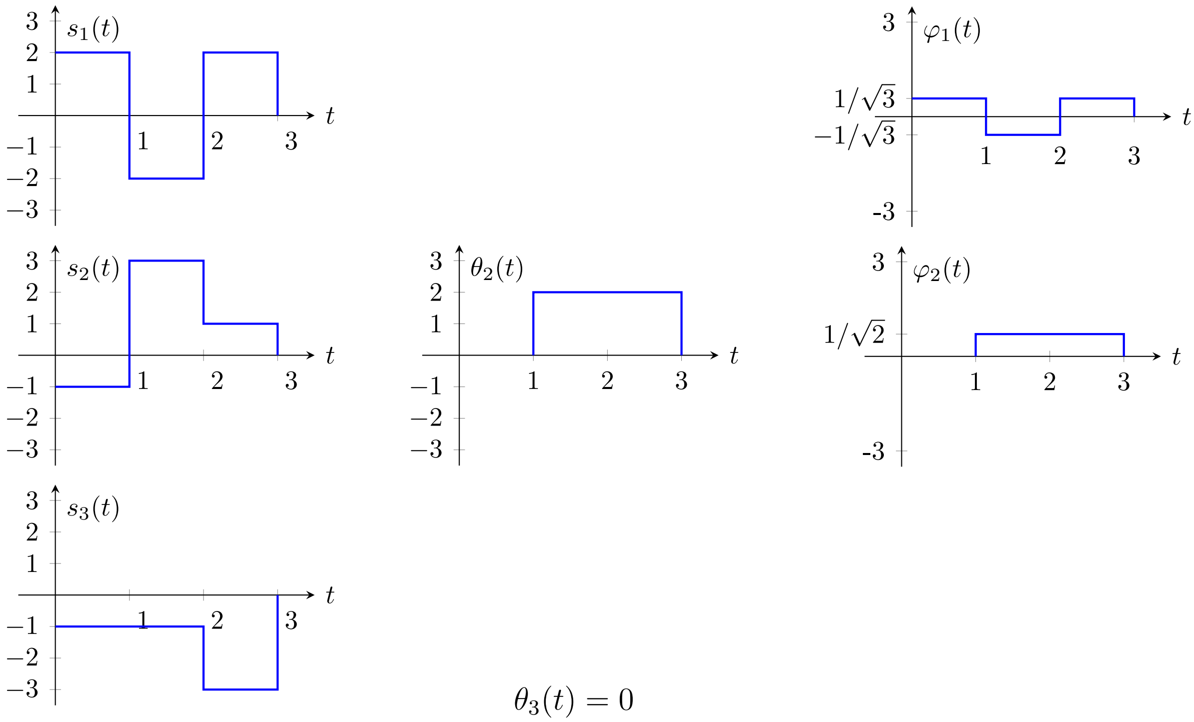

Figure 5.5: Gram-Schmidt procedure. This set of waveforms $\{s_1(t), s_2(t), s_3(t)\}$ leads to the vector diagram in Fig. 5.6.

determine the energy E_1 of the first signal $s_1(t)$

$$E_1 = 4 + 4 + 4 = 12. \tag{5.14}$$

Therefore the first building-block waveform $\varphi_1(t)$ is

$$\varphi_1(t) = \frac{s_1(t)}{\sqrt{E_1}} = \frac{s_1(t)}{2\sqrt{3}}, \text{ and thus, } s_{11} = 2\sqrt{3}. \tag{5.15}$$

Now we continue with the second signal $s_2(t)$. First we determine the projection s_{21} of $s_2(t)$ on the first dimension, i.e., the dimension that corresponds to $\varphi_1(t)$:

$$s_{21} = \int_{-\infty}^{\infty} s_2(t)\varphi_1(t)dt = \frac{1}{\sqrt{3}}(-1 - 3 + 1) = -\sqrt{3}. \tag{5.16}$$

hence the auxiliary signal $\theta_2(t)$ is now

$$\theta_2(t) = s_2(t) + \sqrt{3}\varphi_1(t). \tag{5.17}$$

Next we determine the energy E_{θ_2} of the auxiliary signal $\theta_2(t)$:

$$E_{\theta_2} = 4 + 4 = 8, \tag{5.18}$$

and the second building-block waveform $\varphi_2(t)$ is

$$\varphi_2(t) = \frac{\theta_2(t)}{\sqrt{E_{\theta_2}}} = \frac{\theta_2(t)}{2\sqrt{2}}. \tag{5.19}$$

Now we obtain for the signal $s_2(t)$:

$$\begin{aligned} s_2(t) &= \theta_2(t) - \sqrt{3}\varphi_1(t) \\ &= 2\sqrt{2}\varphi_2(t) - \sqrt{3}\varphi_1(t), \text{ thus } s_{22} = 2\sqrt{2}. \end{aligned} \tag{5.20}$$

For the third signal $s_3(t)$ we can now determine the projections s_{31} and s_{32} and the auxiliary signal $\theta_3(t)$:

$$\begin{aligned} s_{31} &= \int_{-\infty}^{\infty} s_3(t)\varphi_1(t)dt = \frac{1}{\sqrt{3}}(-1+1-3) = -\sqrt{3} \\ s_{32} &= \int_{-\infty}^{\infty} s_3(t)\varphi_2(t)dt = \frac{1}{\sqrt{2}}(-1-3) = -2\sqrt{2} \text{ hence} \\ \theta_3(t) &= s_3(t) + \sqrt{3}\varphi_1(t) + 2\sqrt{2}\varphi_2(t) \equiv 0. \end{aligned} \tag{5.21}$$

Since this auxiliary signal is always 0, we can express the third signal $s_3(t)$ in terms of $\varphi_1(t)$ and $\varphi_2(t)$ as follows:

$$s_3(t) = -\sqrt{3}\varphi_1(t) - 2\sqrt{2}\varphi_2(t), \tag{5.22}$$

hence the coefficients corresponding to $s_3(t)$ are

$$\begin{aligned} s_{31} &= -\sqrt{3} \text{ and} \\ s_{32} &= -2\sqrt{2}. \end{aligned} \tag{5.23}$$

We have now obtained three vectors of coefficients, one for each signal:

$$\begin{aligned} \underline{s}_1 &= (s_{11}, s_{12}) = (2\sqrt{3}, 0), \\ \underline{s}_2 &= (s_{21}, s_{22}) = (-\sqrt{3}, 2\sqrt{2}), \text{ and} \\ \underline{s}_3 &= (s_{31}, s_{32}) = (-\sqrt{3}, -2\sqrt{2}). \end{aligned} \tag{5.24}$$

The vectors obtained in (5.24) are depicted in Fig. 5.6. This can be seen as a geometric interpretation of the waveforms. This will be discussed in more detail in Sec. 5.4. Note that the Gram-Schmidt procedure always yields a basis with the smallest possible dimension. In the example above, $N = 2 < |\mathcal{M}| = 3$.

One should also note that a given set of signals can be expanded in many different orthogonal sets of building-block waveforms, possibly with a larger dimension. What remains constant is the geometrical configuration of the vector representations of the signals.

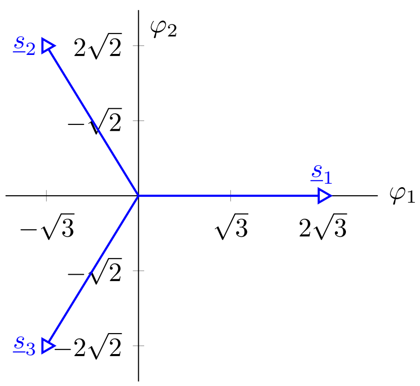

Figure 5.6: A vector representation of the signals $s_m(t), m = 1, 2, 3$ of Fig. 5.5.

For example, the procedure above applied to the waveforms $s_2(t)$, $s_1(t)$ and $s_3(t)$ (in that order) will lead to a different set of building-block waveforms. The resulting vector representation of the signals, however, will remain the same as the one in Fig. 5.6.

5.4 Geometric Interpretation of Signals

In the previous section we have seen that for each set of waveforms $s_1(t), s_2(t), \ldots, s_{|\mathcal{M}|}(t)$ we can construct an orthonormal basis such that each waveform $s_m(t)$ for $m \in \mathcal{M}$ is a linear combination of the building-block waveforms $\varphi_1(t), \varphi_2(t), \ldots, \varphi_N(t)$ that form the basis, i.e.,

$$s_m(t) = \sum_{i=1}^{N} s_{mi}\varphi_i(t). \tag{5.25}$$

Thus, each waveform $s_m(t)$ can be represented using a *vector* with N coefficients

$$\underline{s}_m = (s_{m1}, s_{m2}, \ldots, s_{mN}). \tag{5.26}$$

The coefficients s_{mi} are the projections of the waveform $s_m(t)$ on the building-block waveforms $\varphi_i(t), i = 1, \ldots, N$. The set of waveforms $\{s_1(t), s_2(t), \ldots, s_{|\mathcal{M}|}(t)\}$ can therefore be represented as a set of vectors $\{\underline{s}_1, \underline{s}_2, \ldots, \underline{s}_{|\mathcal{M}|}\}$ in an N-dimensional space. This space is called the *signal space*. The set of vectors $\{\underline{s}_1, \underline{s}_2, \ldots, \underline{s}_{|\mathcal{M}|}\}$ is called the *signal structure* or *signal constellation*.

Example 5.4 Consider for $m = 1, 2, 3, 4$ the set of phase-modulated transmitter waveforms

$$s_m(t) = \begin{cases} \sqrt{\frac{2E_s}{T}}\cos(2\pi f_0 t + \frac{m\pi}{2}) & \text{for } 0 \le t < T \text{ and} \\ 0 & \text{elsewhere,} \end{cases} \tag{5.27}$$

where f_0 is an integral multiple of $1/T$. Note that

$$\cos\left(2\pi f_0 t + \frac{m\pi}{2}\right) = \cos(2\pi f_0 t)\cos\frac{m\pi}{2} - \sin(2\pi f_0 t)\sin\frac{m\pi}{2}. \tag{5.28}$$

If we now take as building-block waveforms

$$\begin{aligned} \varphi_1(t) &= \sqrt{2/T}\cos(2\pi f_0 t), \text{ and} \\ \varphi_2(t) &= \sqrt{2/T}\sin(2\pi f_0 t), \end{aligned} \tag{5.29}$$

for $0 \le t < T$ and zero elsewhere, we obtain the following vector-representations for the signals:

$$\begin{aligned} \underline{s}_1 &= (0, -\sqrt{E_s}), \\ \underline{s}_2 &= (-\sqrt{E_s}, 0), \\ \underline{s}_3 &= (0, \sqrt{E_s}), \\ \underline{s}_4 &= (\sqrt{E_s}, 0). \end{aligned} \tag{5.30}$$

These vectors are depicted in Fig. 5.7.

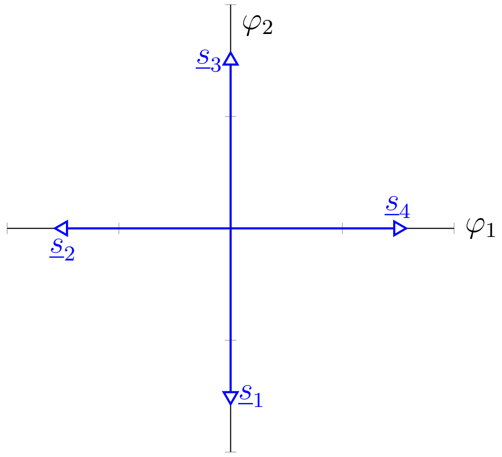

Figure 5.7: Four signals represented as vectors in a two-dimensional space. The length of all signal vectors is $\sqrt{E_s}$.

Example 5.5 Consider now the four waveforms shown in Fig. 5.8 and the basis $\{\varphi_1(t), \varphi_2(t)\}$ shown in the same figure. It can be shown that the signal structure (with respect to this basis) is the same as the signals defined in (5.27). We will later show in this chapter that both sets of waveforms also have identical error behavior.

5.5 Recovery of Signal Vectors

We have seen in Sec. 5.2 how to synthesize the waveform $s_m(t)$ for an $m \in \mathcal{M}$ if we know the corresponding signal vector $\underline{s}_m$ and the basis $\{\varphi_1(t), \varphi_2(t), \ldots, \varphi_N(t)\}$. On the other hand it is also easy to determine the signal vector $\underline{s}_m$ from the waveform $s_m(t)$. To see this note that

$$\begin{aligned}\int_{-\infty}^{\infty} s_m(t)\varphi_i(t)dt &= \int_{-\infty}^{\infty} \left(\sum_{j=1}^{N} s_{mj}\varphi_j(t) \right) \varphi_i(t)dt \\ &= \sum_{j=1}^{N} s_{mj} \int_{-\infty}^{\infty} \varphi_j(t)\varphi_i(t)dt = \sum_{j=1}^{N} s_{mj}\delta_{ji} = s_{mi} \end{aligned} \tag{5.31}$$

because of the orthonormality of the building-block waveforms. In our derivation we used the Kronecker delta function which is defined as

$$\delta_{ji} \triangleq \begin{cases} 1 & \text{if } j = i \\ 0 & \text{if } j \neq i. \end{cases} \tag{5.32}$$

If we carry out (5.31) for all $i = 1, \ldots, N$ we find all coefficients s_{mi} of the vector $\underline{s}_m = (s_{m1}, s_{m2}, \ldots, s_{mN})$. The block diagram in Fig. 5.9 could be used to detect which of the waveforms $s_m(t)$ with $m \in \mathcal{M}$ was present at its input. It is waveform $s_m(t)$ if the vector $\underline{s}_m$ appears at the outputs of the circuit. Note that it is definitely easier to check an N-dimensional vector than a waveform for $-\infty < t < \infty$!

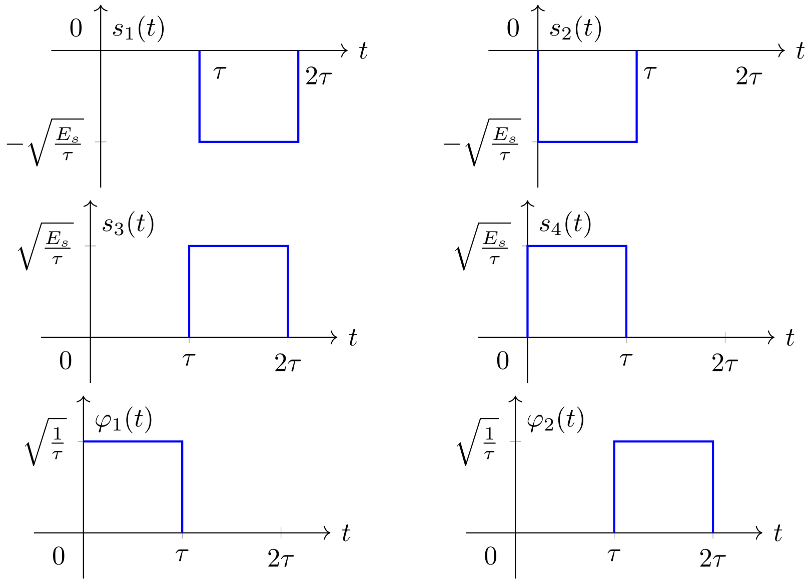

Figure 5.8: Another set of waveforms that leads to the vector diagram in Fig. 5.7 when the basis $\varphi_1(t)$ and $\varphi_2(t)$ shown above is used.

5.6 Irrelevant Data

We are now ready to discuss a receiver for the waveform communication system in Fig. 5.1. Such a receiver observes

$$r(t) = s_m(t) + n_w(t) \tag{5.33}$$

for some $m \in \mathcal{M}$, and where $n_w(t)$ is a realization of a white Gaussian noise process. If the noise $n_w(t)$ would be zero everywhere we could use the circuit in Fig. 5.9 to detect which waveform $s_m(t)$ was actually sent by the transmitter. However, in practice, a noisy version of the vector $\underline{s}_m$ will be produced by the channel. This is due to the noise $n_w(t)$. In what follows we will show that it is possible to make an optimal decision based only on this noisy version of the signal vector $\underline{s}_m$. This noisy version version of $\underline{s}_m$ is the N-dimensional vector $\underline{r}_1 = (r_1, r_2, \ldots, r_N)$ whose components are determined as follows (see Fig. 5.10):

$$r_i \triangleq \int_{-\infty}^{\infty} r(t)\varphi_i(t)dt \text{ for } i = 1, 2, \ldots, N. \tag{5.34}$$

Since $r(t) = s_m(t) + n_w(t)$ we have that

$$\begin{aligned} r_i &= \int_{-\infty}^{\infty} r(t)\varphi_i(t)dt \\ &= \int_{-\infty}^{\infty} s_m(t)\varphi_i(t)dt + \int_{-\infty}^{\infty} n_w(t)\varphi_i(t)dt = s_{mi} + n_i, \end{aligned} \tag{5.35}$$

with

$$n_i \triangleq \int_{-\infty}^{\infty} n_w(t)\varphi_i(t)dt. \tag{5.36}$$

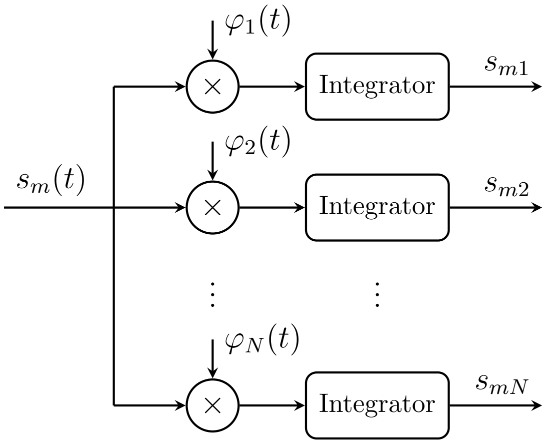

Figure 5.9: Recovering the vector $\underline{s}_m = (s_{m1}, s_{m2}, \ldots, s_{mN})$ from the waveform $s_m(t)$.

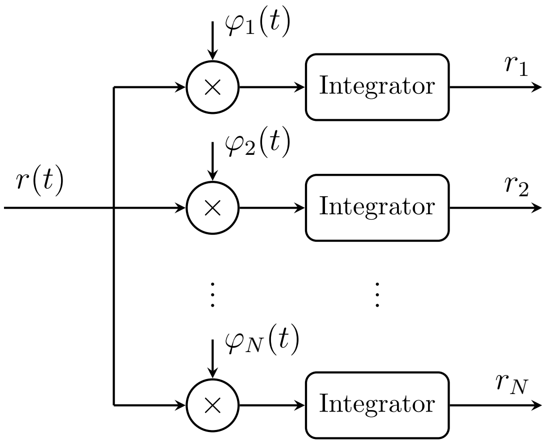

Figure 5.10: Forming the vector $\underline{r}_1 = (r_1, r_2, \ldots, r_N)$ from the received waveform $r(t)$.

Hence also

$$\underline{r}_1 = \underline{s}_m + \underline{n} \tag{5.37}$$

with $\underline{r}_1 = (r_1, r_2, \ldots, r_N)$, $\underline{s}_m = (s_{m1}, s_{m2}, \ldots, s_{mN})$, and $\underline{n} = (n_1, n_2, \ldots, n_N)$.

It is our objective to prove that the optimum receiver only needs $\underline{r}_1$ *for the determination of* $\hat{m}$. The waveforms that correspond to the vectors $\underline{n}$ and $\underline{r}_1$ are defined to be

$$\begin{aligned}
n(t) &\stackrel{\Delta}{=} \sum_{i=1}^{N} n_i \varphi_i(t) \text{ and} \\
r_1(t) &\stackrel{\Delta}{=} \sum_{i=1}^{N} r_i \varphi_i(t) = \sum_{i=1}^{N} (s_{mi} + n_i) \varphi_i(t) \\
&= \sum_{i=1}^{N} s_{mi} \varphi_i(t) + \sum_{i=1}^{N} n_i \varphi_i(t) = s_m(t) + n(t)
\end{aligned} \tag{5.38}$$

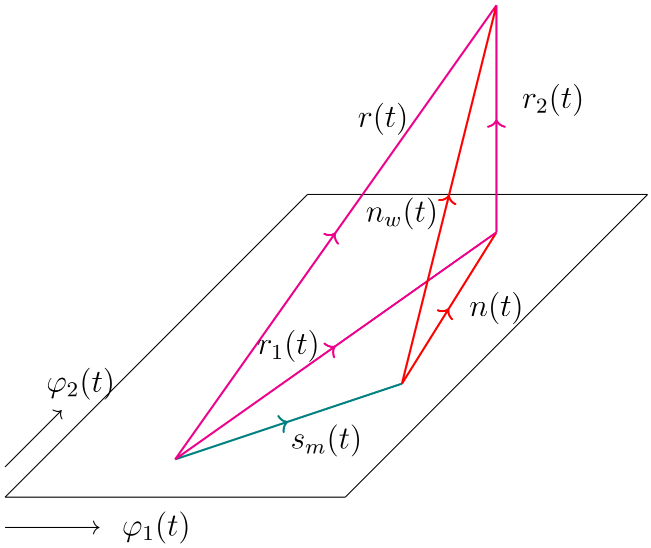

Figure 5.11: Waveforms $r(t)$ and $n_w(t)$ and their projections onto the signal space. Note that both the signal $s_m(t)$ and $r_1(t)$ are in the signal space while $r_2(t)$ is perpendicular to the signal space.

since $s_m(t) = \sum_{i=1}^{N} s_{mi}\varphi_i(t)$. These waveforms can be considered as projections of the waveforms $n_w(t)$ and $r(t)$ onto the signal space, i.e., the space with basis $\{\varphi_i(t), i = 1, \ldots, N\}$, see Fig. 5.11.

Now we can consider the difference $r_2(t)$ between the actually received signal $r(t)$ and the projection $r_1(t)$ of $r(t)$ onto the signal space. This $r_2(t)$ is the part of the received waveform that can not be expressed as a linear combination of building-block waveforms. It is defined as

$$\begin{aligned} r_2(t) &\stackrel{\Delta}{=} r(t) - r_1(t) \\ &= (s_m(t) + n_w(t)) - (s_m(t) + n(t)) = n_w(t) - n(t). \end{aligned} \tag{5.39}$$

This waveform only depends on the realization $n_w(t)$ of the noise process. It is also the part of the noise $n_w(t)$ that can not be expressed as a linear combination of building-block waveforms.

Note first that a receiver can make optimum decisions also from $r_1(t)$ and $r_2(t)$ by the *theorem of reversibility* (Theorem 4.7). This can be proved by assuming that the function G in Theorem 4.7 is the decomposition of $r(t)$ into $r_1(t)$ and $r_2(t)$, i.e., $G\{r(t)\} = (r_1(t), r_2(t))$. We can see that G has a inverse given by $G^{-1}\{(r_1(t), r_2(t))\} = r_1(t) + r_2(t)$, since $r(t) = r_1(t) + r_2(t)$. Therefore, by Theorem 4.7, the receiver can make optimum decisions only based on $r_1(t)$ and $r_2(t)$, i.e., based on $G\{r(t)\}$ instead of $r(t)$. We will next show however that the waveform $r_2(t)$ is *irrelevant* given $r_1(t)$. First note that $r_2(t)$ is a result from linear operations (addition, integration) on the outcome of the Gaussian process $N_w(t)$. Therefore process $R_2(t)$ is also Gaussian.

Consider any finite set of, say Q, samples from $r_2(t)$. Represent this set of samples as a vector, i.e.,

$$\underline{r}_2 = (r_2(t_1), r_2(t_2), \ldots, r_2(t_Q)). \tag{5.40}$$

Now we can write

$$\begin{aligned} p_{\underline{R}_2}(\underline{r}_2|\underline{S} = \underline{s}_m, \underline{R}_1 = \underline{r}_1) &\stackrel{(a)}{=} p_{\underline{R}_2}(\underline{r}_2|\underline{S} = \underline{s}_m, \underline{N} = \underline{r}_1 - \underline{s}_m) \\ &= \frac{p_{\underline{R}_2,\underline{N},\underline{S}}(\underline{r}_2, \underline{r}_1 - \underline{s}_m, \underline{s}_m)}{p_{\underline{N},\underline{S}}(\underline{r}_1 - \underline{s}_m, \underline{s}_m)} \\ &\stackrel{(b)}{=} \frac{p_{\underline{R}_2,\underline{N}}(\underline{r}_2, \underline{r}_1 - \underline{s}_m) \Pr\{\underline{S} = \underline{s}_m\}}{p_{\underline{N}}(\underline{r}_1 - \underline{s}_m) \Pr\{\underline{S} = \underline{s}_m\}} \\ &= \frac{p_{\underline{R}_2,\underline{N}}(\underline{r}_2, \underline{r}_1 - \underline{s}_m)}{p_{\underline{N}}(\underline{r}_1 - \underline{s}_m)} = p_{\underline{R}_2}(\underline{r}_2|\underline{N} = \underline{r}_1 - \underline{s}_m). \end{aligned} \tag{5.41}$$

Equality (a) follows from the fact that, since $\underline{r}_1 = \underline{s}_m + \underline{n}$, the pair $\underline{s}_m, \underline{r}_1$ determines the pair $\underline{s}_m, \underline{n}$ and vice versa. Since the noise vector $\underline{n}$ and the vector $\underline{r}_2$ depend only on the outcome $n_w(t)$ of the white Gaussian noise process $N_w(t)$ which is independent of the signal vector $\underline{S}$, we get equality (b).

From (5.41) we see that we can ignore the *vector* $\underline{r}_2$ when the random vector $\underline{R}_2$ is independent of the random vector $\underline{N}$. The *process* $R_2(t)$ is irrelevant if for each finite set of samples $\underline{r}_2$ the random vector $\underline{R}_2$ is independent of the random vector $\underline{N}$, in other words if the process $R_2(t)$ is statistically independent of the process $N(t)$.

First note that both $r_2(t)$ and $n(t)$ are the result from linear operations (addition, integration) on the outcome of the Gaussian process $n_w(t)$. Therefore processes $R_2(t)$ and $N(t)$ are *jointly Gaussian*. The processes $N(t)$ and $R_2(t)$ are now statistically independent if for all s and t the covariance

$$E[(N(s) - E[N(s)])(R_2(t) - E[R_2(t)])] = 0. \tag{5.42}$$

Since $E[N(s)] = 0$ and $E[R_2(t)] = 0$ we have to show that

$$E[N(s)R_2(t)] = 0 \tag{5.43}$$

for all s and t. Since

$$E[N(s)R_2(t)] = E\left[R_2(t) \sum_{i=1}^{N} N_i \varphi_i(s)\right] = \sum_{i=1}^{N} E[N_i R_2(t)] \varphi_i(s) \tag{5.44}$$

we only need to show that

$$E[N_i R_2(t)] = 0 \tag{5.45}$$

for all $i = 1, \ldots, N$ and all t. Furthermore

$$\begin{aligned} E[N_i R_2(t)] &= E[N_i(N_w(t) - N(t))] \\ &= E[N_i N_w(t)] - E[N_i N(t)]. \end{aligned} \tag{5.46}$$

Now

$$\begin{aligned} E[N_i N_w(t)] &= E\left[\left(\int_{-\infty}^{\infty} N_w(\alpha)\varphi_i(\alpha)d\alpha\right) N_w(t)\right] \\ &= \int_{-\infty}^{\infty} E\left[N_w(\alpha)N_w(t)\right]\varphi_i(\alpha)d\alpha \\ &= \int_{-\infty}^{\infty} \frac{N_0}{2}\delta(t-\alpha)\varphi_i(\alpha)d\alpha = \frac{N_0}{2}\varphi_i(t), \end{aligned} \tag{5.47}$$

and

$$E[N_i N(t)] = E\left[N_i \sum_{j=1}^{N} N_j \varphi_j(t)\right] = \sum_{j=1}^{N} E[N_i N_j]\varphi_j(t) \tag{5.48}$$

where

$$\begin{aligned} E[N_i N_j] &= E\left[\int_{-\infty}^{\infty}\int_{-\infty}^{\infty} N_w(\alpha)N_w(\beta)\varphi_i(\alpha)\varphi_j(\beta)d\alpha d\beta\right] \\ &= \int_{-\infty}^{\infty}\int_{-\infty}^{\infty} E[N_w(\alpha)N_w(\beta)]\varphi_i(\alpha)\varphi_j(\beta)d\alpha d\beta \\ &= \int_{-\infty}^{\infty}\int_{-\infty}^{\infty} \frac{N_0}{2}\delta(\alpha-\beta)\varphi_i(\alpha)\varphi_j(\beta)d\alpha d\beta \\ &= \int_{-\infty}^{\infty} \frac{N_0}{2}\varphi_i(\alpha)\varphi_j(\alpha)d\alpha = \frac{N_0}{2}\delta_{ij}. \end{aligned} \tag{5.49}$$

Therefore

$$E[N_i N(t)] = \sum_{j=1}^{N} E[N_i N_j]\varphi_j(t) = \sum_{j=1}^{N} \frac{N_0}{2}\delta_{ij}\varphi_j(t) = \frac{N_0}{2}\varphi_i(t). \tag{5.50}$$

If we now substitute (5.47) and (5.50) into (5.46) we obtain that

$$E[N_i R_2(t)] = E[N_i N_w(t)] - E[N_i N(t)] = \frac{N_0}{2}\varphi_i(t) - \frac{N_0}{2}\varphi_i(t) = 0 \tag{5.51}$$

for all $i = 1, \ldots, N$ and t, i.e., we have proved that $N(t)$ and $R_2(t)$ are statistically independent.

RESULT 5.2 *We have proved that $r_2(t)$ is irrelevant and an optimum receiver for the waveform channel only needs to consider the relevant output vector $\underline{r}_1$ to estimate which message and corresponding waveform was transmitted.*

5.7 Joint Density of the Relevant Noise

In the previous section we have seen that the only relevant signal for the receiver is $\underline{r}_1$. Recall that

$$\underline{r}_1 = \underline{s}_m + \underline{n} \tag{5.52}$$

with $\underline{n} = (n_1, n_2, \ldots, n_N)$. Therefore the relevant signal $\underline{r}_1$ is a noisy version of the transmitted vector $\underline{s}_m$ if message m is to be conveyed over the channel. The noise components are jointly Gaussian, since they result from linear operations on the Gaussian process $N_w(t)$. Note that for $i = 1, \ldots, N$

$$E[N_i] = E\left[\int_{-\infty}^{\infty} N_w(t)\varphi_i(t)dt\right] = \int_{-\infty}^{\infty} E\left[N_w(t)\right]\varphi_i(t)dt = 0 \tag{5.53}$$

and for $i = 1, \ldots, N$ and $j = 1, \ldots, N$ by (5.49)

$$E[N_i N_j] = \begin{cases} \frac{N_0}{2} & \text{if } i = j \\ 0 & \text{if } i \neq j. \end{cases} \tag{5.54}$$

RESULT 5.3 *The joint density function of the relevant noise vector* $\underline{n}$ *is*

$$p_{\underline{N}}(\underline{n}) = \frac{1}{(\pi N_0)^{N/2}} \exp\left(-\frac{\|\underline{n}\|^2}{N_0}\right), \tag{5.55}$$

hence, the noise is **spherically symmetric** *and depends on the magnitude but not on the direction of* $\underline{n}$. *The noise projected on each direction has variance* $\frac{N_0}{2}$.

5.8 Relation Between Waveform and Vector Channels

We have seen that to each set of waveforms there corresponds a set of building-block waveforms such that each waveform is a linear combination of these building-block waveforms. The waveform $s_m(t)$ can be constructed from the vector $\underline{s}_m$ of coefficients in this linear combination and we can also say that instead of the waveform $s_m(t)$ the vector $\underline{s}_m$ is transmitted over the channel.

We have also seen that an optimum receiver only needs to consider the projections of the received signal $r(t)$ onto the building-block waveforms. It can base its decision only on what is called the relevant vector $\underline{r}_1$. It is important to note that these conclusions depend on the fact that the channel adds white Gaussian noise to the input waveform.

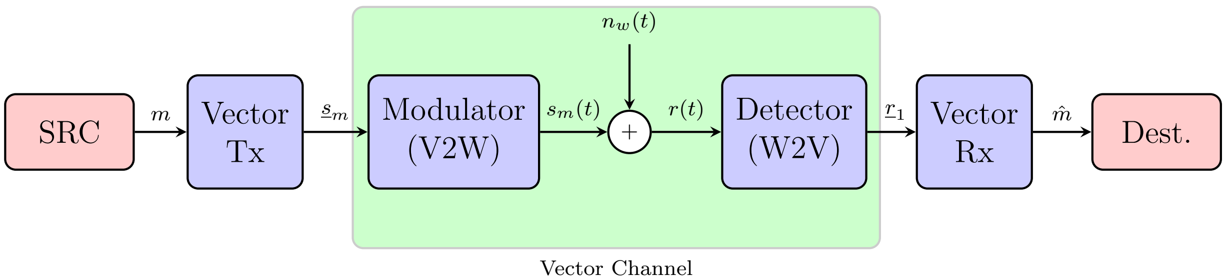

Figure 5.12: Reduction of a waveform channel into a vector channel.

From the above we may conclude that transmission over a waveform channel for which the noise is additive white Gaussian can actually be considered as transmission over a vector channel as shown in Fig. 5.12. A vector transmitter produces the vector $\underline{s}_m$ when message m is generated by the source. This vector is transformed into the waveform $s_m(t)$ by the modulator, i.e., via a vector to waveform (V2W) conversion. The waveform $s_m(t)$ is input to the channel that adds noise. The detector or demodulator operates on the received waveform $r(t)$ and forms the relevant vector $\underline{r}_1$ via a waveform to vector (W2V) operation. A vector receiver determines the estimate $\hat{m}$ of the message that was sent from $\underline{r}_1$. The combination modulator - waveform channel - detector is an additive Gaussian noise vector channel. In the previous chapter we have seen how an optimum receiver for such a channel can be constructed. The decision function that applies to this situation can be found in (4.41).

The final conclusion is that, we can convert the problem of designing an optimum receiver for an additive white Gaussian noise waveform channel to the problem of designing an optimum receiver for an AWGN vector channel. And this latter problem we have already solved!

Since the error behavior of the waveform communication system is only determined by the set of signal vectors (the signal structure), we should realize that depending on the chosen building-block waveforms we can have different sets of waveforms that yield the same error performance. See for example the discussions in Examples 5.4 and 5.5. What building-block waveforms are actually chosen by the communication engineer depends possibly on other factors as, e.g., bandwidth requirements as we will see in the next part of this course reader.

We conclude this chapter by emphasizing that we have shown that a waveform channel with AWGN is equivalent to a vector channel with additive independent and identically distributed Gaussian noise. This is why we often call this vector channel the White Gaussian Noise (AWGN) channel. In other words, one of the key results in this chapter is that the waveform channel problem in Fig. 5.12 can be converted into the problem in Fig. 5.13.

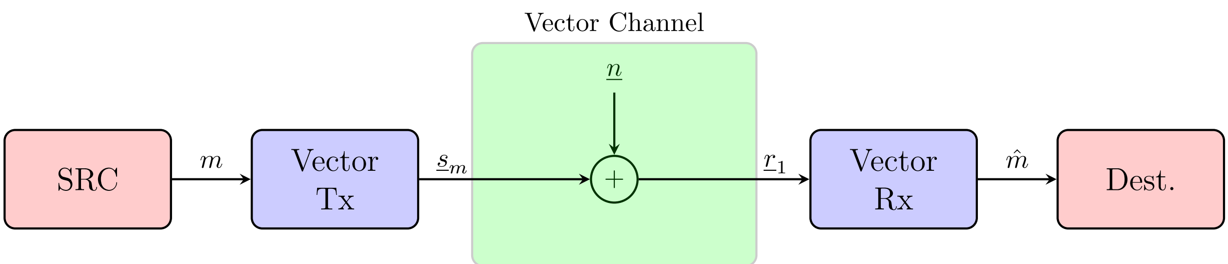

Figure 5.13: The communication system in Fig. 5.12 can be converted into a communication system based on a vector channel with AGN.

Chapter 6

Receiver Implementation, Matched Filters

Summary: We discuss receiver structures for optimum waveform communication here. We will discuss three ways of implementing an optimum receivers: correlation receiver, matched-filter receiver, and direct receiver. We will also show that a matched filter maximizes the signal-to-noise ratio.

6.1 Introduction

The receiver for communication of messages over a waveform channel we discussed in the previous chapter first determines $\underline{r} = (r_1, r_2, \ldots, r_N)$, i.e., the relevant received vector (that was named $\underline{r}_1$ in Sec. 5.6). The received vector $\underline{r}$ is then used to find the $m \in \mathcal{M}$ that minimizes (see 4.41)

$$\|\underline{r} - \underline{s}_m\|^2 - 2\sigma^2 \ln \Pr\{M = m\} = \|\underline{r} - \underline{s}_m\|^2 - N_0 \ln \Pr\{M = m\}, \tag{6.1}$$

where we substituted $N_0/2$ for σ^2. This receiver is optimum because it is based on only on relevant data (relevant for determining $\hat{m}$), and because it uses the optimum MAP detection rule in (6.1).

The vector $\underline{r}$ is given by

$$r_i = \int_{-\infty}^{\infty} r(t)\varphi_i(t)dt \text{ for } i = 1, 2, \ldots, N. \tag{6.2}$$

The problem that we investigate in this chapter is whether these operations can be simplified. It turns out that instead of multiplying and integrating, we can also do a filter-operation with a suitably chosen filter and sample the output of the filter.

Using dot products defined as

$$(\underline{a} \cdot \underline{b}) \triangleq \sum_{i=1}^{N} a_i b_i, \tag{6.3}$$

we can rewrite the first term in (6.1) as follows:

$$\begin{aligned} \|\underline{r}-\underline{s}_m\|^2 &= (\underline{r}-\underline{s}_m)\cdot(\underline{r}-\underline{s}_m) \\ &= (\underline{r}\cdot\underline{r}) - 2(\underline{r}\cdot\underline{s}_m) + (\underline{s}_m\cdot\underline{s}_m) = \|\underline{r}\|^2 - 2(\underline{r}\cdot\underline{s}_m) + \|\underline{s}_m\|^2. \end{aligned} \tag{6.4}$$

Since $\|\underline{r}\|^2$ does not depend on m, we can ignore it when (6.4) is used in (6.1), as shown in the following result.

RESULT 6.1 *The optimum receiver applies the rule*

$$\hat{m} = \underset{m\in\mathcal{M}}{\operatorname{argmax}}\{(\underline{r}\cdot\underline{s}_m) + c_m\} \tag{6.5}$$

with

$$c_m \triangleq \frac{N_0}{2}\ln \Pr\{M=m\} - \frac{\|\underline{s}_m\|^2}{2}. \tag{6.6}$$

6.2 Correlation Receiver

The method described in Result 6.1 immediately suggests the receiver structure shown in Fig. 6.1. There we first see a bank of N multipliers and integrators. This bank yields the vector $\underline{r}$ and it implements (6.2). It correlates $r(t)$ with all building-block waveforms. Note that this part of the optimum receiver also was shown in Fig. 5.10 and was subject of investigation of the previous chapter. It also appeared as the detector (demodulator) in Fig. 5.12 at the end of the previous chapter.

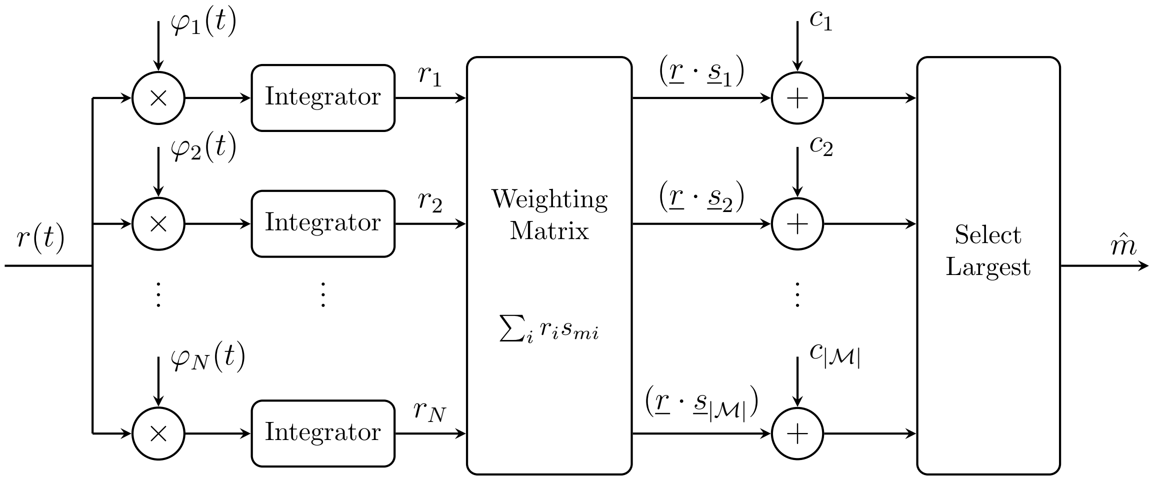

Figure 6.1: The structure of the correlation receiver.

After having determined $\underline{r}$ we use matrix multiplication to obtain the dot products

$(\underline{r} \cdot \underline{s}_m)$ for $m \in \mathcal{M}$.

$$\begin{pmatrix} (\underline{r} \cdot \underline{s}_1) \\ (\underline{r} \cdot \underline{s}_2) \\ \vdots \\ (\underline{r} \cdot \underline{s}_{|\mathcal{M}|}) \end{pmatrix} = \begin{pmatrix} s_{11} & s_{12} & \dots & s_{1N} \\ s_{21} & s_{22} & \dots & s_{2N} \\ \vdots & \vdots & \ddots & \vdots \\ s_{|\mathcal{M}|1} & s_{|\mathcal{M}|2} & \dots & s_{|\mathcal{M}|N} \end{pmatrix} \begin{pmatrix} r_1 \\ r_2 \\ \vdots \\ r_N \end{pmatrix}. \quad (6.7)$$

Adding the constants c_m and picking the m that achieves the largest sum yields an optimum receiver. This is shown in Fig. 6.1.

6.3 Matched-Filter Receiver

If for all $i = 1, \dots, N$ the building-block waveforms are such that $\varphi_i(t) \equiv 0$ for $t < 0$ and $t > T$, then we can replace the N multipliers and integrators by N *matched filters* and samplers. This can be advantageous in analog implementations since accurate multipliers are then hard to build while filters are more easily designed.

Consider a filter with an impulse response $h_i(t) = \varphi_i(T-t)$ for some $i \in \{1, 2, \dots, N\}$, as shown in Fig. 6.2. Note that $h_i(t) \equiv 0$ for $t < 0$ (i.e., the filter is causal) and also for $t > T$. An example of the relationship between $\varphi_i(t)$ and $h_i(t)$ is shown in Fig. 6.3.

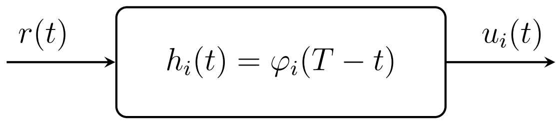

Figure 6.2: A filter matched to the building-block waveform $\varphi_i(t)$.

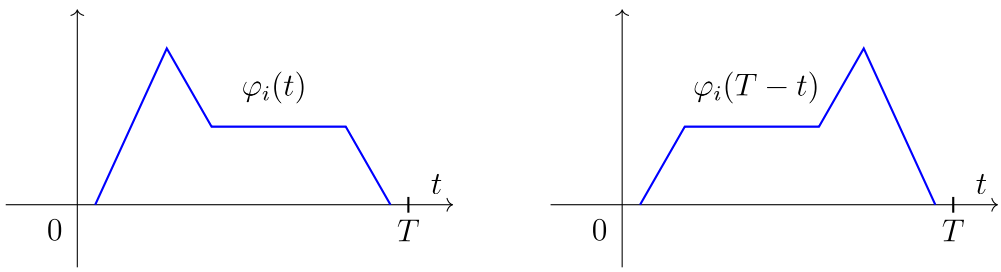

Figure 6.3: A building-block waveform $\varphi_i(t)$ and the impulse response $\varphi_i(T-t)$ of the corresponding matched filter.

For the output of this filter we then get

$$\begin{aligned} u_i(t) &= r(t) * h_i(t) \\ &= \int_{-\infty}^{\infty} r(\alpha) h_i(t-\alpha) d\alpha \\ &= \int_{-\infty}^{\infty} r(\alpha) \varphi_i(T-t+\alpha) d\alpha. \end{aligned} \quad (6.8)$$

For $t = T$ the matched-filter output

$$u_i(T) = \int_{-\infty}^{\infty} r(\alpha)\varphi_i(\alpha)d\alpha = r_i, \tag{6.9}$$

hence we can determine the i-th component of the relevant vector $\underline{r}$ in this way, i.e., by filtering with $h_i(t)$ and sampling at $t = T$.

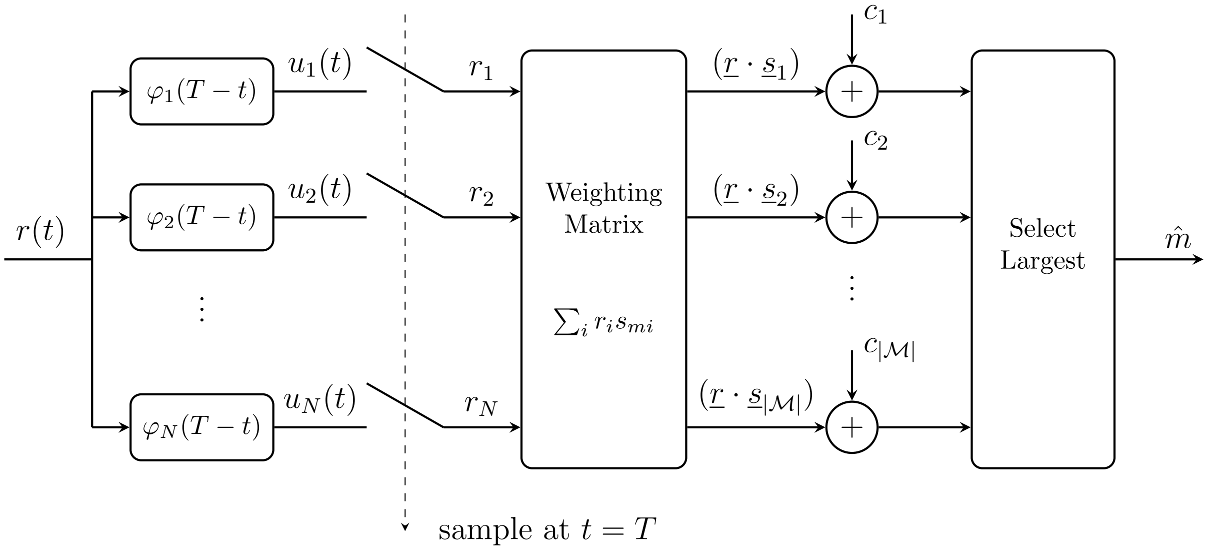

Figure 6.4: Matched-filter receiver

A filter whose impulse response is a delayed time-reversed version of a signal $\varphi_i(t)$ is called matched to $\varphi_i(t)$. A receiver that is equipped with such filters is called a matched-filter receiver. This is shown in Fig. 6.4.

6.4 Parseval Relationships

Consider an orthonormal basis $\{\varphi_i(t), i = 1, 2, \ldots, N\}$ and two waveforms $f(t)$ and $g(t)$ that can be expressed in terms of the building-block waveforms that make up this base, i.e.,

$$\begin{aligned} f(t) &= \sum_{i=1}^{N} f_i \varphi_i(t), \\ g(t) &= \sum_{i=1}^{N} g_i \varphi_i(t). \end{aligned} \tag{6.10}$$

The vector-representations that correspond to $f(t)$ and $g(t)$ are

$$\begin{aligned} \underline{f} &= (f_1, f_2, \ldots, f_N) \text{ and} \\ \underline{g} &= (g_1, g_2, \ldots, g_N). \end{aligned} \tag{6.11}$$

RESULT 6.2 *The correlation between $f(t)$ and $g(t)$ can be expressed as*

$$\begin{aligned}\int_{-\infty}^{\infty} f(t)g(t)dt &= \int_{-\infty}^{\infty} \sum_{i=1}^{N}\sum_{j=1}^{N} f_i g_j \varphi_i(t)\varphi_j(t)dt \\ &= \sum_{i=1}^{N}\sum_{j=1}^{N} f_i g_j \int_{-\infty}^{\infty} \varphi_i(t)\varphi_j(t)dt \\ &= \sum_{i=1}^{N}\sum_{j=1}^{N} f_i g_j \delta_{ij} = \sum_{i=1}^{N} f_i g_i = (\underline{f}\cdot\underline{g}). \end{aligned} \tag{6.12}$$

Result 6.2 says that the *correlation* of $f(t)$ and $g(t)$, which is defined as the integral of their product, is equal to the dot product of the corresponding vectors. Note that this result can be regarded as an analogue to the Parseval relation in Fourier analysis (see Appendix A) which says that

$$\int_{-\infty}^{\infty} f(t)g(t)dt = \int_{-\infty}^{\infty} F(f)G^*(f)df, \tag{6.13}$$

with

$$\begin{aligned} F(f) &= \int_{-\infty}^{\infty} f(t)\exp(-j2\pi ft)dt \text{ and} \\ f(t) &= \int_{-\infty}^{\infty} F(f)\exp(j2\pi ft)df. \end{aligned} \tag{6.14}$$

Here $G^*(f)$ is the complex conjugate of $G(f)$. The consequences of Result 6.2 are:

- Take $g(t) \equiv f(t)$ then
$$\int_{-\infty}^{\infty} f^2(t)dt = (\underline{f}\cdot\underline{f}) = \|\underline{f}\|^2. \tag{6.15}$$
This means that the energy of waveform $f(t)$ is simply the square of the length of the corresponding vector $\underline{f}$. We therefore also call the squared length of a vector its *energy*.

  Note that now we can rewrite (6.6) as
$$c_m = \frac{N_0}{2}\ln \Pr\{M=m\} - \frac{\|\underline{s}_m\|^2}{2} = \frac{N_0}{2}\ln \Pr\{M=m\} - \frac{E_m}{2}, \tag{6.16}$$
where
$$E_m \triangleq \int_{-\infty}^{\infty} s_m^2(t)dt, \tag{6.17}$$
is the energy corresponding to the waveform $s_m(t)$, for $m \in \mathcal{M} = \{1,2,\ldots,|\mathcal{M}|\}$.

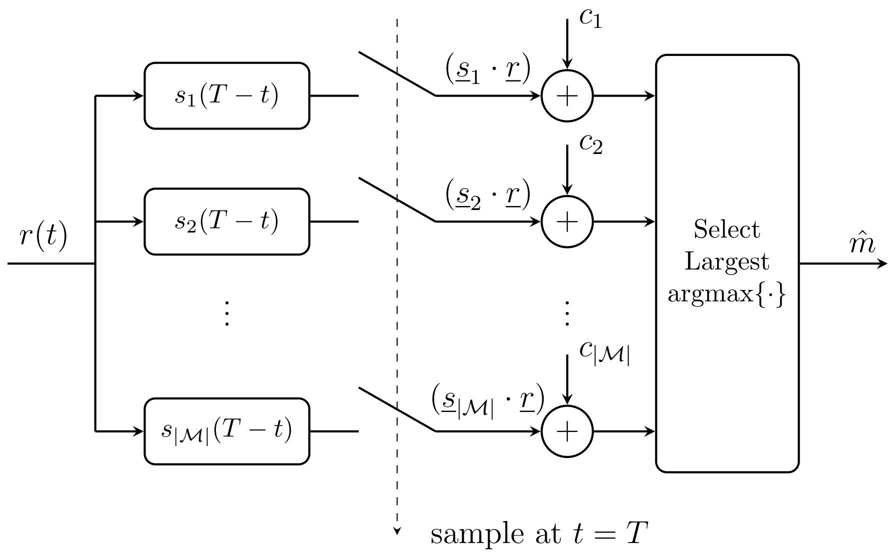

Figure 6.5: Direct receiver.

- Consider

$$\begin{aligned}\int_{-\infty}^{\infty} r(t)s_m(t)dt &= \int_{-\infty}^{\infty} r(t)\sum_{i=1}^{N} s_{mi}\varphi_i(t)dt \\ &= \sum_{i=1}^{N} s_{mi}\int_{-\infty}^{\infty} r(t)\varphi_i(t)dt = \sum_{i=1}^{N} s_{mi}r_i = (\underline{s}_m \cdot \underline{r}). \qquad (6.18)\end{aligned}$$

This is a result similar to (6.12) but *not identical* since $r(t) \neq \sum_{i=1}^{N} r_i\varphi_i(t)$, i.e., $r(t)$ can not be expressed as a linear combination of building-block waveforms. Note that the dot product in (6.18) is what we need to calculate for an optimum receiver (see Result 6.1).
If we now, for all $m \in \mathcal{M}$, take a filter with impulse response $s_m(T-t)$, let the waveform channel output $r(t)$ be the input of all these filters and sample the M filter outputs at $t = T$, we obtain

$$\int_{-\infty}^{\infty} r(\alpha)s_m(T-t+\alpha)d\alpha \overset{t=T}{=} \int_{-\infty}^{\infty} r(\alpha)s_m(\alpha)d\alpha = (\underline{s}_m \cdot \underline{r}). \qquad (6.19)$$

This gives another method to determine $(\underline{s}_m \cdot \underline{r})$, and hence, to form an optimum receiver. This is shown in Fig. 6.5. This receiver is called a *direct receiver* since the filters are matched directly to the signals $\{s_m(t), m \in \mathcal{M}\}$. We again assume that the signals are non-zero only for $0 \leq t \leq T$.

Note that a direct receiver is usually more expensive than a receiver with filters matched to the building-block waveforms, since always $M \geq N$ and in practice even often $M \gg N$. The weighting-matrix operations are not needed here however.

6.5 Signal-to-Noise Ratio

We have seen in the previous section that a matched-filter receiver is optimum, i.e., minimizes the expected error probability P_e. Not only in this sense is the matched filter optimum, we will show next that it also maximizes the *signal-to-noise ratio* (SNR). To see

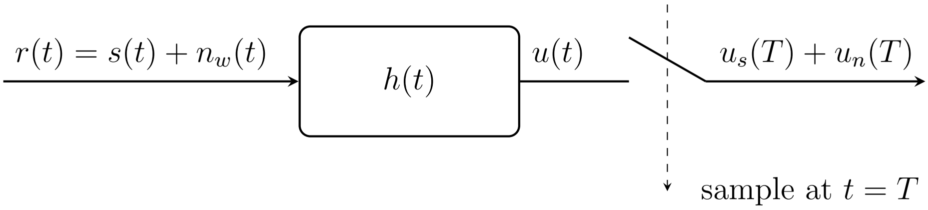

Figure 6.6: A matched filter maximizes SNR.

what we mean by this, consider the communication situation shown in Fig. 6.6. A signal $s(t)$ is assumed to be non-zero only for $0 \leq t \leq T$. This signal is observed in additive white noise, i.e., the observer receives $r(t) = s(t) + n_w(t)$. The process $N_w(t)$ is a zero-mean white Gaussian noise process with power density $S_w(f) = N_0/2$ for all $-\infty < f < \infty$.

We now want to decide whether the signal $s(t)$ was present in the noise or not. A matched-filter receiver uses a linear time-invariant filter with impulse response $h(t)$ and samples the filter output at time $t = T$.

For the sampled filter output $u(t)$ at time $t = T$ we can write

$$u(T) = \int_{-\infty}^{\infty} r(T-\alpha)h(\alpha)d\alpha = u_s(T) + u_n(T), \tag{6.20}$$

with

$$u_s(T) \triangleq \int_{-\infty}^{\infty} s(T-\alpha)h(\alpha)d\alpha \tag{6.21}$$

$$u_n(T) \triangleq \int_{-\infty}^{\infty} n_w(T-\alpha)h(\alpha)d\alpha, \tag{6.22}$$

where $u_s(T)$ is the signal component and $u_n(T)$ the noise component in the sampled filter output.

Definition 6.1 *We can now define the* signal-to-noise ratio *(SNR) as*

$$SNR \triangleq \frac{u_s^2(T)}{E[U_n^2(T)]}, \tag{6.23}$$

i.e., the ratio between signal energy and noise variance.

The noise variance can be expressed as

$$
\begin{aligned}
E[U_n^2(T)] &= E\left[\int_{-\infty}^{\infty} N_w(T-\alpha)h(\alpha)d\alpha \int_{-\infty}^{\infty} N_w(T-\beta)h(\beta)d\beta\right] \\
&= \int_{-\infty}^{\infty}\int_{-\infty}^{\infty} E[N_w(T-\alpha)N_w(T-\beta)]h(\alpha)h(\beta)d\alpha d\beta \\
&= \frac{N_0}{2}\int_{-\infty}^{\infty}\int_{-\infty}^{\infty} \delta(\beta-\alpha)h(\alpha)h(\beta)d\alpha d\beta \\
&= \frac{N_0}{2}\int_{-\infty}^{\infty} h^2(\alpha)d\alpha. \qquad (6.24)
\end{aligned}
$$

On the other hand, the signal energy is upper bounded as

$$
\begin{aligned}
u_s^2(T) &= \left[\int_{-\infty}^{\infty} s(T-\alpha)h(\alpha)d\alpha\right]^2 \\
&\leq \int_{-\infty}^{\infty} s^2(T-\alpha)d\alpha \int_{-\infty}^{\infty} h^2(\alpha)d\alpha \qquad (6.25)
\end{aligned}
$$

where the inequality follows from Schwarz inequality (see Appendix D)[1] Using (6.24) and (6.25) gives the following result.

RESULT 6.3 *The maximum attainable SNR is*

$$
\begin{aligned}
SNR &\leq \frac{\int_{-\infty}^{\infty} s^2(T-\alpha)d\alpha \int_{-\infty}^{\infty} h^2(\alpha)d\alpha}{\frac{N_0}{2}\int_{-\infty}^{\infty} h^2(\alpha)d\alpha} \qquad (6.27) \\
&= \frac{\int_{-\infty}^{\infty} s^2(T-\alpha)d\alpha}{\frac{N_0}{2}} \qquad (6.28) \\
&= \frac{2E_s}{N_0}. \qquad (6.29)
\end{aligned}
$$

Equality in Result 6.3 is obtained if and only if $h(t) = Cs(T-t)$ for some constant C, i.e., if the filter $h(t)$ is matched to the signal $s(t)$. This shows that the matched-filter receiver achieves the upper bound in (6.27). Note that this maximum SNR depends only on the energy of the waveform $s(t)$.

In this section we have demonstrated a much weaker form of optimality for the matched filter than the one that we have obtained in the previous chapter. The matched filter is not only the filter that maximizes SNR, but can be used for optimum detection as well.

[1]For two finite-energy waveforms $a(t)$ and $b(t)$ the inequality

$$
\left(\int_{-\infty}^{\infty} a(t)b(t)dt\right)^2 \leq \int_{-\infty}^{\infty} a^2(t)dt \int_{-\infty}^{\infty} b^2(t)dt \qquad (6.26)
$$

holds. Equality is obtained if and only if $b(t) = Ca(t)$ for some constant C.

6.6 Dwight O. North

The matched filter as a filter for maximizing the SNR was invented by North [8] in 1943. Matched filters are extremely important in communications and signal processing but they also important for, e.g., radars. North's result was published in a classified report at RCA Labs in Princeton. The name "matched filter" was coined by Van Vleck and Middleton who independently published the result a year later in a Harvard Radio Research Lab report [14]. Dwight O. North was one of the recipients of the IEEE Information Society's Golden Jubilee Awards for Technological Innovation, where he was cited for his invention of the matched filter.

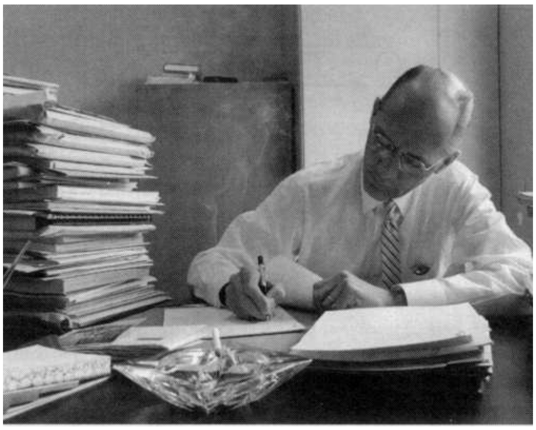

Figure 6.7: Dwight O. North, inventor of the matched filter. Photo IEEE-IT Soc. Newsl., Dec. 1998.

Part III

CHANNEL PROCESSING: TRANSMITTERS

Chapter 7

Signal Energy Considerations, Orthogonal Signals

SUMMARY: The collection of vectors that corresponds to the signal-waveforms is called the signal structure. If the signal structure is translated or rotated the error probability need not change. In this chapter we determine the translation vector that minimizes the average signal energy. After that we demonstrate that binary orthogonal signaling achieves a certain error performance only when the energy is twice that of antipodal signals. In the second part of the chapter we investigate orthogonal signaling. In this case the waveforms that correspond to the messages are orthogonal. We determine the average error probability for such signals. It appears that this error probability can be made arbitrary small by increasing the number of waveforms if only the energy per transmitted bit is larger than $N_0 \ln 2$. This is a channel capacity result!

7.1 Translation and Rotation of Signal Structures

In the additive white[1] Gaussian noise case, if a signal structure, i.e., the collection of vectors $\underline{s}_1, \underline{s}_2, \ldots, \underline{s}_{|\mathcal{M}|}$, is *translated or rotated* the error probability P_e will not change. To see why, just assume that the corresponding decision regions $\mathcal{I}_1, \mathcal{I}_2, \ldots, \mathcal{I}_{|\mathcal{M}|}$ (which need not be optimum) are translated or rotated in the same way. Then, because the AWGN-vector is spherically symmetric in all dimensions in the signal space, and since distances between decoding regions and signal points did not change, the error probability remains the same. However, in general, the average signal energy changes if a signal structure is translated. On the other hand, rotation about the origin has no effect on the average signal energy. We are now interested in finding out which translation vector minimizes the average signal energy.

[1]Although we are concerned with an AGN vector channel, we use the word "white" to emphasize that this vector channel is equivalent to a waveform channel with AWGN.

7.2 Signal Energy

Here we want to stress again that

$$E_{s_m} = \int_0^T s_m^2(t)dt = \|\underline{s}_m\|^2, \tag{7.1}$$

and therefore, we only need to know the collection of signal vectors, i.e., the signal structure, and the message probabilities to determine the average signal. This average signal energy is defined as

$$E_{\text{av}} \stackrel{\Delta}{=} \sum_{m\in\mathcal{M}} \Pr\{M=m\}E_{s_m} = \sum_{m\in\mathcal{M}} \Pr\{M=m\}\|\underline{s}_m\|^2 = E[\|\underline{S}\|^2]. \tag{7.2}$$

7.3 Translating a Signal Structure

The smallest possible average error probability of a waveform communication system only depends on the signal structure, i.e., on the collection of vectors $\underline{s}_1, \underline{s}_2, \dots, \underline{s}_{|\mathcal{M}|}$. It does not change if the entire signal structure is translated. The optimum decision regions simply translate too. Translation has an effect on the average signal energy however. We next determine the translation vector that minimizes the average signal energy.

Consider a certain signal structure. Let $E_{\text{av}}(\underline{a})$ denote the average signal energy when the structure is translated over $-\underline{a}$, or equivalently when the origin of the coordinate system is moved to $\underline{a}$ as shown in Fig. 7.1. Then

$$\begin{aligned} E_{\text{av}}(\underline{a}) &= \sum_{m\in\mathcal{M}} \Pr\{M=m\}\|\underline{s}_m - \underline{a}\|^2 \\ &= E\left[\|\underline{S}-\underline{a}\|^2\right]. \end{aligned} \tag{7.3}$$

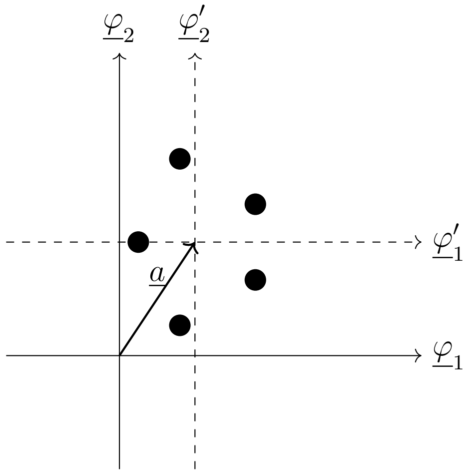

Figure 7.1: Translation of a signal structure, moving the origin of the coordinate system to $\underline{a}$.

We now have to find out how we should choose the translation vector $\underline{a}$ that minimizes $E_{\text{av}}(\underline{a})$. It turns out that the best choice is

$$\underline{a} = \sum_{m\in\mathcal{M}} \Pr\{M=m\}\underline{s}_m = E[\underline{S}]. \tag{7.4}$$

This follows from considering an alternative translation vector $\underline{b}$. The energy of the signal structure after translation by $\underline{b}$ is

$$\begin{aligned} E_{\text{av}}(\underline{b}) = E\left[\|\underline{S}-\underline{b}\|^2\right] &= E\left[\|(\underline{S}-\underline{a})+(\underline{a}-\underline{b})\|^2\right] \\ &= E\left[\|\underline{S}-\underline{a}\|^2+2(\underline{S}-\underline{a})\cdot(\underline{a}-\underline{b})+\|\underline{a}-\underline{b}\|^2\right] \\ &= E\left[\|\underline{S}-\underline{a}\|^2\right]+2(E[\underline{S}]-\underline{a})\cdot(\underline{a}-\underline{b})+\|\underline{a}-\underline{b}\|^2 \\ &= E\left[\|\underline{S}-\underline{a}\|^2\right]+\|\underline{a}-\underline{b}\|^2 \\ &\geq E\left[\|\underline{S}-\underline{a}\|^2\right], \end{aligned} \tag{7.5}$$

where equality in the third line follows from $\underline{a} = E[\underline{S}]$. Observe that $E_{\text{av}}(\underline{b})$ is minimized only for $\underline{b} = \underline{a} = E[\underline{S}]$.

If we do not translate, i.e., when $\underline{b} = \underline{0}$, the average signal energy

$$E_{\text{av}}(\underline{0}) = E\left[\|\underline{S}-\underline{a}\|^2\right]+\|\underline{a}\|^2, \tag{7.6}$$

hence we can save $\|\underline{a}\|^2$ if we translate the center of the coordinate system to $\underline{a}$.

RESULT 7.1 *To minimize the average signal energy we should choose the* **center of gravity** *of the signal structure as the origin of the coordinate system. If the center of gravity of the signal structure $\underline{a} \neq \underline{0}$ we can decrease the average signal energy by $\|\underline{a}\|^2$ by moving the origin of the coordinate system to $\underline{a}$.*

In what follows we will discuss some examples.

7.4 Orthogonal vs. Antipodal Signaling

Let $\mathcal{M} = \{1, 2\}$ and $\Pr\{M = 1\} = \Pr\{M = 2\} = 1/2$. Consider a first signal set of two *orthogonal* waveforms (see the two sub-figures in the top row in Fig. 7.2)

$$\begin{aligned} s_1(t) &= \sqrt{2E_s}\sin(10\pi t) \\ s_2(t) &= \sqrt{2E_s}\sin(12\pi t), \text{ for } 0 \leq t < 1, \end{aligned} \tag{7.7}$$

and a second signal set of two *antipodal* signals (see the bottom row sub-figures in Fig. 7.2)

$$\begin{aligned} s_1(t) &= \sqrt{2E_s}\sin(10\pi t) \\ s_2(t) &= -\sqrt{2E_s}\sin(10\pi t), \text{ also for } 0 \leq t < 1. \end{aligned} \tag{7.8}$$

Note that binary FSK (frequency-shift keying) is the same as orthogonal signaling, while binary PSK (phase-shift keying) is identical to antipodal signaling.

The vector representations of the signal sets are

$$\begin{aligned} \underline{s}_1 &= (\sqrt{E_s}, 0), \\ \underline{s}_2 &= (0, \sqrt{E_s}), \end{aligned} \tag{7.9}$$

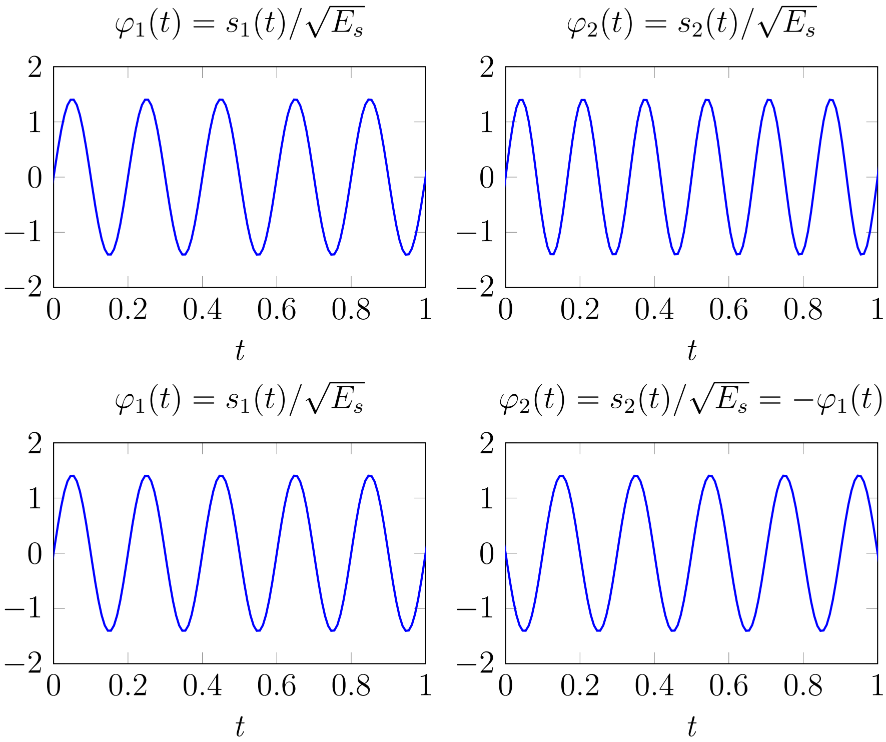

Figure 7.2: The two signal sets of (7.7) and (7.8) in waveform representation.

for the first (orthogonal) set, and

$$\begin{aligned} \underline{s}_1 &= (\sqrt{E_s}, 0), \\ \underline{s}_2 &= (-\sqrt{E_s}, 0), \end{aligned} \tag{7.10}$$

for the second (antipodal) set. These vector representations are shown in Fig. 7.3.

The average signal energy for both sets is equal to E_s. For the error probabilities in the case of AWGN with power spectral density $N_0/2$ we get

$$\begin{aligned} P_{\mathrm{e}}^{\mathrm{orthog.}} &= Q\left(\frac{\sqrt{2E_s}}{2\sqrt{\frac{N_0}{2}}}\right) = Q\left(\sqrt{E_s/N_0}\right), \\ P_{\mathrm{e}}^{\mathrm{antipod.}} &= Q\left(\frac{2\sqrt{E_s}}{2\sqrt{\frac{N_0}{2}}}\right) = Q\left(\sqrt{2E_s/N_0}\right). \end{aligned} \tag{7.11}$$

Note that the distance d between the signal points differs by a factor $\sqrt{2}$ and $P_{\mathrm{e}} = Q(d/2\sigma)$.

These error probabilities are depicted in Fig. 7.4. We observe a difference in the error probabilities of 3.0 dB. By this we mean that, in order to achieve a certain value of P_{e}, we have to make the signal energy twice as large for orthogonal signaling than for antipodal

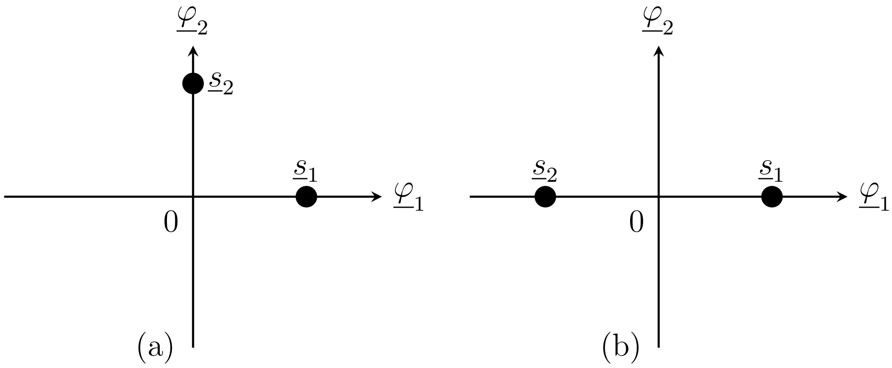

Figure 7.3: Vector representation of the orthogonal (a) and the antipodal signal set (b).

signaling. The better performance of antipodal signaling relative to orthogonal signaling is best explained by the fact that for antipodal signaling the center of gravity is the origin of the coordinate system while for orthogonal signaling this is certainly not the case.

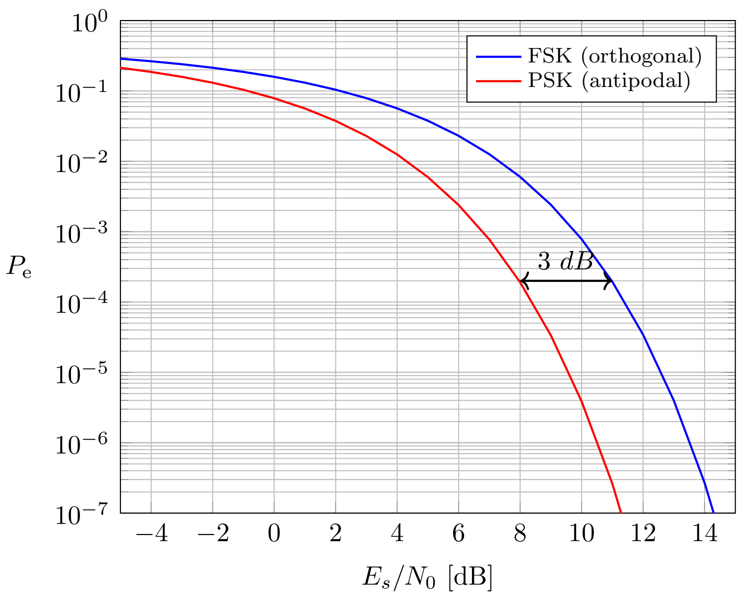

Figure 7.4: Probability of error for binary antipodal and orthogonal signaling as function of E_s/N_0 in dB. It is assumed that $\Pr\{M = 1\} = \Pr\{M = 2\} = 1/2$. Observe the difference of 3 dB between both curves.

We may conclude that binary PSK modulation achieves a better error-performance than binary FSK. An advantage of FSK modulation is however that efficient FSK receivers can be designed that do not recover the phase. PSK on the other hand requires coherent demodulation.

7.5 Orthogonal Signal Structures

Consider $|\mathcal{M}|$ signals $s_m(t)$, or in vector representation $\underline{s}_m$, with a-priori probabilities $\Pr\{M = m\} = 1/|\mathcal{M}|$ for $m \in \mathcal{M} = \{1, 2, \dots, |\mathcal{M}|\}$. We now define an orthogonal signal set in the following way:

Definition 7.1 *All signals in an orthogonal set are assumed to have equal energy and are orthogonal i.e.,*

$$\underline{s}_m \stackrel{\Delta}{=} \sqrt{E_s}\underline{\varphi}_m \text{ for } m \in \mathcal{M}, \tag{7.12}$$

where $\underline{\varphi}_m$ is the unit-vector corresponding to dimension m. There are as many building-block waveforms $\varphi_m(t)$ and dimensions in the signal space as there are messages.

The signals that we have defined are now orthogonal since

$$\int_{-\infty}^{\infty} s_m(t)s_k(t)dt = (\underline{s}_m \cdot \underline{s}_k) = E_s\left(\underline{\varphi}_m \cdot \underline{\varphi}_k\right) = E_s\delta_{mk} \text{ for } m \in \mathcal{M} \text{ and } k \in \mathcal{M}. \tag{7.13}$$

Note that all signals have energy equal to E_s.

So far we have not been very explicit about the actual signals. However we can, e.g., think of (disjoint) shifts of a pulse (pulse-position modulation, PPM) or sines and cosines with an integer number of periods over $[0, T)$ (frequency-shift keying, FSK). FSK with $|\mathcal{M}| = 2$ was analyzed in Sec. 7.2.

7.6 Optimum Receiver

How does the optimum receiver decide when it receives the vector $\underline{r} = (r_1, r_2, \dots, r_{|\mathcal{M}|})$? It has to choose the message $m \in \mathcal{M}$ that minimizes the squared Euclidean distance between $\underline{s}_m$ and $\underline{r}$, i.e.,

$$\begin{aligned} \|\underline{r} - \underline{s}_m\|^2 &= \|\underline{r}\|^2 + \|\underline{s}_m\|^2 - 2(\underline{r} \cdot \underline{s}_m) \\ &= \|\underline{r}\|^2 + E_s - 2\sqrt{E_s}r_m. \end{aligned} \tag{7.14}$$

RESULT 7.2 *Since only the term $-2\sqrt{E_s}r_m$ depends on m, the optimum receiver for orthogonal signaling chooses $\hat{m}$ such that*

$$r_{\hat{m}} \geq r_m \text{ for all } m \in \mathcal{M}. \tag{7.15}$$

In other words, the optimum receiver finds the largest component in the vector $\underline{r} = (r_1, r_2, \dots, r_{|\mathcal{M}|})$. The position of that component gives the value of $\hat{m}$. Now we can find an expression for the error probability.

7.7 Error Probability

To determine the error probability for orthogonal signaling we may assume, because of symmetry, that signal $s_1(t)$ was actually sent. Then

$$\begin{aligned} r_1 &= \sqrt{E_s} + n_1, \\ r_m &= n_m, \text{ for } m = 2, 3, \ldots, |\mathcal{M}|, \\ \text{with } p_{\underline{N}}(\underline{n}) &= \prod_{m=1}^{|\mathcal{M}|} \frac{1}{\sqrt{\pi N_0}} \exp\left(-\frac{n_m^2}{N_0}\right). \end{aligned} \tag{7.16}$$

Note that the noise vector $\underline{n} = (n_1, n_2, \ldots, n_{|\mathcal{M}|})$ consists of $|\mathcal{M}|$ independent components all with mean 0 and variance $N_0/2$.

Suppose that the first component of the received vector is α. Then we can write for the correct probability, conditional on the fact that message 1 was sent and that the first component of $\underline{r}$ is α,

$$\begin{aligned} \Pr\{\hat{M} = 1 | M = 1, R_1 = \alpha\} &= \Pr\{N_2 < \alpha, N_3 < \alpha, \ldots, N_{|\mathcal{M}|} < \alpha\} \\ &= (\Pr\{N_2 < \alpha\})^{|\mathcal{M}|-1} \\ &= \left(\int_{-\infty}^{\alpha} p_N(\beta) d\beta\right)^{|\mathcal{M}|-1}. \end{aligned} \tag{7.17}$$

Therefore, the correct probability can be expressed as

$$P_c = \int_{-\infty}^{\infty} P_{R_1}(\alpha | M = 1) \Pr\{\hat{M} = 1 | M = 1, R_1 = \alpha\} d\alpha \tag{7.18}$$

$$= \int_{-\infty}^{\infty} p_N\left(\alpha - \sqrt{E_s}\right) \left(\int_{-\infty}^{\alpha} p_N(\beta) d\beta\right)^{|\mathcal{M}|-1} d\alpha. \tag{7.19}$$

We rewrite this correct probability as follows

$$\begin{aligned} P_c &= \int_{-\infty}^{\infty} \frac{1}{\sqrt{\pi N_0}} \exp\left(-\frac{(\alpha - \sqrt{E_s})^2}{N_0}\right) \left(\int_{-\infty}^{\alpha} \ldots d\beta\right)^{|\mathcal{M}|-1} d\alpha \\ &= \int_{-\infty}^{\infty} \frac{1}{\sqrt{2\pi}} \exp\left(-\frac{(\alpha/\sqrt{N_0/2} - \sqrt{E_s}/\sqrt{N_0/2})^2}{2}\right) \left(\int_{-\infty}^{\alpha} \ldots d\beta\right)^{|\mathcal{M}|-1} d\alpha/\sqrt{N_0/2} \\ &= \int_{-\infty}^{\infty} \frac{1}{\sqrt{2\pi}} \exp\left(-\frac{(\mu - \sqrt{2E_s/N_0})^2}{2}\right) \left(\int_{-\infty}^{\mu\sqrt{N_0/2}} \ldots d\beta\right)^{|\mathcal{M}|-1} d\mu \end{aligned} \tag{7.20}$$

with $\mu = \alpha/\sqrt{N_0/2}$. Furthermore

$$\begin{aligned} \int_{-\infty}^{\mu\sqrt{N_0/2}} \frac{1}{\sqrt{\pi N_0}} \exp\left(-\frac{\beta^2}{N_0}\right) d\beta &= \int_{-\infty}^{\mu\sqrt{N_0/2}} \frac{1}{\sqrt{2\pi}} \exp\left(-\frac{(\beta/\sqrt{N_0/2})^2}{2}\right) d\beta/\sqrt{N_0/2} \\ &= \int_{-\infty}^{\mu} \frac{1}{\sqrt{2\pi}} \exp\left(-\frac{\lambda^2}{2}\right) d\lambda \end{aligned} \tag{7.21}$$

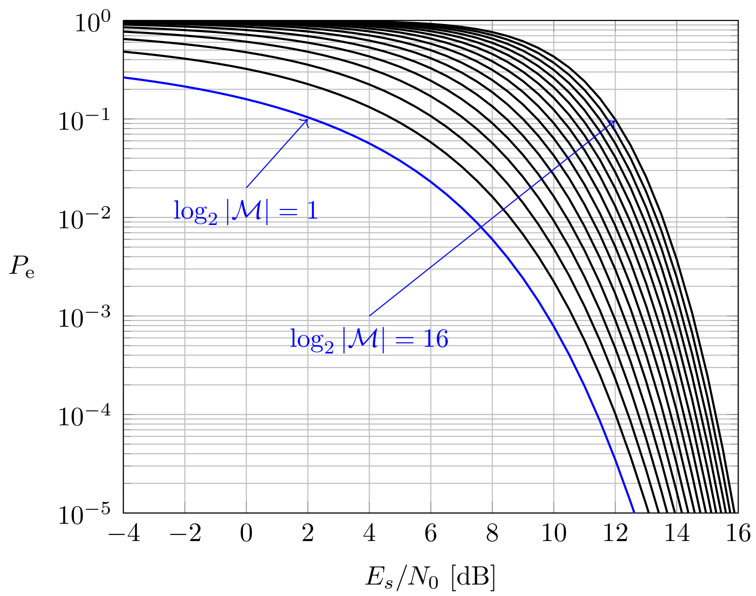

Figure 7.5: Error probability P_e for $|\mathcal{M}|$ orthogonal signals as a function of E_s/N_0 in dB for $\log_2 |\mathcal{M}| = 1, 2, \ldots, 16$. Note that P_e increases with $|\mathcal{M}|$ for fixed E_s/N_0.

with $\lambda = \beta/\sqrt{N_0/2}$. Therefore

$$P_c = \int_{-\infty}^{\infty} p(\mu - b) \left(\int_{-\infty}^{\mu} p(\lambda) d\lambda \right)^{|\mathcal{M}|-1} d\mu, \tag{7.22}$$

with $p(\gamma) = \frac{1}{\sqrt{2\pi}} \exp\left(-\frac{\gamma^2}{2}\right)$ and $b = \sqrt{2E_s/N_0}$. Note that $p(\gamma)$ is the probability density function of a Gaussian random variable with mean zero and variance 1.

From (7.22) we conclude that for a given $|\mathcal{M}|$ the correct probability P_c depends only on b, i.e., on the ratio E_s/N_0. This can be regarded as a signal to noise ratio since E_s is the signal energy and N_0 is twice the variance of the noise in each dimension.

Example 7.1 In Fig. 7.5 the error probability $P_e = 1 - P_c$ is depicted for values of $\log_2 |\mathcal{M}| = 1, 2, \ldots, 16$ and as a function of E_s/N_0. The case $\log_2 |\mathcal{M}| = 1$ corresponds to binary FSK in Fig. 7.4.

7.8 Capacity

Consider the following experiment. We keep increasing $|\mathcal{M}|$ and want to know how we should increase E_s/N_0 such that the error probability P_e gets smaller and smaller. This is known as reliable communication. It turns out that it is the energy per bit that counts. We define E_b as the energy per transmitted bit of information, i.e.,

$$E_b \triangleq \frac{E_s}{\log_2 |\mathcal{M}|}. \tag{7.23}$$

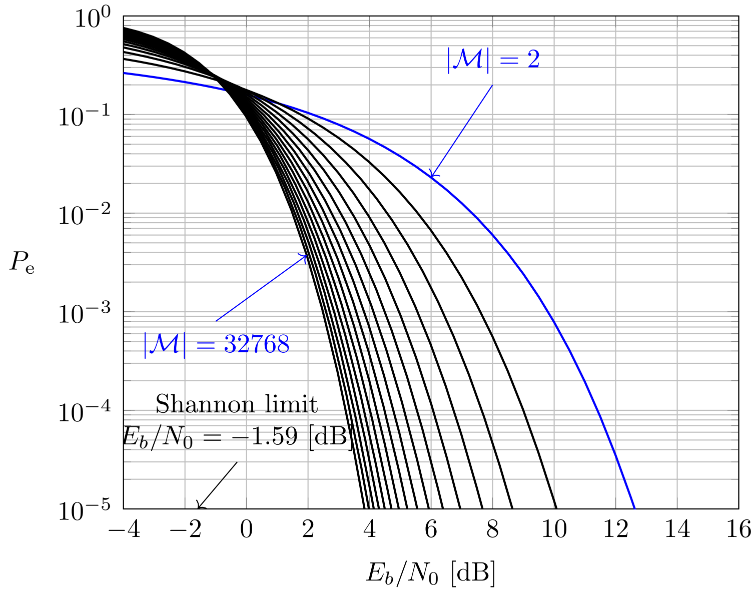

Figure 7.6: Error probability for $|\mathcal{M}| = 2, 4, 8, \ldots, 32768$ now as function of the ratio E_b/N_0 in dB.

The following result shows that reliable communication is possible as long as $E_b > N_0 \ln 2$.

RESULT 7.3 *The error probability for orthogonal signalling satisfies*

$$P_e \leq \begin{cases} 2\exp\left(-[E_b/(2N_0) - \ln 2]\log_2|\mathcal{M}|\right), & \text{if } E_b/N_0 \geq 4\ln 2. \\ 2\exp\left(-[\sqrt{E_b/N_0} - \sqrt{\ln 2}]^2 \log_2|\mathcal{M}|\right), & \text{if } \ln 2 \leq E_b/N_0 \leq 4\ln 2. \end{cases} \tag{7.24}$$

The proof of this result can be found in Appendix F.

The consequence of (7.24) is that if E_b, i.e., the energy per bit, is larger than $N_0 \ln 2$ we can get an arbitrary small error probability by increasing $|\mathcal{M}|$, the dimensionality of the signal space. **This a channel capacity result!**

Note that the number of bits that we transmit each time is $\log_2|\mathcal{M}|$ and this number grows much slower than $|\mathcal{M}|$ itself.

Example 7.2 In Fig. 7.6 we have plotted the error probability P_e as a function of the ratio E_b/N_0. It appears that for ratios larger than $\ln 2 = -1.5917$ dB (this number is called the Shannon limit) the error probability decreases by making $|\mathcal{M}|$ larger.

Finally note that if we use a transmitter with power P_s then, since reliable transmission of a bit requires at least energy $N_0 \ln 2$, up to

$$C = \frac{P_s}{N_0 \ln 2} \left[\frac{\text{bits}}{\text{seconds}}\right] \tag{7.25}$$

can be transmitted reliably. We will see later that this is the so-called wideband capacity.

7.9 Energy of $|\mathcal{M}|$ Orthogonal Signals

The average energy E_{av} of the signals in an orthogonal set (all signals having energy E_s) is

$$E_{\text{av}} = E\left[\|\underline{S}\|^2\right] = \sum_{m\in\mathcal{M}} \Pr\{M=m\}\|\underline{s}_m\|^2 = E_s. \tag{7.26}$$

The center of gravity of our orthogonal signal structure is

$$\underline{a} = \left(\frac{1}{|\mathcal{M}|}, \frac{1}{|\mathcal{M}|}, \dots, \frac{1}{|\mathcal{M}|}\right)\sqrt{E_s}. \tag{7.27}$$

We know from (7.6) that

$$E_{\text{av}}(\underline{0}) = E_{\text{av}}(\underline{a}) + \|\underline{a}\|^2 \tag{7.28}$$

thus, since $E_{\text{av}}(\underline{0}) = E_{\text{av}}$,

$$E_s = E_{\text{av}}(\underline{a}) + \frac{E_s}{|\mathcal{M}|} \tag{7.29}$$

or

$$E_{\text{av}}(\underline{a}) = E_s\left(1 - \frac{1}{|\mathcal{M}|}\right). \tag{7.30}$$

Observe that $E_{\text{av}}(\underline{a})$ is the average signal energy after translating the coordinate system such that its origin is the center of gravity of the signal structure. For $|\mathcal{M}| \to \infty$ the difference between the $E_{\text{av}}(\underline{a})$ and E_s can be neglected. Therefore, we conclude that an orthogonal signal set is not optimal in the sense that for a given error performance some energy could be saved (by translating the signal set). However, that difference diminishes if $|\mathcal{M}| \to \infty$.

Chapter 8

Message Sequences, Bandwidth

SUMMARY: In this chapter we will describe the problem of transmitting a continuous stream of messages. How should we use the available signal power in such a way that we achieve a large information rate together with a small error probability ? It will be shown that we can use block-orthogonal signaling to achieve these goals. Drawback of block-orthogonal signaling is however that it requires a large number of dimensions per second. Then we show that a channel with bandwidth W can only accommodate roughly $2W$ dimensions per second. Hence block-orthogonal signaling is only practical when the available bandwidth is large.

8.1 A Stream of Messages

In the previous part we have considered transmission of a **single randomly-chosen message** $m \in \mathcal{M}$, over a waveform channel. In real life the signals corresponding to the messages have a finite duration (at least approximately). Therefore we can assume that the signals are only non-zero inside the time-interval $0 \leq t < T$. The **problem** that was to be solved was to determine the optimum receiver, i.e., the receiver that minimizes the error probability P_e for a channel with AWGN.

In this chapter we shall investigate the more practical situation where we have a **continuous stream of messages** that are to be transmitted over our AWGN waveform channel. This is schematically shown in Fig. 8.1.

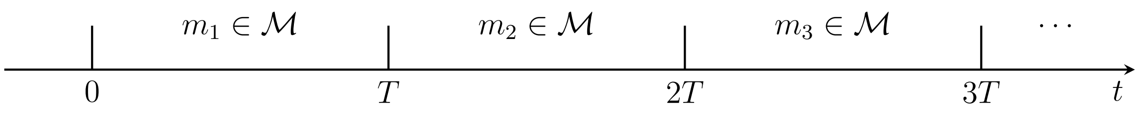

Figure 8.1: A continuous stream of messages.

Definition 8.1 *We assume that each T seconds one out of $|\mathcal{M}|$ messages is to be transmitted. The messages are* **equally likely***, i.e.,* $\Pr\{M = m\} = 1/|\mathcal{M}|$ *for all* $m \in \mathcal{M}$.

The waveform that corresponds to message $m \in \mathcal{M}$ is $s_m(t)$. It is non-zero only for $0 \leq t < T$. If the message in the k-th interval $[(k-1)T, kT)$ is m, the signal in that interval is $s_{k,m}(t) = s_m(t-(k-1)T)$.

Definition 8.2 *If the* **available transmit power** *is P_s (Joule/sec or Watt) then for each signal $s_m(t)$ for $m \in \mathcal{M}$ the* **available energy** *is $E_s = P_s T$ and hence*

$$P_s T = E_s \geq \int_0^T s_m^2(t)dt \qquad [\text{Joule}]. \tag{8.1}$$

Definition 8.3 *The* **transmission rate** *R is defined as*

$$R \triangleq \frac{\log_2 |\mathcal{M}|}{T} \qquad \left[\frac{\text{bits}}{\text{seconds}}\right]. \tag{8.2}$$

Definition 8.4 *Now the* **available energy per transmitted bit** *is defined as*

$$E_b \triangleq \frac{E_s}{\log_2 |\mathcal{M}|} \qquad \left[\frac{\text{Joule}}{\text{bit}}\right]. \tag{8.3}$$

From the above definitions we can deduce for the available energy per transmitted bit that

$$E_b = \frac{E_s}{T}\frac{T}{\log_2 |\mathcal{M}|} = \frac{P_s}{R}. \tag{8.4}$$

Our problem is now to determine the **maximum rate at which we can communicate reliably** over a waveform channel when the available power is P_s. What are the signals that are to be used to achieve this maximum rate? In the next sections we will first consider two extremal situations, namely bit-by-bit signaling and block-orthogonal signaling. In Chapter 9, we will discuss optimal transmitters.

8.2 Bit-by-Bit Signaling

8.2.1 Description

Suppose that in T seconds, we want to transmit K binary digits $b_1 b_2 \ldots b_K$. Then

$$\begin{aligned} |\mathcal{M}| &= 2^K, \\ R &= \frac{\log_2 |\mathcal{M}|}{T} = \frac{K}{T}. \end{aligned} \tag{8.5}$$

We can realize this by transmitting a signal $s(t)$ that is composed out of K pulses $p(t)$ that are shifted in time. More precisely

$$s(t) = \sum_{i=1}^{K} (-1)^{b_i+1} p(t-(i-1)\tau) \tag{8.6}$$

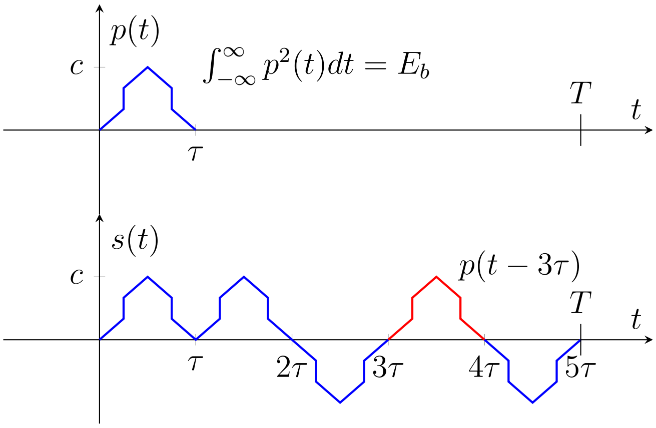

Figure 8.2: A bit-by-bit waveform for $K = 5$ and message 11010.

Here $p(t)$ is a pulse with energy E_b and duration τ. An example of this approach is shown in Fig. 8.2.

To evaluate the performance of bit-by-bit signaling we first have to determine the building-block waveforms that are the basis of our signals. It will be clear that if we take for $i = 1, 2, \ldots, K$

$$\varphi_i(t) \triangleq \frac{p(t-(i-1)\tau)}{\sqrt{E_b}} \tag{8.7}$$

then for $i = 1, 2, \ldots, K$ and $j = 1, 2, \ldots, K$

$$\int_{-\infty}^{\infty} \varphi_i(t)\varphi_j(t)dt = \delta_{ij}, \tag{8.8}$$

and we have an orthonormal basis. Hence the building-block waveforms are the time-shifts over multiples of τ of the normalized pulse $p(t)/\sqrt{E_b}$ as is shown in Fig. 8.3. Now we can

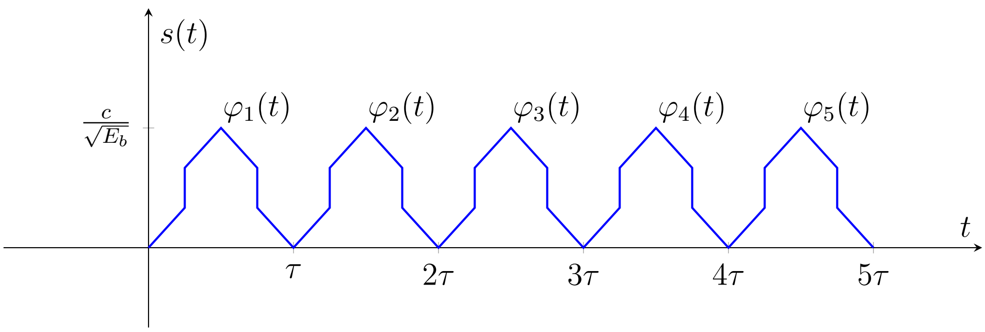

Figure 8.3: Our $K = 5$ building-block waveforms.

determine the signal structures that correspond to all the signals. For $K = 1, 2, 3$ we have shown the signal structures for bit-by-bit signaling in Fig. 8.4. The structure is always a K-dimensional *hypercube*.

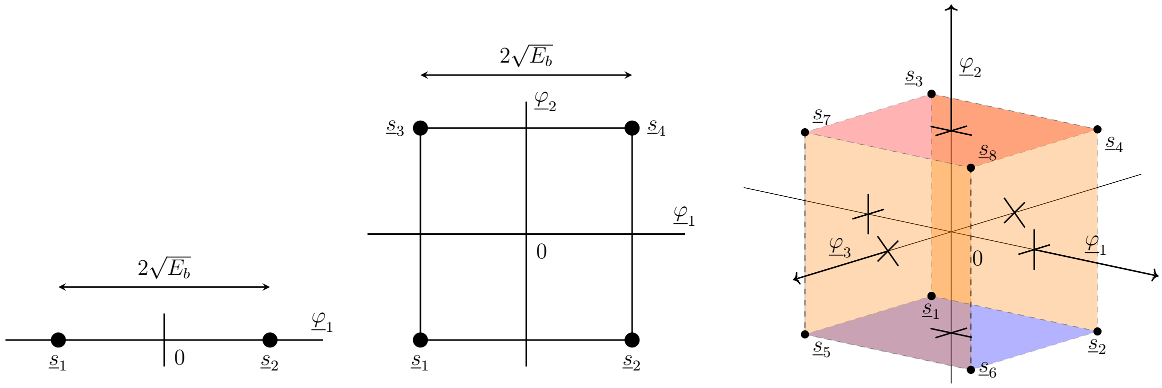

Figure 8.4: Bit-by-bit signal structure for $K = 1, 2, 3$.

To see how the decision regions look like note first that

$$\underline{s}_1 = \left(-\sqrt{E_b}, -\sqrt{E_b}, \ldots, -\sqrt{E_b}\right). \tag{8.9}$$

and observe that the optimum receiver decides $\hat{m} = 1$ if

$$r_i < 0, \text{ for all } i = 1, ..., K \tag{8.10}$$

Now for messages other than for $m = 1$ similar arguments show that the decision regions are separated by hyperplanes $r_i = 0$ for $i = 1, ..., K$.

To find an expression for P_e note that the signal hypercube is symmetrical and assume that $\underline{s}_1$ was transmitted. No error occurs if $r_i = -\sqrt{E_b} + n_i < 0$ for all $i = 1, ..., K$ or, in other words, if

$$n_i < \sqrt{E_b} \text{ for all } i = 1, ..., K, \tag{8.11}$$

hence, noting that $\sigma^2 = N_0/2$, we get

$$P_\mathrm{c} = \left(1 - Q(\sqrt{2E_b/N_0})\right)^K. \tag{8.12}$$

Therefore

$$P_\mathrm{e} = 1 - \left(1 - Q(\sqrt{2E_b/N_0})\right)^K. \tag{8.13}$$

Observe that to estimate bit b_i for $i = 1, ..., K$, an optimum receiver only needs to consider the received signal r_i in dimension i.

8.2.2 Probability of error considerations

Now we fix the transmit power P_s and the rate R. Note that for bit-by-bit signaling $K = RT$ (see equation (8.5)) and that $E_b = P_s/R$ (see equation (8.4)) and substitute this in (8.13), our expression for P_e. We then obtain

$$P_\mathrm{e} = 1 - \left(1 - Q\left(\sqrt{\frac{2P_s}{RN_0}}\right)\right)^{RT}. \tag{8.14}$$

Based on this expression for P_e we can now investigate what happens if we increase T (by multiples of $1/R$).

- For fixed average power P_s and fixed rate R the average error probability increases and approaches 1 if we increase T.

Since we cannot improve reliability by increasing T, we consider the minimum value $T = 1/R$, i.e., $K = 1$. For $K = 1$ we get

$$P_e = Q\left(\sqrt{\frac{2P_s}{RN_0}}\right). \tag{8.15}$$

Now we can conclude that:

- The average error probability P_e can only be decreased by increasing the power P_s or by decreasing the rate R.

This seemed to be "the end of the story" for communication engineers before Shannon presented his ideas in [12] and [13]. We will return to this at the end of Sec. 8.3.

8.3 Block-Orthogonal Signaling

8.3.1 Description

Next we will consider block-orthogonal signaling. We again want to transmit K bits in T seconds. We do this by sending one out of 2^K orthogonal pulses every T seconds. If we use pulse-position modulation (PPM) the $|\mathcal{M}| = 2^K$ signals are

$$s_m(t) = \sqrt{E_s}\varphi(t - (m-1)\tau), \text{ for } m = 1, ..., 2^K, \tag{8.16}$$

where $\varphi(t)$ has energy 1 and duration not more than τ with

$$\tau = \frac{T}{2^K}. \tag{8.17}$$

All signals *within the block* $[0, T)$ are orthogonal and have energy E_s. That is why we call our signaling method block-orthogonal. A block-orthogonal system with $K = 5$ is shown in Fig. 8.5.

8.3.2 Probability of error considerations

To determine the error probability P_e for block-orthogonal signaling we assume that

$$E_b/N_0 = (1+\epsilon)^2 \ln 2, \text{ for } 0 \le \epsilon \le 1, \tag{8.18}$$

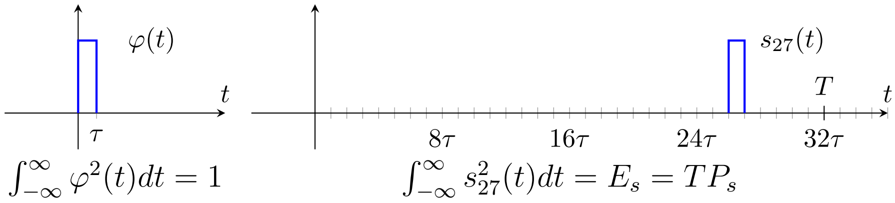

Figure 8.5: A block-orthogonal waveform for $K = 5$ and message 11010 or $m = 27$.

i.e., we are willing to spend slightly more than $N_0 \ln 2$ [Joule] per transmitted bit of information. Now we obtain from (7.24) that

$$\begin{aligned} P_{\mathrm{e}} &\leq 2\exp\left(-\left[\sqrt{(1+\epsilon)^2 \ln 2} - \sqrt{\ln 2}\right]^2 \log_2 |\mathcal{M}|\right) \\ &= 2\exp\left(-[\epsilon^2 \ln 2] \log_2 |\mathcal{M}|\right). \end{aligned} \tag{8.19}$$

Finally substitution of $\log_2 |\mathcal{M}| = RT$ (see (8.3)) yields

$$P_{\mathrm{e}} \leq 2\exp(-\epsilon^2 RT \ln 2). \tag{8.20}$$

What does (8.18) imply for the rate R? Note that $E_b = P_s/R$ (see (8.4)). This results in

$$E_b/N_0 = P_s/RN_0 = (1+\epsilon)^2 \ln 2, \tag{8.21}$$

in other words

$$R = \frac{1}{(1+\epsilon)^2} \frac{P_s}{N_0 \ln 2}. \tag{8.22}$$

Based on (8.20) and (8.22) we can now investigate what we should do to improve the reliability of our system. This leads to the following result.

THEOREM 8.1 *For an available average power P_s we can achieve rates R smaller than but arbitrarily close to*

$$C_\infty \triangleq \frac{P_s}{N_0 \ln 2} \qquad \left[\frac{bit}{second}\right] \tag{8.23}$$

while the error probability P_{e} can be made arbitrarily small by increasing T. Observe that C_∞, the channel **capacity**, *depends only on the available power P_s and power spectral density $N_0/2$ of the noise.*

This is a Shannon-type of result. The reliability can be increased not only by increasing the power P_s or decreasing the rate R (as discussed in Sec. 8.2.2) but also by increasing the "codeword-lengths" T. It is also important to note that only rates up to the capacity C_∞ can be achieved reliably. We will see later that rates larger than C_∞ are indeed not achievable. Therefore it is correct to use the term channel capacity here.

One might get the feeling that this could finish our investigations. We have found the capacity of the waveform channel with AWGN. In the next chapter we will see that so far we have ignored an important property of signal sets: their dimensionality.

Signaling	Dimensions per block	Dimensions per second
Bit-by-Bit	$K = RT$	$K/T = R$
Block Orthogonal	$2^K = 2^{RT}$	$2^K/T = 2^{RT}/T$

Table 8.1: Comparison between bit-by-bit and orthogonal signaling blocks.

8.4 Dimensions Needed for Bit-by-Bit and for Block-Orthogonal Signaling

We again assume that in an interval of duration T we have to transmit K bits. For bit-by-bit signaling, we need $K = RT$ dimensions per block (see Sec. 8.2.1). For block-orthogonal signaling we need $2^K = 2^{RT}$ dimensions per block (see Sec. 8.3.1). Therefore for bit-by-bit signaling we need $K/T = R$ dimensions per second. For block-orthogonal signaling we need $2^K/T = 2^{RT}/T$ dimensions per second. This discussion is summarized in Table 8.1.

Note that for block-orthogonal signaling the number of dimensions per second explodes by increasing T (see Table 8.1). In the next section we will see that a channel with a finite bandwidth cannot accommodate all these dimensions. Increasing T is however necessary to improve the reliability of a block-orthogonal system hence finite bandwidth creates a problem.

8.5 Bandwidth, time, and dimensions

The following result will not be proved. Intuitively it relates to the sampling theorem. For more information on this subject check Wozencraft and Jacobs [15]. The Fourier transform is described briefly in Appendix A.

RESULT 8.2 (Dimensionality theorem) *Let $\varphi_i(t)$, for $i = 1, ..., N$ denote any set of orthonormal waveforms. Assume that for all waveforms $\varphi_i(t)$ for $i = 1, \dots, N$*

1. *$\varphi_i(t) = 0$ for all t outside $[0, T)$, and*
2. *its Fourier transform satisfies $\int_{-W}^{+W} |\Phi_i(f)|^2 df \approx 1$.*

Then the number of orthogonal waveforms (dimensions) N is (roughly) upper-bounded by $2WT$. The parameter W is called **bandwidth** *(in Hz).*

The theorem says that if we require almost all spectral energy of the waveforms to be in the frequency range $[-W, W]$, the number of waveforms cannot be much more than roughly $2WT$, in other words the number of dimensions is not much more than $2W$ per second.

Now that we know that the maximum number of dimensions is $2W$ per second we are interested in sets of building-block waveforms achieving this upper bound. Therefore consider $N = 2K + 1$ orthogonal waveforms that are always zero except for $0 \leq t < T$, which are defined as

$$
\begin{aligned}
\varphi_0(t) &= \sqrt{\frac{1}{T}} \\
\varphi_1^c(t) &= \sqrt{\frac{2}{T}} \cos\left(2\pi\frac{t}{T}\right) \quad \text{and} \quad \varphi_1^s(t) = \sqrt{\frac{2}{T}} \sin\left(2\pi\frac{t}{T}\right) \\
\varphi_2^c(t) &= \sqrt{\frac{2}{T}} \cos\left(4\pi\frac{t}{T}\right) \quad \text{and} \quad \varphi_2^s(t) = \sqrt{\frac{2}{T}} \sin\left(4\pi\frac{t}{T}\right) \\
&\vdots \qquad\qquad\qquad\qquad\qquad\qquad \vdots \\
\varphi_K^c(t) &= \sqrt{\frac{2}{T}} \cos\left(2K\pi\frac{t}{T}\right) \quad \text{and} \quad \varphi_K^s(t) = \sqrt{\frac{2}{T}} \sin\left(2K\pi\frac{t}{T}\right).
\end{aligned} \tag{8.24}
$$

Recall that in block-orthogonal signaling the error probability can be reduced by increasing the duration T. However, as shown in Table 8.1, the number of dimensions per second for block-orthogonal signaling grows exponentially on T. On the other hand, the dimensionality theorem states that the number of dimensions per second is roughly $2W$. Because of this, it becomes clear that block-orthogonal signaling has a very unpleasant property that concerns bandwidth: to decrease P_{e} the channel bandwidth also has to grow.

8.6 Time or Frequency Limitations

In this chapter we have studied building-block waveforms that are time-limited. As a consequence these waveforms have a spectrum which is not frequency-limited. We can also investigate building-block waveforms that are frequency-limited. However this limitation implies that these waveforms are not time-limited anymore. Chapter 10 on pulse modulation deals with such building blocks.

Chapter 9

Capacity of the Baseband and Wideband Channels

SUMMARY: Here we determine first the channel capacity of the baseband AWGN waveform channel. We approach this problem in a geometrical way. The key idea is random selection or random code generation (Shannon, 1948). Then we find the capacity of the AWGN waveform channel in the case of unlimited bandwidth resources (i.e., the wideband AWGN channel). The result that is obtained in this way shows that block-orthogonal signaling is optimal.

9.1 Introduction, Capacity of the Vector Channel

In the previous chapter we have seen that for a waveform channel with bandwidth W, the number of available dimensions per second is roughly $2W$. We have also seen that reliable block-orthogonal signaling requires a lot of dimensions per second which is quite bad considering bandwidth. On the other hand bit-by-bit signaling requires as many dimensions as there are bits to be transmitted, which is acceptable from the bandwidth perspective. But bit-by-bit signaling can only made reliable by increasing the transmitter power P_s or by decreasing the rate R.

This raises the question whether we can achieve reliable transmission at certain rates R by increasing T, when both the bandwidth W and available power P_s are fixed. The following sections show that this is indeed possible. We will describe the results obtained by Shannon [13]. His analysis has a strong geometrical flavor. These early results may not be as strong as possible but they certainly are very surprising and give the right intuition.

We start by stating a result that will be proved in Sec. 9.5:

RESULT 9.1 *For the AGN vectorial channel, there exist for N large enough, sets of $|\mathcal{M}|$ vectors, $\underline{s}_1, \underline{s}_2, \ldots, \underline{s}_{|\mathcal{M}|}$ where $\|\underline{s}_m\|^2 \approx NE_N$ for all $m = 1, 2, \ldots, |\mathcal{M}|$ and where $P_{\mathrm{e}} \approx 0$*

as long as

$$R_N \triangleq \frac{\log_2 |\mathcal{M}|}{N} < C_N \triangleq \frac{1}{2}\log_2\left(\frac{E_N + N_0/2}{N_0/2}\right) \qquad \left[\frac{\textit{bit}}{\textit{dimension}}\right], \tag{9.1}$$

where all vectors have length N, are equiprobable, and where E_N is the available energy per dimension. It can also be shown that P_e cannot be small if the rate per dimension $R_N > C_N$.

We call C_N the channel **capacity** of the additive Gaussian vector channel in bits per dimension. We focus here on the *capacity per dimension*, not per unit of bandwidth, as we are dealing with the AGN channel.

9.2 Capacity of the baseband (AWGN) Channel

In the previous chapter we have seen that a waveform channel with bandwidth W can accommodate (roughly) at most $2W$ dimensions per second. With $2W$ dimensions per second, the available energy per dimension is $E_N = P_s/(2W)$ if P_s is the available transmitter power. In that case the channel capacity in bit per dimension is

$$C_N = \frac{1}{2}\log_2\left(\frac{\frac{P_s}{2W} + N_0/2}{N_0/2}\right) = \frac{1}{2}\log_2\left(1 + \frac{P_s}{WN_0}\right). \tag{9.2}$$

Therefore we obtain the following result, which gives an expression for the channel capacity of the baseband AWGN channel in Sec. 2.1.3.

THEOREM 9.2 *For a waveform channel with spectral noise density $N_0/2$, frequency bandwidth W, and available transmitter power P_s, the capacity in bit per second is*

$$C = 2WC_N = W\log_2\left(1 + \frac{P_s}{WN_0}\right) \qquad \left[\frac{\textit{bit}}{\textit{second}}\right]. \tag{9.3}$$

Thus reliable communication is possible for rates R in bit per second smaller than C, while rates larger than C are not realizable with arbitrary small P_e.

9.3 Capacity of the Wideband AWGN Channel

We have seen in Sec. 8.3.2 that with block-orthogonal signaling we can achieve reliable communication at rates

$$R < \frac{P_s}{N_0 \ln 2} \qquad \left[\frac{\text{bit}}{\text{second}}\right], \tag{9.4}$$

if we only had access to as much bandwidth as we would want. We will show next that rates larger than $P_s/(N_0 \ln 2)$ are not realizable with reliable signaling schemes. Therefore we may indeed call $P_s/(N_0 \ln 2)$ the capacity of the wideband AWGN channel.

In the previous section (see Theorem 9.2) the capacity of a waveform channel with frequency bandwidth limited to W was shown to be

$$C = W \log_2 \left(1 + \frac{P_s}{W N_0}\right) \quad \left[\frac{\text{bit}}{\text{second}}\right]. \tag{9.5}$$

We can easily determine the wideband capacity by letting $W \to \infty$. This is shown in the next result.

RESULT 9.3 *The capacity C_∞ of the* **wideband AWGN channel** *with power spectral density $N_0/2$, when the transmitter power is P_s, follows from:*

$$\begin{aligned} C_\infty &= \lim_{W \to \infty} W \log_2 \left(1 + \frac{P_s}{W N_0}\right) \\ &= \lim_{W \to \infty} \frac{P_s}{N_0 \ln 2} \frac{\ln\left(1 + \frac{P_s}{W N_0}\right)}{\frac{P_s}{W N_0}} = \frac{P_s}{N_0 \ln 2}. \end{aligned} \tag{9.6}$$

Note that, expressed in nats per second, this capacity would be equal to P_s/N_0.

9.4 Relation Between Capacities and SNR

Note that we can express the capacity of the baseband AWGN channel as

$$\begin{aligned} C &= W \log_2 \left(1 + \frac{P_s}{W N_0}\right) \\ &= \frac{P_s}{N_0 \ln 2} \frac{\ln\left(1 + \frac{P_s}{W N_0}\right)}{\frac{P_s}{W N_0}} = C_\infty \frac{\ln(1 + \text{SNR})}{\text{SNR}}, \text{ with SNR} \triangleq \frac{P_s}{W N_0}. \end{aligned} \tag{9.7}$$

Here SNR is the signal-to-noise ratio of the waveform channel. Note that the total noise power is equal to the frequency band $2W$ times the power spectral density $N_0/2$ of the noise. We have plotted the ratio $\ln(1 + \text{SNR})/\text{SNR}$ in Fig. 9.1. Using the SNR definition above, we can express the capacity in (9.3) as $C/N = \log_2(1 + \text{SNR})$. This is also shown in Fig. 9.1.

RESULT 9.4 *If we note that $C = W \log_2(1 + SNR)$ then we can can distinguish between two cases.*

$$C \approx \begin{cases} C_\infty & \text{if } SNR \ll 1, \\ W \log_2(SNR) & \text{if } SNR \gg 1. \end{cases} \tag{9.8}$$

The case $SNR \ll 1$ is called the **power-limited** *regime. There is enough bandwidth. When on the other hand $SNR \gg 1$ we speak about* **bandwidth-limited** *channels.*

Finally we give some other ways to express the signal-to-noise ratio (under the assumption that the number of dimensions per second is exactly $2W$):

$$\text{SNR} = \frac{P_s}{W N_0} = \frac{E_N}{N_0/2} = 2R_N \frac{E_b}{N_0} = \frac{R}{W} \frac{E_b}{N_0}. \tag{9.9}$$

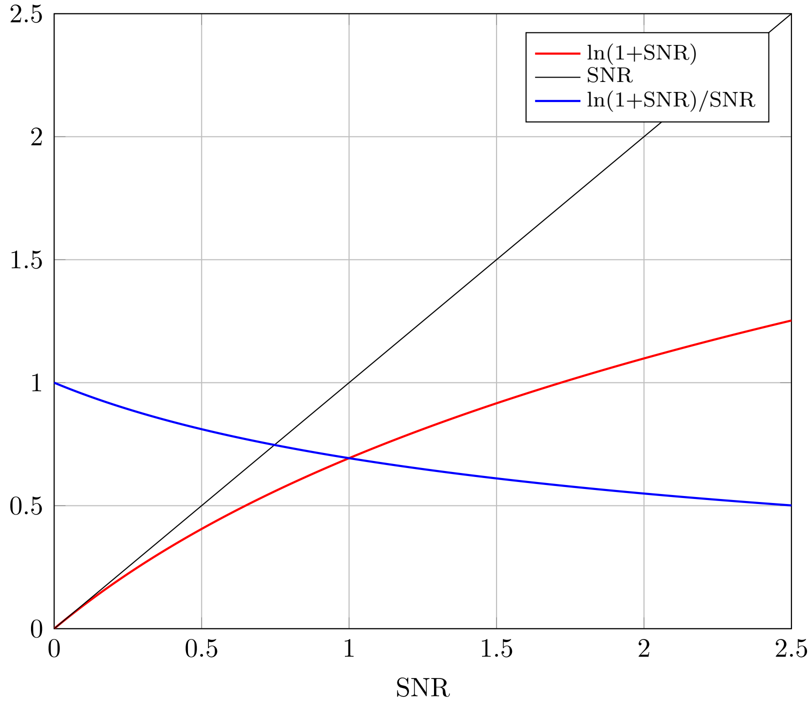

Figure 9.1: The ratio $\ln(1 + \text{SNR})/\text{SNR}$ and $\ln(1 + \text{SNR})$ as function of the SNR.

9.5 Capacity Proof, Random Selection

In this section we will prove Result 9.1.

9.5.1 Normalized Vectors

It has advantages to consider here *normalized* versions of the signal, noise and received vectors. These normalized versions are defined in the following way:

Definition 9.1 *The normalized version $\underline{r}'$ of the received vector $\underline{r}$ is defined by*

$$\underline{r}' \triangleq \underline{r}/\sqrt{N}.$$

As usual N is the number of components in $\underline{r}$ or the number of dimensions. Similar definitions hold for normalized signal vectors $\underline{s}'_m$, for $m \in \mathcal{M}$, and for the normalized noise vector $\underline{n}'$.

9.5.2 Sphere Hardening - Gaussian Vectors

We will first show that Gaussian spheres, when the number of dimensions N grows, become harder and harder. We will see next what this means.

The random Gaussian vector $\underline{G}$ has N components, each with mean 0 and variance σ_g^2. The normalized noise vector $\underline{G}' = \underline{G}/\sqrt{N}$. Its expected squared length is

$$E\left[\|\underline{G}'\|^2\right] = E\left[\frac{1}{N}\sum_{i=1}^{N} G_i^2\right] = \frac{1}{N}\sum_{i=1}^{N} E\left[G_i^2\right] = \frac{1}{N}\sum_{i=1}^{N}\sigma_g^2 = \sigma_g^2. \tag{9.10}$$

For the case of the original vector $\underline{G}$, we have

$$E\left[\|\underline{G}\|^2\right] = N\sigma_g^2. \tag{9.11}$$

For the variance of the squared length of $\underline{G}'$ we find that

$$\begin{aligned}
\text{var}\left[\|\underline{G}'\|^2\right] &= \frac{1}{N^2}\text{var}\left[\sum_{i=1}^{N} G_i^2\right] = \frac{1}{N^2}\sum_{i=1}^{N}\text{var}\left[G_i^2\right] \\
&= \frac{1}{N^2}\sum_{i=1}^{N}\left(E[G_i^4] - (E[G_i^2])^2\right) \\
&= \frac{1}{N^2}\sum_{i=1}^{N}\left(3\sigma_g^4 - (\sigma_g^2)^2\right) = \frac{2\sigma_g^4}{N}.
\end{aligned} \tag{9.12}$$

The second equality in this derivation holds since $G_1, G_2, \ldots, G_N$ are independent. Moreover we have used that $E[G_i^4] = 3\sigma_g^4$. Finally observe that $\frac{2\sigma_g^4}{N}$ approaches zero for $N \to \infty$.

Chebyshev's inequality[1] can be now used to show that the probability of observing a normalized noise vector with squared length smaller than $\sigma_g^2 - \varepsilon$ or larger than $\sigma_g^2 + \varepsilon$ for any fixed $\varepsilon > 0$ approaches zero for $N \to \infty$. More precisely

$$\begin{aligned}
\Pr\left\{\left|\|\underline{G}'\|^2 - \sigma_g^2\right| > \varepsilon\right\} &\leq \frac{\text{var}\left[\|\underline{G}'\|^2\right]}{\varepsilon^2} \\
&= \frac{2\sigma_g^4/N}{\varepsilon^2} \\
&= \frac{2}{N}\frac{\sigma_g^4}{\varepsilon^2}.
\end{aligned} \tag{9.13}$$

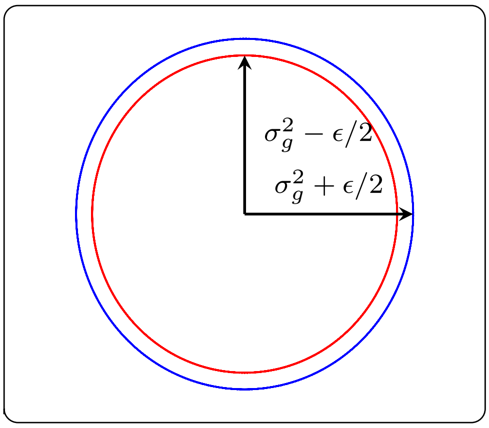

Figure 9.2: Hardening of Gaussian sphere.

This shows the "hardening" effect, which is represented in Fig. 9.2.

RESULT 9.5 *The normalized received vector $\underline{g}$ is (roughly speaking)* **on the surface of a hypersphere** *with radius $\sqrt{\sigma_g^2}$. Fluctuations are possible, however for $N \to \infty$ these fluctuations disappear.*

[1] This inequality states that for a random variable X with mean μ and variance σ^2, $\Pr\{|X - \mu| \geq \varepsilon\} \leq \sigma^2/\varepsilon^2$ for every ε.

9.5.3 Capacity-achieving signals sets

Shannon [13] constructed an *existence proof* to show that there are signal sets that allow reliable communication and that contain surprisingly many signals. His argument involved *random coding*. This concept is discussed in this section.

Generating a random code

Fix the number of signal vectors $|\mathcal{M}|$ and their number of components (dimensions) N. To obtain a signal set, we select $|\mathcal{M}|$ signal vectors $\underline{s}_1, \underline{s}_2, \ldots, \underline{s}_{|\mathcal{M}|}$ *at random*, independently of each other. Each vector-component is a random sample from a Gaussian density with mean 0 and variance E_N. Consider the ensemble of all signal sets that can be chosen in this way.

Note that the noise vectors $\underline{n}$ are Gaussian too, with all components being independent of each other, and having mean 0 and variance $N_0/2$.

The resulting channel output-vector $\underline{r} = \underline{s}_m + \underline{n}$ is the sum of two independent Gaussian vectors is consequently also Gaussian, with all components having mean 0 and variance $E_N + N_0/2$. The total variance is $N(E_N + N_0/2)$.

Energy per dimension

Note that the *expected energy per dimension* in this way is equal to the variance of the Gaussian density that is used to generate the components of the signal vectors. By the sphere-hardening argument in (9.11) we can also say that the *energies of the vectors* are actually roughly NE_N.

Error probability

We are now interested in P_e^{av}, i.e., the error probability P_e *averaged over the ensemble of signal sets*, i.e.,

$$P_{\mathrm{e}}^{\mathrm{av}} = \int_{\mathbb{R}^{N\cdot|\mathcal{M}|}} p(\underline{s}_1, \underline{s}_2, \ldots, \underline{s}_{|\mathcal{M}|}) P_{\mathrm{e}}(\underline{s}_1, \underline{s}_2, \ldots, \underline{s}_{|\mathcal{M}|}) d\underline{s}_1 d\underline{s}_2 \ldots d\underline{s}_{|\mathcal{M}|}. \tag{9.14}$$

The averaging corresponds to the selection of the signal sets $\{\underline{s}_1, \underline{s}_2, \ldots, \underline{s}_{|\mathcal{M}|}\}$. Once we know P_e^{av} we claim that there exists *at least one signal set* $\{\underline{s}_1, \underline{s}_2, \ldots, \underline{s}_{|\mathcal{M}|}\}$ with error probability $P_e(\underline{s}_1, \underline{s}_2, \ldots, \underline{s}_{|\mathcal{M}|}) \leq P_e^{av}$. Therefore we will first show that P_e^{av} is small enough.

Consider Fig. 9.3, in which we focus on the normalized vectors $\underline{s}'_m$, $\underline{n}'$, and $\underline{r}'$. Suppose that the signal $\underline{s}'_m$ for some fixed $m \in \mathcal{M}$ was actually sent. The noise vector $\underline{n}'$ is added to the signal vector and hence the received vector turns out to be $\underline{r}' = \underline{s}'_m + \underline{n}'$. Now an optimum receiver will decode the message m only if there are no other signals $\underline{s}'_k, k \neq m$, inside a hypersphere with radius $\|\underline{n}'\|$ around $\underline{r}'$. This is shown with a red line in Fig. 9.3. This is a consequence of Result 4.4 that says that minimum Euclidean distance decoding is optimum if all messages are equally likely.

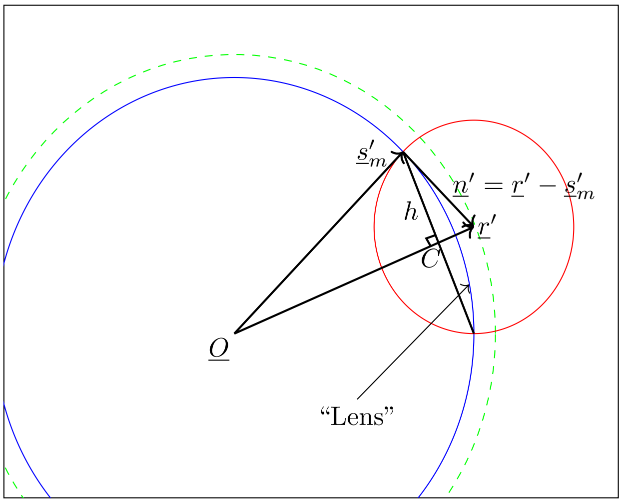

Figure 9.3: Random coding situation. The blue sphere has radius $\sqrt{E_N}$ and the dashed green sphere has radius $\sqrt{E_N + N_0/2}$.

- Note that Result 9.5 implies that, for $N \to \infty$, the signal $\underline{s}'_m$ was chosen on the surface of a sphere with radius $\sqrt{E_N}$. This is a consequence of the random selection procedure of the signal vectors based on Gaussian random variables. Note that each component had mean 0 and variance E_N. Therefore we may assume that $\|\underline{s}'_m\|^2 = E_N$.

- Now consider the received vector $\underline{r}'$. By Result 9.5 the normalized received vector $\underline{r}'$ is now, for $N \to \infty$, on the surface of a sphere with radius $\sqrt{E_N + N_0/2}$ centered at the origin, and thus, $\|\underline{r}'\|^2 = E_N + N_0/2$.

- Moreover the normalized noise vector $\underline{n}'$ is on the surface of a sphere with radius $\sqrt{N_0/2}$ hence $\|\underline{n}'\|^2 = N_0/2$ again by the sphere-hardening argument (see Result 9.5).

Observing the lengths of $\underline{s}'_m$, $\underline{n}'$, and $\underline{r}'$, we may conclude that the angle between the normalized signal vector $\underline{s}'_m$ and the normalized noise vector $\underline{n}'$ is $\pi/2$ (Pythagoras).

First we have to determine the probability that the signal corresponding to some message $k \neq m$ is inside the sphere with center $\underline{r}'$ and radius $\|\underline{n}'\|$. Therefore we need to know the surface area A_{lens} of the "lens" in the Fig. 9.3, the part that is on the surface of the sphere on which the signals-vectors are. Determining this surface area is not so easy but we know that it is not larger than the surface area of a sphere with radius h, see Fig. 9.3, and center coinciding with the center C of the lens. This hypersphere contains the lens. Our next problem is therefore to find out how large h is.

Now we can use simple geometry to determine the length h:

$$h = \frac{\sqrt{E_N}\sqrt{\frac{N_0}{2}}}{\sqrt{E_N + \frac{N_0}{2}}}, \tag{9.15}$$

and consequently[2]

$$A_{\text{lens}} \leq B_N h^{N-1} = B_N \left(\frac{E_N \frac{N_0}{2}}{E_N + \frac{N_0}{2}} \right)^{(N-1)/2} . \tag{9.16}$$

The probability that a signal $\underline{s}_k$ for a specific $k \neq m$ was selected on the surface of the lens is now given by the surface area of the lens divided by the surface area of the sphere where the signal vectors are. This ratio can be upper-bounded as follows

$$\frac{A_{\text{lens}}}{B_N E_N^{(N-1)/2}} \leq \left(\frac{\frac{N_0}{2}}{E_N + \frac{N_0}{2}} \right)^{(N-1)/2} . \tag{9.17}$$

By the union bound[3] the probability that any signal $\underline{s}_k$ for $k \neq m$ is chosen inside the lens is at most $|\mathcal{M}| - 1$ times as large as the ratio (probability) considered in (9.17). Therefore we obtain for the error probability averaged over the ensemble of signal sets

$$P_{\text{e}}^{\text{av}} \leq |\mathcal{M}| \left(\frac{\frac{N_0}{2}}{E_N + \frac{N_0}{2}} \right)^{(N-1)/2} . \tag{9.18}$$

Now fix any $\delta > 0$. Suppose that the number of signals $|\mathcal{M}|$ as a function of the number of dimensions N is given by

$$|\mathcal{M}| = 2^{-\delta N} \left(\frac{E_N + \frac{N_0}{2}}{\frac{N_0}{2}} \right)^{N/2} , \tag{9.19}$$

and consequently the rate (in bits per dimension)

$$R_N = \frac{\log_2 |\mathcal{M}|}{N} = C_N - \delta, \tag{9.20}$$

then

$$\lim_{N \to \infty} P_{\text{e}}^{\text{av}} \leq \lim_{N \to \infty} 2^{-\delta N} \sqrt{\frac{E_N + N_0/2}{N_0/2}} = 0. \tag{9.21}$$

Since this holds for all $\delta > 0$ we may conclude that there exist signal sets, one for each value of N, for all values of the rate $R_N < C_N$, for which $\lim_{N \to \infty} P_{\text{e}} = 0$. This completes the proof of Result 9.1.

[2] Note that the surface of an N-dimensional hypersphere of radius r is $B_N \cdot r^{N-1}$, where B_N is a constant that depends only on N.

[3] For K events $E_1, E_2, \ldots, E_K$ the probability $\Pr\{E_1 \cup E_2 \cup \ldots \cup E_K\} \leq \Pr\{E_1\} + \Pr\{E_2\} + \ldots + \Pr\{E_K\}$.

9.6 How well can we do in practice?

In the previous section we have shown that signal sets exist that allow reliable communication at rates arbitrarily close to the capacity. That is, signal sets exist that achieve negligible error probability for $N \to \infty$. The obvious follow-up question is: How can we find such signal sets, and what is their performance in terms of error probability given a practical value of N? The answer to the first part of the question is given by the achievability proof in the previous section: we can use randomly generated codes.

Example 9.1 In Fig. 9.4 we have depicted the behavior of randomly generated codes. In a MATLAB program we have generated codes (signal sets) with $R_N = 1$ bit/dimension and vector-lengths $N = 4, 8, 12,$ and 16. Note that reliable transmission of $R_N = 1$-codes is only possible for signal-to-noise ratios $E_N/\frac{N_0}{2} \geq 3$, or 4.7 dB. These codes are therefore tested with $E_N/\frac{N_0}{2}$ between 3 and 11 dB. The resulting error probabilities for vector-lengths 4,8,12, and 16 are listed in Fig. 9.4. For each experiment we have generated 32 codes, and each code was tested with 256 randomly-generated messages. The resulting number of errors was divided by 8192 to give an estimate of the error probability. The figure clearly shows that increasing N results in decreasing error-probabilities for $E_N/\frac{N_0}{2} \geq 5$ dB. Simulations for $N \geq 20$ turned out to be unfeasible in MATLAB.

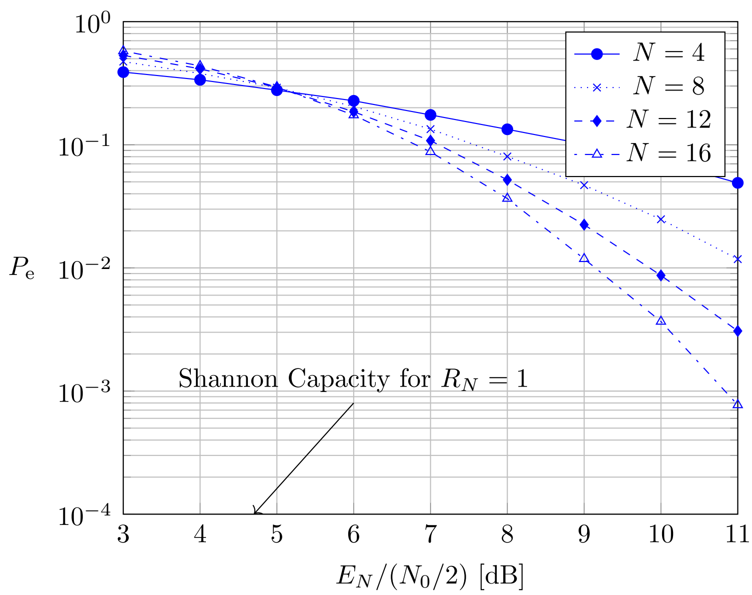

Figure 9.4: Error probability as a function of $E_N/\frac{N_0}{2}$ for codes with different lengths.

The disadvantage of a randomly generated code is its lack of structure. As a result, storing the mapping from messages to corresponding codewords (as well as the decoder mapping) is very inefficient and quickly becomes infeasible for large N. Over the years, various codes have been proposed that have a certain structure, and thus, allow for a more efficient encoding and decoding. Examples of very good codes are the so-called turbo codes, low-density parity-check (LDPC) codes, and (more recently) polar codes.

Example 9.2 In Fig. 9.5 we have depicted the behavior of polar codes, a family of modern, capacity-approaching codes. In a MATLAB program we have generated codes (signal sets) with $R_N = 1/2$ bit/dimension and vector-lengths $N = 2^8$, till $N = 2^{14}$. Note that reliable transmission of $R_N = 1/2$-codes is only possible for signal-to-noise ratios $E_N/\frac{N_0}{2} \geq 1$, i.e., 0 dB. These codes are therefore tested with $E_N/\frac{N_0}{2}$ above -0.5 dB. The resulting error probabilities are listed in Fig. 9.5. This figure shows that these codes perform very close to the capacity limit. Furthermore, these codes are well-structured and decoding can be performed with relatively low complexity even for large lengths.

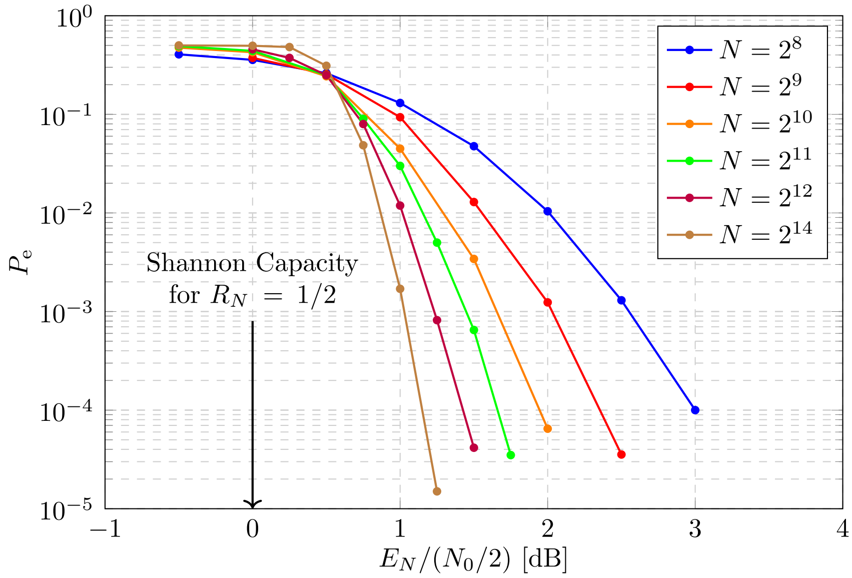

Figure 9.5: Error probability as a function of $E_N/\frac{N_0}{2}$ for Polar Codes codes with different lengths.

Chapter 10

Pulse Transmission

SUMMARY: In this chapter we discuss serial pulse amplitude modulation. This method provides us with a new channel dimension every T seconds if we choose the pulse according to the so-called Nyquist criterion. The Nyquist criterion implies that the required channel bandwidth W is larger than $1/(2T)$.

10.1 Problem Description

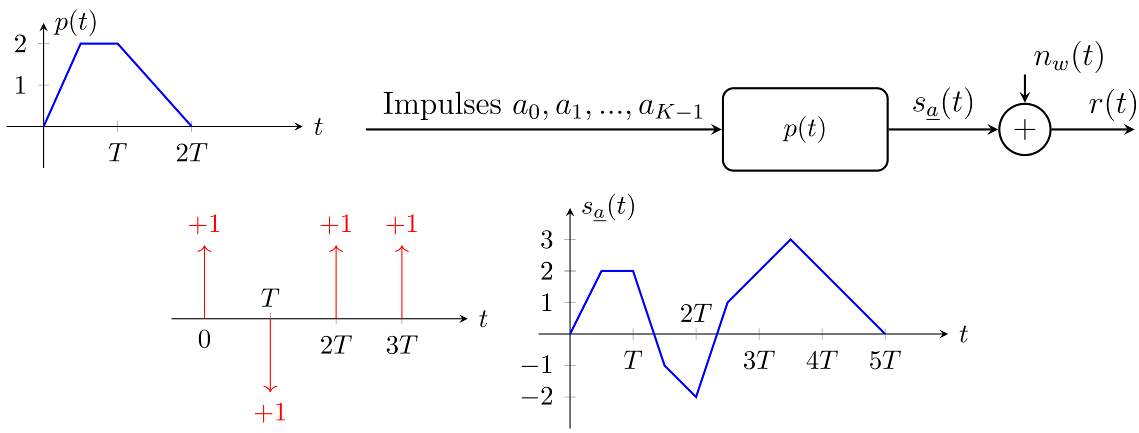

Figure 10.1: A serial pulse-amplitude modulation system.

We have observed before that a channel with a bandwidth of W Hz can accommodate roughly $2WT$ dimensions each T seconds. We considered building-block waveforms of finite duration, therefore the bandwidth constraint could only be met approximately. Here we will investigate whether it is possible to get a new dimension every $1/(2W)$ seconds. We allow the building blocks to have a non finite duration. Moreover all these building blocks are time-shifts of the same "pulse". The subject of this chapter is therefore called *serial pulse transmission.*

Consider Fig. 10.1. We assume that the transmitter sends a signal $s_{\underline{a}}(t)$ that consists of amplitude-modulated time shifts of a pulse $p(t)$ by an integer multiple k of the so-called *modulation interval* T, hence

$$s_{\underline{a}}(t) = \sum_{k=0}^{K-1} a_k p(t - kT). \tag{10.1}$$

The vector of amplitudes $\underline{a} = (a_0, a_1, \ldots, a_{K-1})$ consists of symbols $a_k, k = 0, ..., K-1$ taking values in the alphabet $\mathcal{A}$. We call this modulation method serial *pulse-amplitude modulation (PAM)*. We are now interested in the property of a pulse that makes all its shifts orthonormal. Serial PAM can be seen as a generalization of the bit-by-bit signaling we studied in Sec. 8.2. The differences are that here we will consider BW-limited pulses and nonbinary alphabets $\mathcal{A}$.

10.2 Orthonormal Pulses: the Nyquist Criterion

10.2.1 The Nyquist result

If we have the possibility to choose the pulse $p(t)$ ourselves we can choose it in such a way that all time shifts of the pulse form an orthonormal base. In that case the pulse $p(t)$ has to satisfy

$$\int_{-\infty}^{\infty} p(t - kT)p(t - k'T)dt = \begin{cases} 1 & \text{if } k = k', \\ 0 & \text{if } k \neq k', \end{cases} \tag{10.2}$$

for integer k and k'. This is equivalent to

$$\int_{-\infty}^{\infty} p(\alpha)p(\alpha - kT)d\alpha = p(t) * p(-t)|_{t=kT} = h(kT) = \begin{cases} 1 & \text{if } k = 0, \\ 0 & \text{if } k \neq 0, \end{cases} \tag{10.3}$$

where $h(t) \triangleq p(t) * p(-t)$. This time-domain restriction on the pulse $p(t)$ is called the zero-forcing (ZF) criterion. Later we will see why. This restriction is imposed so that no intersymbol interference occurs. In other words, when detecting the symbol at time k, we would like not to see interference from other symbols.

THEOREM 10.1 *The frequency-domain equivalent to (10.3) which is known as the Nyquist criterion for zero intersymbol interference is*

$$\begin{aligned} Z(f) &= \frac{1}{T} \sum_{m=-\infty}^{\infty} H(f + m/T) \\ &= \frac{1}{T} \sum_{m=-\infty}^{\infty} |P(f + m/T)|^2 = 1 \quad \textit{for all } f, \end{aligned}$$

where $H(f) = P(f)P^*(f) = |P(f)|^2$ is the Fourier transform of $h(t) = p(t) * p(-t)$. Note that $|P(f)|$ is the modulus of $P(f)$. Moreover $Z(f)$ is called the $1/T$-aliased spectrum of $H(f)$.

Later in this section we will give the proof of this theorem. First we will discuss the theorem and consider an important consequence of it.

10.2.2 Discussion

Since $p(t)$ is a real signal, the real part of its spectrum $P(f)$ is even in f, and the imaginary part of this spectrum is odd. Therefore the modulus $|P(f)|$ of $P(f)$ is an even function of the frequency f.

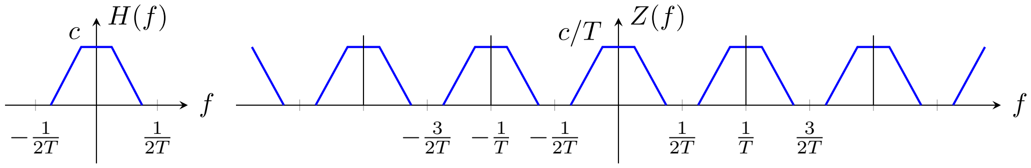

Figure 10.2: The spectrum $H(f) = |P(f)|^2$ corresponding to a pulse $p(t)$ that does not satisfy the Nyquist criterion.

If the bandwidth W of the pulse $p(t)$ is strictly smaller than $1/(2T)$ (see Fig. 10.2), then the Nyquist criterion, which is based on $H(f) = |P(f)|^2$, can not be satisfied. Thus no pulse $p(t)$ that satisfies a bandwidth-W constraint, can lead to orthogonal signaling if $W < 1/(2T)$.

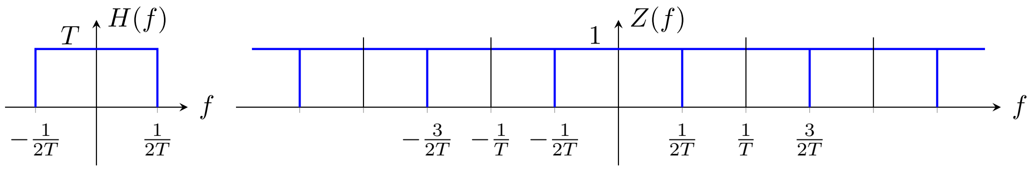

Figure 10.3: The ideally bandlimited spectrum $H(f) = |P(f)|^2$. Note that $P(f)$ is a spectrum with the smallest possible bandwidth satisfying the Nyquist criterion.

The smallest possible bandwidth W of a pulse that satisfies the Nyquist criterion is $1/(2T)$. The "basic" pulse with bandwidth $1/(2T)$ for which the Nyquist criterion holds has a so-called brick-wall (ideally bandlimited) spectrum, which is given by

$$P(f) = \begin{cases} \sqrt{T} & \text{if } |f| < 1/(2T), \\ 0 & \text{if } |f| > 1/(2T), \end{cases} \tag{10.4}$$

and $\sqrt{T/2}$ for $|f| = 1/(2T)$. The corresponding $H(f) = |P(f)|^2$ and $1/T$-aliased spectrum $Z(f)$ can be found in Fig. 10.3.

The basic pulse $p(t)$ that corresponds to the ideally bandlimited spectrum is shown in Fig. 10.4. It is the well-known sinc-pulse

$$p(t) = \frac{1}{\sqrt{T}} \frac{\sin(\pi t/T)}{\pi t/T}. \tag{10.5}$$

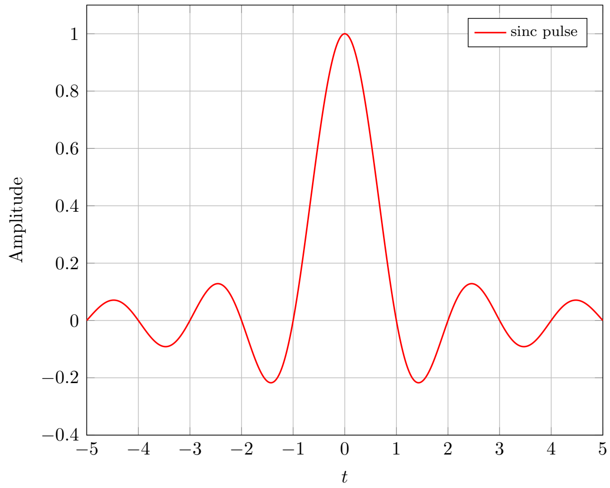

Figure 10.4: The sinc-pulse that corresponds to $T = 1$, i.e., $p(t) = \sin(\pi t)/(\pi t)$.

A pulse with a bandwidth larger than $1/(2T)$ can also satisfy the Nyquist criterion as can be seen in Fig. 10.5. Note that the so-called *excess bandwidth*, i.e., the bandwidth minus $1/(2T)$, can be larger than $1/(2T)$.

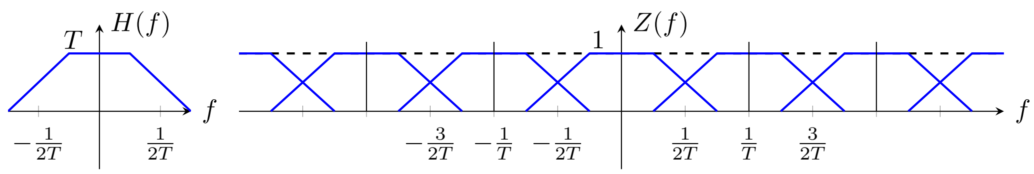

Figure 10.5: A spectrum $H(f)$ with a positive excess bandwidth satisfying the Nyquist criterion.

Now we are ready to state the implication of the previous discussion.

RESULT 10.2 *The smallest possible bandwidth W of a pulse that satisfies the Nyquist criterion is $W = \frac{1}{2T}$. The sinc-pulse $p(t) = \frac{1}{\sqrt{T}}\frac{\sin(\pi t/T)}{\pi t/T}$ has this property. This way of serial pulse transmission leads to exactly $\frac{1}{T} = 2W$ dimensions per second.*

The fact that the sinc-pulse is not causal is not really important. In practice we can use a delayed version that has the same properties as the "real" sinc pulse. In theory the delay should be infinity (as $p(t)$ is infinitely long). In practice, however, $p(t)$ is typically truncated.

10.2.3 Proof of the Nyquist result

We will next give the proof of Theorem 10.1, the Nyquist result.

Proof: Since $H(f)$ is the Fourier transform of $h(t)$, the condition (10.3) can be rewritten as

$$h(kT) = \int_{-\infty}^{\infty} H(f)\exp(j2\pi fkT)df = \begin{cases} 1 & \text{if } k = 0, \\ 0 & \text{if } k \neq 0. \end{cases} \tag{10.6}$$

We now break up the integral in parts, a part for each integer m, and obtain

$$\begin{aligned} h(kT) &= \sum_{m=-\infty}^{\infty} \int_{(2m-1)/2T}^{(2m+1)/2T} H(f)\exp(j2\pi fkT)df \\ &= \sum_{m=-\infty}^{\infty} \int_{-1/2T}^{1/2T} H\left(f+\frac{m}{T}\right)\exp(j2\pi fkT)df \\ &= \int_{-1/2T}^{1/2T} \left[\sum_{m=-\infty}^{\infty} H\left(f+\frac{m}{T}\right)\right]\exp(j2\pi fkT)df \\ &= T\int_{-1/2T}^{1/2T} Z(f)\exp(j2\pi fkT)df \end{aligned} \tag{10.7}$$

where we have defined $Z(f)$ by

$$Z(f) \triangleq \frac{1}{T}\sum_{m=-\infty}^{\infty} H\left(f+\frac{m}{T}\right). \tag{10.8}$$

Observe that $Z(f)$ is a periodic function in f with period $1/T$. Therefore it can be expanded in terms of its Fourier series coefficients $\dots, z_{-1}, z_0, z_1, z_2, \dots$ as

$$Z(f) = \sum_{k'=-\infty}^{\infty} z_{k'}\exp(j2\pi k' fT) \tag{10.9}$$

where

$$z_{k'} = T\int_{-1/2T}^{1/2T} Z(f)\exp(-j2\pi fk'T)df. \tag{10.10}$$

If we now combine (10.7) and (10.9) we obtain that

$$h(-kT) = z_k, \tag{10.11}$$

for all integers k. Condition (10.3) now tells us that only $z_0 = 1$ and all other z_k are zero. This implies that (see (10.9))

$$Z(f) = 1, \tag{10.12}$$

or equivalently (see (10.8))

$$\frac{1}{T}\sum_{m=-\infty}^{\infty} H\left(f+\frac{m}{T}\right) = 1. \tag{10.13}$$

□

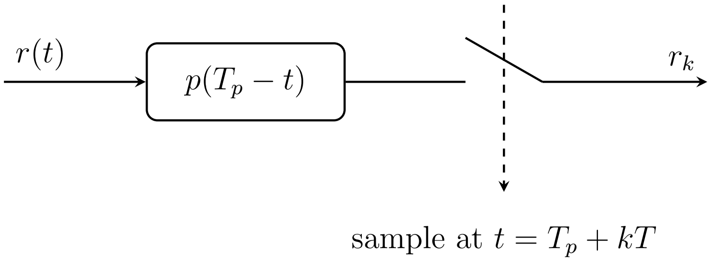

Figure 10.6: The optimum receiver front-end for detection of serially transmitted orthonormal pulses.

10.3 Receiver Implementation

If we use serial PAM with orthonormal pulses $p(t - kT), k = 0, ..., K - 1$, then we can use a single matched-filter $m(t) = p(T_p - t)$ for the computations of the correlations of the received waveform $r(t)$ with all building-block waveforms, i.e., with all pulses. Assume that the delay T_p is chosen in such a way that $m(t)$ is (effectively[1]) causal. The output of this filter $m(t)$ when $r(t)$ is the input signal is

$$u(t) = \int_{-\infty}^{\infty} r(\alpha)m(t - \alpha)d\alpha = \int_{-\infty}^{\infty} r(\alpha)p(T_p - t + \alpha)d\alpha. \tag{10.14}$$

At time $t = T_p + kT$ we see at the filter output

$$r_k = u(T_p + kT) = \int_{-\infty}^{\infty} r(\alpha)p(\alpha - kT)d\alpha, \tag{10.15}$$

which is what the optimum receiver should determine, i.e., the correlation of $r(t)$ with the pulse $p(t - kT)$. This leads to the very simple receiver structure shown in Fig. 10.6. Processing the samples $r_k, k = 1, ..., K$, should be done in the usual way.

When there is no noise $r(t) = \sum_{k=0}^{K-1} a_k p(t - kT)$. Then at time $t = T_p + kT$ we see at the filter output

$$\begin{aligned} r_k = u(T_p + kT) &= \int_{-\infty}^{\infty} r(\alpha)p(\alpha - kT)d\alpha \\ &= \int_{-\infty}^{\infty} \sum_{k=0}^{K-1} a_{k'} p(\alpha - k'T)p(\alpha - kT)d\alpha \\ &= \sum_{k'=0}^{K-1} a_{k'} \int_{-\infty}^{\infty} p(\alpha - k'T)p(\alpha - kT)d\alpha \\ &= a_k, \end{aligned} \tag{10.16}$$

[1]Note that $p(t)$ has a nonfinite duration in general.

by the orthonormality of the pulses. Conclusion is that there is no intersymbol interference present in the samples. In other words the Nyquist criterion forces the intersymbol interference to be zero. This is why we called the time restriction in (10.3) the zero-forcing (ZF) criterion.

10.4 Performance in AWGN

Here we briefly discuss the performance of the optimum receiver front-end of Fig. 10.6 in the presence of AGWN. In this case, $r(t) = s_{\underline{a}}(t) + n_w(t)$. When this signal is passed through the linear filter in Fig. 10.6, two components are generated. The first one is the signal component, which we showed in (10.16) to be equal to the transmitted signal at time k, i.e., a_k. The noise component can be shown to be a Gaussian random variable with zero mean and variance $N_0/2$. We can therefore conclude that the concatenation of the transmitter that maps the symbols $a_1, a_2, \ldots$ to a waveform, the channel, and the receiver in Fig. 10.6 can be modeled via a DICO AWG channel $r_k = a_k + n_k$. This is a very powerful result because it allows us to study optimum detection for a waveform channel using the techniques we discussed in Chapter 4.

Chapter 11

Pass-Band Channels

SUMMARY: Here we consider transmission over an ideal passband channel with bandwidth $2W$. We show that building-block waveforms for transmission over a passband channel can be constructed from baseband building-block waveforms having a bandwidth not larger than W. A first set of orthonormal baseband building-block waveforms can be modulated on a cosine carrier, a second orthonormal set on a sine carrier, and the resulting passband waveforms are all orthogonal to each other. This technique is called quadrature multiplexing. We determine the optimum receiver for this signaling method and the capacity of the passband channel. We finally discuss quadrature amplitude modulation (QAM).

11.1 Introduction

So far we have only considered *baseband communication*. In baseband communication the channel allows signaling only in the frequency band $[-W, W]$. But what should we do if the channel only accepts signals with a spectrum in the frequency band $\pm[f_0 - W, f_0 + W]$? In the present chapter we will describe a method that can be used for signaling over such a channel.

Consider Fig. 11.1, that shows an *ideal* passband channel. The input signal $s(t)$ to the passband channel is first sent through a filter $W_p(f)$. This filter $W_p(f)$ is an ideal passband

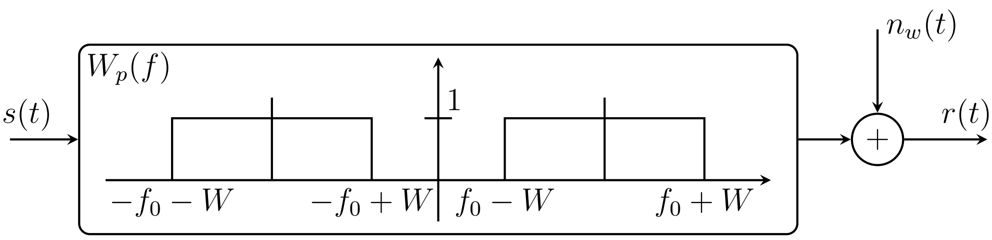

Figure 11.1: Ideal passband channel with AWGN.

filter with bandwidth $2W$ and center frequency $f_0 > W$. It has transfer function

$$W_p(f) \triangleq \begin{cases} 1 & \text{if } f_0 - W < |f| < f_0 + W, \\ 0 & \text{elsewhere.} \end{cases} \tag{11.1}$$

The noise process $N_w(t)$ is assumed to be stationary, Gaussian, zero-mean, and white. The noise has power spectral density function

$$S_{N_w}(f) = N_0/2 \text{ for } -\infty < f < \infty, \tag{11.2}$$

and autocorrelation function $R_{N_w}(t,s) \triangleq E[N_w(t)N_w(s)] = \frac{N_0}{2}\delta(t-s)$. The noise-waveform $n_w(t)$ is added to the output of the passband filter $W_0(f)$ which results in $r(t)$, the output of the passband channel.

In the next section we will describe a signaling method for a passband channel. This method is called *quadrature multiplexing*.

11.2 Quadrature Multiplexing

In quadrature multiplexing we combine two waveforms with a baseband spectrum into a waveform with a spectrum that matches with the passband channel. We assume that the two baseband waveforms together contain a single message.

Consider a first set of baseband waveforms $\{s_1^c(t), s_2^c(t), \ldots, s_{|\mathcal{M}|}^c(t)\}$ with waveform $s_m^c(t)$ for all $m \in \{1, 2, \ldots, |\mathcal{M}|\}$, having bandwidth smaller than W, i.e., with a spectrum $S_m^c(f) \equiv 0$ for $|f| \geq W$. To this set of baseband-waveforms there corresponds a set of building-block waveforms $\{\phi_i(t), i = 1, 2, \ldots, N_c\}$. For all $i = \{1, 2, \ldots, N_c\}$ the spectrum of the corresponding building-block waveform $\Phi_i(f) \equiv 0$ for $|f| \geq W$ since the building-block waveforms are linear combinations of the signal waveforms (Gram-Schmidt procedure, see Sec. 5.3).

Also consider a second set of baseband waveforms $\{s_1^s(t), s_2^s(t), \ldots, s_{|\mathcal{M}|}^s(t)\}$ with waveform $s_m^s(t)$ for all $m \in \{1, 2, \ldots, |\mathcal{M}|\}$ having bandwidth smaller than W, i.e., $S_m^s(f) \equiv 0$ for $|f| \geq W$. To this second set of waveforms there corresponds a set of building-block waveforms $\{\psi_j(t), j = 1, 2, \ldots, N_s\}$. For all $j = \{1, 2, \ldots, N_s\}$ the spectrum of the corresponding building-block waveform $\Psi_j(f) \equiv 0$ for $|f| \geq W$.

Now, to obtain a passband signal, the two waveforms $s_m^c(t)$ and $s_m^s(t)$ are combined into a signal $s_m(t)$ by modulating them on a cosine resp. sine wave with frequency f_0 and then adding the resulting signals together (see Fig. 11.2), thus

$$s_m(t) = s_m^c(t)\sqrt{2}\cos(2\pi f_0 t) + s_m^s(t)\sqrt{2}\sin(2\pi f_0 t). \tag{11.3}$$

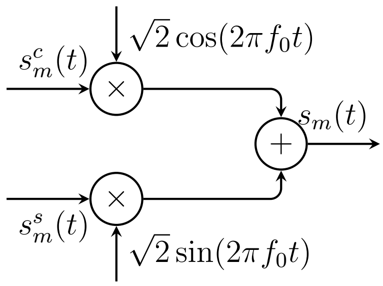

Figure 11.2: Quadrature multiplexing.

We now make (11.3) more precise. Note that to each message $m \in \mathcal{M}$ there corresponds a waveform $s_m^c(t) =$

$\sum_{i=1}^{N_c} s^c_{mi}\phi_i(t)$ and a waveform $s^s_m(t) = \sum_{j=1}^{N_s} s^s_{mj}\psi_j(t)$. Therefore we write:

$$\begin{aligned} s_m(t) &= s^c_m(t)\sqrt{2}\cos(2\pi f_0 t) + s^s_m(t)\sqrt{2}\sin(2\pi f_0 t) \\ &= \sum_{i=1}^{N_c} s^c_{mi}\phi_i(t)\sqrt{2}\cos(2\pi f_0 t) + \sum_{j=1}^{N_s} s^s_{mj}\psi_j(t)\sqrt{2}\sin(2\pi f_0 t). \end{aligned} \tag{11.4}$$

This means that the signal $s_m(t)$ can be regarded as a linear combination of "building-block" waveforms $\phi_i(t)\sqrt{2}\cos(2\pi f_0 t)$ and $\psi_j(t)\sqrt{2}\sin(2\pi f_0 t)$. To see whether these waveforms are actually building blocks we have to check whether they form an orthonormal set.

To this end consider the Fourier transforms of the building block waveforms $\phi_i(t)$ and $\psi_j(t)$:

$$\begin{aligned} \Phi_i(f) &= \int_{-\infty}^{\infty} \phi_i(t)\exp(-j2\pi f t)dt, \\ \Psi_j(f) &= \int_{-\infty}^{\infty} \psi_j(t)\exp(-j2\pi f t)dt. \end{aligned} \tag{11.5}$$

Since both sets $\{\phi_i(t), i = 1, N_c\}$ and $\{\psi_i(t), j = 1, N_s\}$ form an orthonormal basis, using the Parseval relation, we have for all i and j and all i' and j' that

$$\begin{aligned} \int_{-\infty}^{\infty} \Phi_i(f)\Phi^*_{i'}(f)df &= \int_{-\infty}^{\infty} \phi_i(t)\phi_{i'}(t)dt = \delta_{i,i'}, \\ \int_{-\infty}^{\infty} \Psi_j(f)\Psi^*_{j'}(f)df &= \int_{-\infty}^{\infty} \psi_j(t)\psi_{j'}(t)dt = \delta_{j,j'}. \end{aligned} \tag{11.6}$$

Now we are ready to determine the spectrum $\Phi_{c,i}(f)$ of a cosine or *in-phase* building-block waveform

$$\phi_{c,i}(t) \triangleq \phi_i(t)\sqrt{2}\cos(2\pi f_0 t) \tag{11.7}$$

and the spectrum $\Psi_{s,j}(f)$ of a sine or *quadrature* building-block waveform

$$\psi_{s,j}(t) \triangleq \psi_j(t)\sqrt{2}\sin(2\pi f_0 t). \tag{11.8}$$

We express these spectra in terms of the baseband spectra $\Phi_i(f)$ and $\Psi_j(f)$ (see also Fig. 11.3).

$$\begin{aligned} \Phi_{c,i}(f) &= \int_{-\infty}^{\infty} \phi_i(t)\sqrt{2}\cos(2\pi f_0 t)\exp(-j2\pi f t)dt \\ &= \frac{1}{\sqrt{2}}\left(\Phi_i(f - f_0) + \Phi_i(f + f_0)\right), \\ \Psi_{s,j}(f) &= \int_{-\infty}^{\infty} \psi_j(t)\sqrt{2}\sin(2\pi f_0 t)\exp(-j2\pi f t)dt \\ &= \frac{1}{j\sqrt{2}}\left(\Psi_j(f - f_0) - \Psi_j(f + f_0)\right). \end{aligned} \tag{11.9}$$

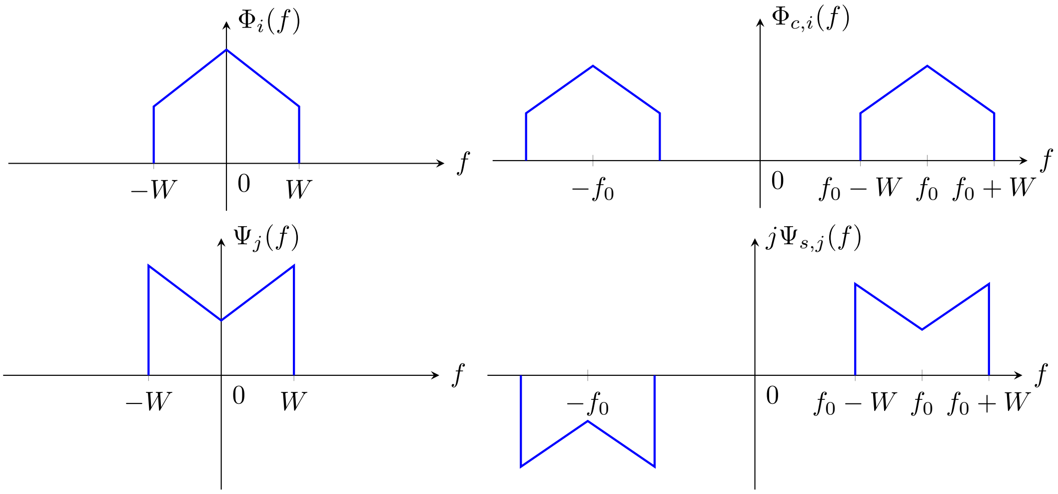

Figure 11.3: Spectra after modulation with $\sqrt{2}\cos 2\pi f_0 t$ and $\sqrt{2}\sin 2\pi f_0 t$. For simplicity it is assumed that the baseband spectra are real.

Note that the spectra $\Phi_{c,i}(f)$ and $\Psi_{s,j}(f)$ are zero outside the passband $\pm[f_0-W, f_0+W]$.

We now first consider the correlation between $\phi_{c,i}(t)$ and $\phi_{c,i'}(t)$ for all i and i'. This leads to

$$\begin{aligned}
\int_{-\infty}^{\infty} \phi_{c,i}(t)\phi_{c,i'}(t)dt &= \int_{-\infty}^{\infty} \Phi_{c,i}(f)\Phi^*_{c,i'}(f)df \\
&= \frac{1}{2}\int_{-\infty}^{\infty} [\Phi_i(f-f_0)+\Phi_i(f+f_0)][\Phi^*_{i'}(f-f_0)+\Phi^*_{i'}(f+f_0)]df \\
&= \frac{1}{2}\int_{-\infty}^{\infty} \Phi_i(f-f_0)\Phi^*_{i'}(f-f_0)df + \frac{1}{2}\int_{-\infty}^{\infty} \Phi_i(f-f_0)\Phi^*_{i'}(f+f_0)df \\
&\quad + \frac{1}{2}\int_{-\infty}^{\infty} \Phi_i(f+f_0)\Phi^*_{i'}(f-f_0)df + \frac{1}{2}\int_{-\infty}^{\infty} \Phi_i(f+f_0)\Phi^*_{i'}(f+f_0)df \\
&\overset{(a)}{=} \frac{1}{2}\int_{-\infty}^{\infty} \Phi_i(f-f_0)\Phi^*_{i'}(f-f_0)df + \frac{1}{2}\int_{-\infty}^{\infty} \Phi_i(f+f_0)\Phi^*_{i'}(f+f_0)df \\
&\overset{(b)}{=} \frac{1}{2}\delta_{i,i'} + \frac{1}{2}\delta_{i,i'} = \delta_{i,i'}. \qquad (11.10)
\end{aligned}$$

Here equality (a) follows from the fact that $f_0 > W$ and the observation that for all $i = 1, ..., N_c$ the spectra $\Phi_i(f) \equiv 0$ for $|f| \geq W$. Therefore the cross-terms are zero, see also Fig. 11.3. Equality (b) follows from (11.6) which holds since the baseband building-blocks $\phi_i(t)$ for $i = 1, ..., N_c$, form an orthonormal base.

In a similar way we can show that for all j and j'

$$\int_{-\infty}^{\infty} \psi_{s,j}(t)\psi_{s,j'}(t)dt = \delta_{j,j'}. \qquad (11.11)$$

What remains to be investigated are the correlations between all in-phase (cosine) building-block waveforms $\phi_{c,i}(t)$ for $i = 1, ..., N_c$ and all quadrature (sine) building-block waveforms $\psi_{s,j}(t)$ for $j = 1, ..., N_s$:

$$\begin{aligned}
\int_{-\infty}^{\infty} \phi_{c,i}(t)\psi_{s,j}(t)dt &= \int_{-\infty}^{\infty} \Phi_{c,i}(f)\Psi^*_{s,j}(f)df \\
&= \frac{j}{2}\int_{-\infty}^{\infty} [\Phi_i(f-f_0)+\Phi_i(f+f_0)][\Psi^*_j(f-f_0)-\Psi^*_j(f+f_0)]df \\
&= \frac{j}{2}\int_{-\infty}^{\infty} \Phi_i(f-f_0)\Psi^*_j(f-f_0)df - \frac{j}{2}\int_{-\infty}^{\infty} \Phi_i(f-f_0)\Psi^*_j(f+f_0)df \\
&\quad +\frac{j}{2}\int_{-\infty}^{\infty} \Phi_i(f+f_0)\Psi^*_j(f-f_0)df - \frac{j}{2}\int_{-\infty}^{\infty} \Phi_i(f+f_0)\Psi^*_j(f+f_0)df \\
&\stackrel{(c)}{=} \frac{j}{2}\int_{-\infty}^{\infty} \Phi_i(f-f_0)\Psi^*_j(f-f_0)df - \frac{j}{2}\int_{-\infty}^{\infty} \Phi_i(f+f_0)\Psi^*_j(f+f_0)df \\
&= 0.
\end{aligned} \tag{11.12}$$

Here equality (c) follows from the fact that $f_0 > W$ and the observation that for all $i = 1, ..., N_c$ the spectra $\Phi_i(f) \equiv 0$ for $|f| \geq W$ and for all $j = 1, ..., N_s$ the spectra $\Psi_j(f) \equiv 0$ for $|f| \geq W$. Therefore the cross-terms are zero. See Fig. 11.3.

RESULT 11.1 *We have shown that all in-phase building-block waveforms $\phi_{c,i}(t)$ for $i = 1, ..., N_c$ and all quadrature building-block waveforms $\psi_{s,j}(t)$ for $j = 1, ..., N_s$ together form an orthonormal base.*
Moreover the spectra $\Phi_{c,i}(f)$ and $\Psi_{s,j}(f)$ of all these building-block waveforms are zero outside the passband $\pm[f_0 - W, f_0 + W]$. Therefore none of these building-block waveforms is hindered by the passband filter $W(f)$ when they are sent over our passband channel.

It is important to note that the baseband building-block waveforms $\phi_i(t)$ and $\psi_j(t)$, for any i and j, need not be orthogonal to each other. Multiplication of these baseband waveforms by $\sqrt{2}\cos(2\pi f_0 t)$ and $\sqrt{2}\sin(2\pi f_0 t)$ results in the orthogonality of the passband building-block waveforms $\phi_{c,i}(t)$ and $\psi_{s,j}(t)$. Also note that all the passband building block waveforms have unit energy. This follows from (11.10) and (11.11). Therefore the energy of $s_m(t)$ is equal to the squared length of the total vector

$$\underline{s}_m = (\underline{s}^c_m, \underline{s}^s_m) = (s^c_{m1}, s^c_{m2}, \ldots, s^c_{mN_c}, s^s_{m1}, s^s_{m2}, \ldots, s^s_{mN_s}). \tag{11.13}$$

11.3 Optimum Receiver for Quadrature Multiplexing

The result of the previous section actually states that by applying quadrature multiplexing for a passband channel we obtain a “normal” waveform channel communication problem. Quadrature multiplexing apparently yields the right building-block waveforms! The building-block waveforms have spectra that are matched to the passband channel. Each message $m \in \mathcal{M}$ results in a signal $s_m(t)$ that is a linear combination of N_c cosine and N_s sine building-block waveforms. Therefore the ideal passband filter at the input of the passband channel has no effect on the transmission of the signals.

We have seen before that a waveform channel is actually equivalent to a vector channel. Also we know how the optimum receiver for a waveform channel should be constructed (see Ch. 6). If we restrict ourselves for a moment to the receiver that correlates the received signal $r(t)$ with the building blocks, we know that it should start with $N_c + N_s$ multipliers followed by integrators:

$$\begin{aligned}\int_{-\infty}^{\infty} r(t)\phi_{c,i}(t)dt &= \int_{-\infty}^{\infty} r(t)\sqrt{2}\cos(2\pi f_0 t)\phi_i(t)dt = r_i^c, \text{ and}\\ \int_{-\infty}^{\infty} r(t)\psi_{s,j}(t)dt &= \int_{-\infty}^{\infty} r(t)\sqrt{2}\sin(2\pi f_0 t)\psi_j(t)dt = r_j^s.\end{aligned} \tag{11.14}$$

After having determined the received vector $\underline{r} = (\underline{r}^c, \underline{r}^s) = (r_1^c, r_2^c, \ldots, r_{N_c}^c, r_1^s, r_2^s, \ldots, r_{N_s}^s)$ we can form the dot-products $(\underline{r}\cdot\underline{s}_m)$ where the signal vector $\underline{s}_m = (\underline{s}_m^c, \underline{s}_m^s) = (s_{m1}^c, s_{m2}^c, \ldots, s_{mN_c}^c, s_{m1}^s, s_{m2}^s, \ldots, s_{mN_s}^s)$:

$$(\underline{r}\cdot\underline{s}_m) = \sum_{i=1}^{N_c} r_i^c s_{mi}^c + \sum_{j=1}^{N_s} r_j^s s_{mj}^s. \tag{11.15}$$

Adding the constants c_m is now the last step before selecting $\hat{m}$ as the message m that maximizes $(\underline{r}\cdot\underline{s}_m) + c_m$ where (see Result (6.1))

$$c_m = \frac{N_0}{2}\ln \Pr\{M = m\} - \frac{\|\underline{s}_m\|^2}{2}, \tag{11.16}$$

with

$$\begin{aligned}\|\underline{s}_m\|^2 = \|\underline{s}_m^c\|^2 + \|\underline{s}_m^s\|^2 &= \sum_{i=1}^{N_c}(s_{mi}^c)^2 + \sum_{j=1}^{N_s}(s_{mj}^s)^2\\ &= \int_{-\infty}^{\infty}(s_m^c(t))^2 dt + \int_{-\infty}^{\infty}(s_m^s(t))^2 dt.\end{aligned} \tag{11.17}$$

Note that $\|\underline{s}_m\|^2 = \int_{-\infty}^{\infty} s_m^2(t)dt$. All this leads to the receiver implementation shown in Fig. 11.4.

11.4 Dimensions per Second

By applying quadrature multiplexing we can not obtain more than $4W$ dimensions per second from our passband channel (see Result 8.2). By choosing both the baseband building-block waveform sets $\{\phi_i(t), i = 1, ..., N_c\}$ and $\{\psi_j(t), j = 1, ..., N_s\}$ as large (rich) as possible given the bandwidth constraint of W Hz, i.e., by taking $2W$ dimensions per second for each of the building-block waveform sets, we obtain the upper bound of $4W$ dimensions per second. Note however that, as usual, this corresponds to 2 dimensions per Hz per second.

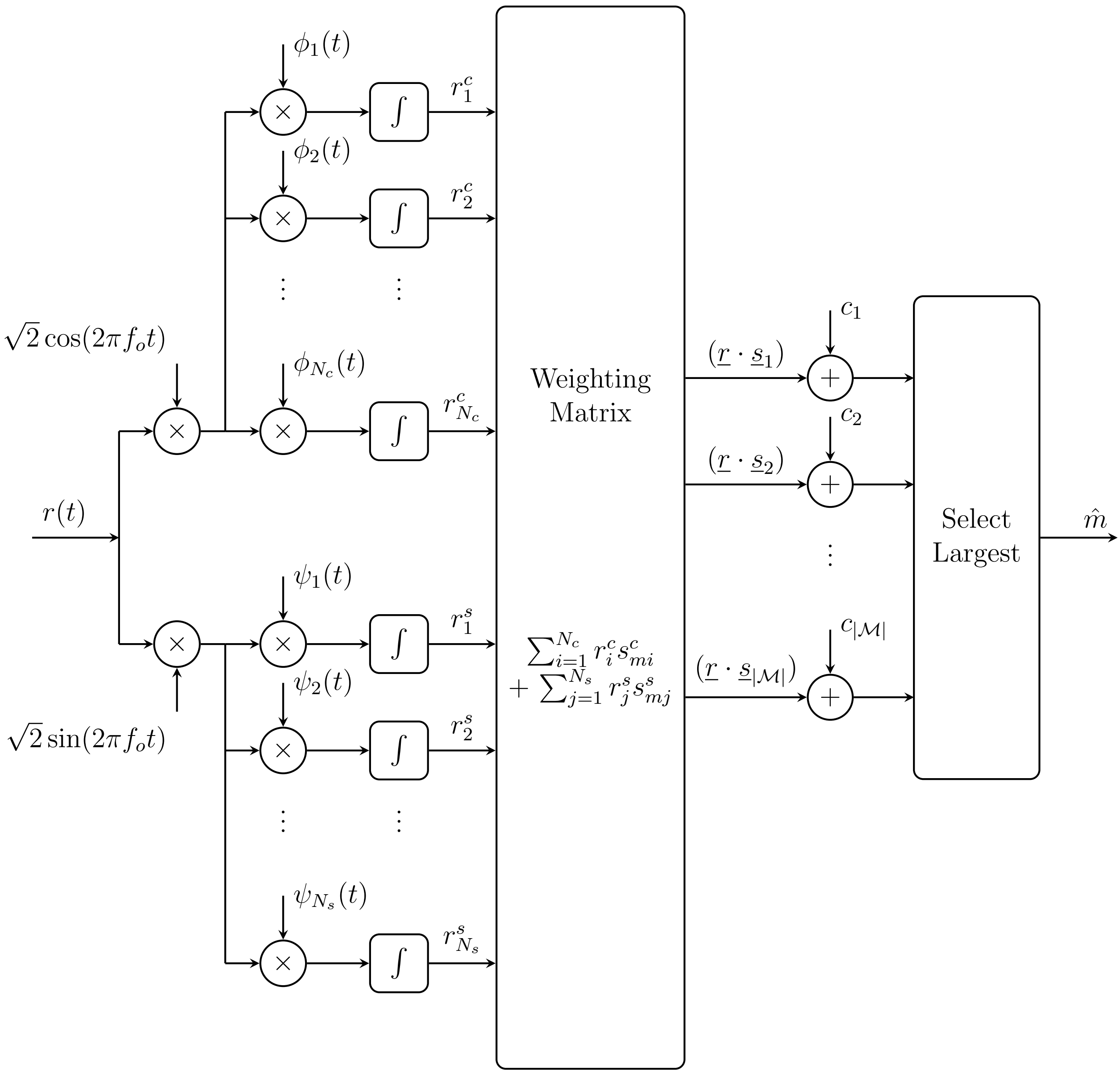

Figure 11.4: Optimum receiver for quadrature-multiplexed signals that are transmitted over a passband channel.

11.5 Capacity of the Pass-Band Channel

In the previous section we saw that the number of dimensions in the case of passband transmission is at most $4W$ per second. Moreover there exist baseband building-block sets that achieve this maximum. Given the transmit power P_s, the available energy per dimension is $E_N = P_s/(4W)$. From Result 9.1 we now obtain the capacity of the passband channel first in bits per dimension, then in bits per second.

RESULT 11.2 *The capacity in bit per dimension of the passband channel with bandwidth* $\pm[f_0 - W, f_0 + W]$ *is*

$$C_N = \frac{1}{2}\log_2\left(1 + \frac{P_s}{2N_0W}\right) \quad \left[\frac{bit}{dimension}\right], \tag{11.18}$$

if the transmitter power is P_s *and the noise spectral density is* $N_0/2$ *for all* f*. Consequently the capacity in bit per second is*

$$C = 4WC_N = 2W\log_2\left(1 + \frac{P_s}{2N_0W}\right) \quad \left[\frac{bit}{second}\right]. \tag{11.19}$$

Note that, as expected, (11.19) coincides with Theorem 9.2 if the bandwidth is $2W$*.*

11.6 Quadrature Amplitude Modulation

We take $N_c = N_s = N$ and the baseband in-phase and quadrature building-block waveforms to be equal, i.e., $\phi_i(t) = \psi_i(t)$ for all $i = 1, \ldots, N$. Then the two dimensions corresponding to the passband building-blocks $\phi_i(t)\sqrt{2}\cos(2\pi f_0 t)$ and $\phi_i(t)\sqrt{2}\sin(2\pi f_0 t)$ for $i = 1, \ldots, N$ are in some way linked together. To see this let

$$s(t) = a\phi(t)\sqrt{2}\cos(2\pi f_0 t) + b\phi(t)\sqrt{2}\sin(2\pi f_0 t), \tag{11.20}$$

hence suppose that we transmit the vector (a, b). If we observe a slightly delayed version of the signal $r(t) = s(t - \Delta) + n_w(t)$ then

$$\begin{aligned} s(t-\Delta) &= a\phi(t-\Delta)\sqrt{2}\cos(2\pi f_0(t-\Delta)) + b\phi(t-\Delta)\sqrt{2}\sin(2\pi f_0(t-\Delta)) \\ &\approx a\phi(t)\sqrt{2}\cos(2\pi f_0(t-\Delta)) + b\phi(t)\sqrt{2}\sin(2\pi f_0(t-\Delta)) \\ &= a\phi(t)\sqrt{2}\left[\cos(2\pi f_0 t)\cos(2\pi f_0\Delta) + \sin(2\pi f_0 t)\sin(2\pi f_0\Delta)\right] \\ &\quad + b\phi(t)\sqrt{2}\left[\sin(2\pi f_0 t)\cos(2\pi f_0\Delta) - \cos(2\pi f_0 t)\sin(2\pi f_0\Delta)\right] \\ &= \left[a\cos(2\pi f_0\Delta) - b\sin(2\pi f_0\Delta)\right]\phi(t)\sqrt{2}\cos(2\pi f_0 t) \\ &\quad + \left[b\cos(2\pi f_0\Delta) + a\sin(2\pi f_0\Delta)\right]\phi(t)\sqrt{2}\sin(2\pi f_0 t). \end{aligned} \tag{11.21}$$

Now note that the "delayed" vector $(a\cos(2\pi f_0\Delta) - b\sin(2\pi f_0\Delta), b\cos(2\pi f_0\Delta) + a\sin(2\pi f_0\Delta))$ is a rotated version of the transmitted vector (a, b), and this demonstrates the coupling of the two dimensions. The approximate equality in the second step holds since $\phi(t)$ is baseband and Δ is small.

We refer to modulation method in (11.20) as quadrature amplitude modulation (QAM).

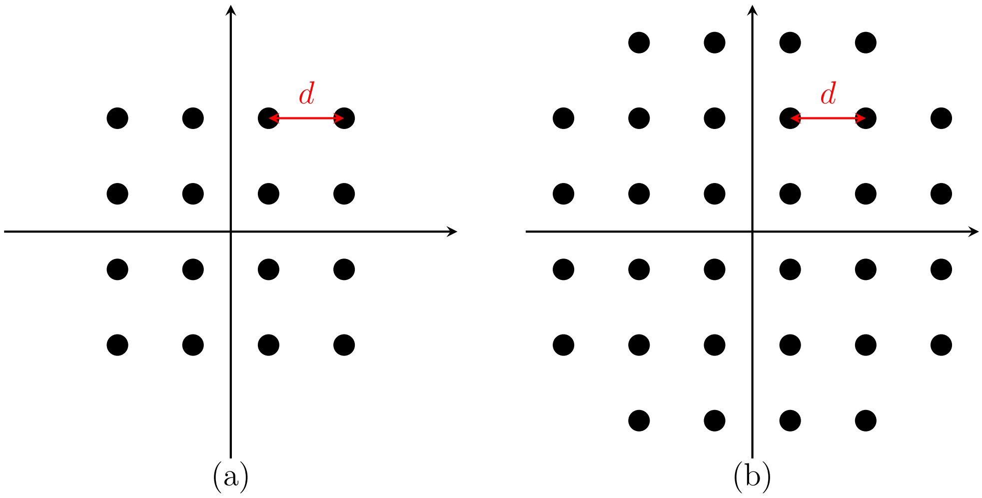

Figure 11.5: Two QAM signal structures, (a) 16-QAM, (b) 32-QAM. Note that 32-QAM is not square!

11.7 Serial Quadrature Amplitude Modulation

It is important to realize that we could use serial pulse amplitude modulation with a pulse $p(t)$ satisfying the Nyquist criterion (see Result 10.1) on both carriers (cosine and sine). A Nyquist pulse corresponds to an orthonormal basis consisting of time shifts of this pulse. Two such sets (based on the same pulse $p(t)$) can be used in a QAM scheme. Note that this signaling method leads to an extremely simple receiver structure.

Example 11.1 QAM modulation results in two-dimensional signal structures. In serial QAM we can take as baseband building blocks

$$\phi_1(t) = \psi_1(t) = \sqrt{2W}\frac{\sin(2\pi W t)}{2\pi W t}, \tag{11.22}$$

and all other baseband building blocks are shifts over multiples of $1/(2W)$ seconds of this sinc-pulse. Therefore the frequency bandwidth of all building blocks is W. After modulation a passband spectrum is obtained, thus the spectra of the signals fit into $\pm[f_0 - W, f_0 + W]$. In each pair of dimensions corresponding to a shift over $(k-1)/(2W)$ seconds we can observe a two-dimensional part (s_k^c, s_k^s) of the signal vector. This part takes values from a two-dimensional signal structure.

In Fig. 11.5 two signal structures are shown. The signal points are placed on a rectangular grid. This implies that their minimum Euclidean distance is not smaller than a certain value d. It is important to place the required number of signal points in such a way on the grid that their average energy is minimal.

Chapter 12

Random Carrier-Phase

SUMMARY: Here we consider carrier modulation under the assumption that the carrier-phase is not known to the receiver. Only one baseband signal $s^b(t)$ will be transmitted. First we determine the optimum receiver for this case. Then we consider the implementation of the optimum receiver when all signals have equal energy. We investigate envelope detection and work out an example in which one of out of two orthogonal signals is transmitted.

12.1 Introduction

Up to this point, we have always assumed that the receiver's local oscillator (the one that produces the term $\cos(2\pi f_0 t)$) is in perfect phase alignment with the phase at the transmitter. Because of oscillator drift or differences in propagation time, it is not always reasonable to assume that the receiver knows the phase of the wave that is used as carrier of the message. In this case *coherent demodulation* is not possible.

To investigate this situation we assume that the transmitter modulates with the[1] baseband signal $s^b(t)$ a wave with a random phase θ, i.e.,

$$s(t) = s^b(t)\sqrt{2}\cos(2\pi f_0 t - \theta), \tag{12.1}$$

where the random phase Θ is assumed to be uniform over $[0, 2\pi)$ hence

$$p_\Theta(\theta) = \frac{1}{2\pi}, \text{ for } 0 \leq \theta < 2\pi. \tag{12.2}$$

Note that, without loss of generality, we can assume that the random phase appears at the transmitter and not at the receiver. More precisely, for each message $m \in \mathcal{M}$, let the signal $s_m^b(t)$ correspond to the vector $\underline{s}_m = (s_{m1}, s_{m2}, \ldots, s_{mN})$ hence

$$s_m^b(t) = \sum_{i=1}^{N} s_{mi}\varphi_i(t). \tag{12.3}$$

[1]Note that there is only one baseband signal involved here. This type of modulation is called double sideband suppressed carrier (DSB-SC) modulation.

We assume as before that the spectrum of the signals $s^b_m(t)$ for all $m \in \mathcal{M}$ is zero outside $[-W, W]$. Note that the same holds for the building-block waveforms $\varphi_i(t)$ for $i = 1, \ldots, N$. This is since the building-block waveforms are linear combinations of the signals. If we now use the trigonometric identity $\cos(a - b) = \cos a \cos b + \sin a \sin b$ we obtain

$$\begin{aligned} s_m(t) &= s^b_m(t)\sqrt{2}\cos(2\pi f_0 t - \theta) \\ &= s^b_m(t)\cos(\theta)\sqrt{2}\cos(2\pi f_0 t) + s^b_m(t)\sin(\theta)\sqrt{2}\sin(2\pi f_0 t) \\ &= \sum_{i=1}^{N} s_{mi}\cos(\theta)\varphi_i(t)\sqrt{2}\cos(2\pi f_0 t) + \sum_{i=1}^{N} s_{mi}\sin(\theta)\varphi_i(t)\sqrt{2}\sin(2\pi f_0 t). \end{aligned} \quad (12.4)$$

If we now turn to the vector approach we can say that, although θ is unknown, this is equivalent to quadrature amplitude modulation where the vector-signals $\underline{s}^c_m$ and $\underline{s}^s_m$ are transmitted satisfying

$$\begin{aligned} \underline{s}^c_m &= \underline{s}_m \cos(\theta), \\ \underline{s}^s_m &= \underline{s}_m \sin(\theta). \end{aligned} \quad (12.5)$$

After receiving the signal $r(t) = s_m(t) + n_w(t)$ an optimum-receiver forms the vectors $\underline{r}^c$ and $\underline{r}^s$ for which

$$\begin{aligned} \underline{r}^c &= \underline{s}^c_m + \underline{n}^c = \underline{s}_m \cos\theta + \underline{n}^c, \\ \underline{r}^s &= \underline{s}^s_m + \underline{n}^s = \underline{s}_m \sin\theta + \underline{n}^s, \end{aligned} \quad (12.6)$$

where both $\underline{n}^c$ and $\underline{n}^s$ are independent Gaussian vectors with independent components all having mean zero and variance $N_0/2$. In the next section we will further determine the optimum receiver for this situation. Note that, unlike quadrature multiplexing/modulation we studied in Chapter 11, here the same data $\underline{s}_m$ appears in both quadrature components.

12.2 Optimum incoherent reception

To determine the optimum receiver we first write out the decision variable for message m, i.e.,

$$\begin{aligned} &\Pr\{M = m\} p_{\underline{R}^c,\underline{R}^s}(\underline{r}^c, \underline{r}^s | M = m) \\ &= \Pr\{M = m\} \int_0^{2\pi} p_\Theta(\theta) p_{\underline{R}^c,\underline{R}^s}(\underline{r}^c, \underline{r}^s | M = m, \Theta = \theta) d\theta. \end{aligned} \quad (12.7)$$

Note that we average over the unknown phase θ. Assume first that all messages are equally likely. Therefore only the integral is relevant. The conditional PDF inside the integral is

$$\begin{aligned} &p_{\underline{R}^c,\underline{R}^s}(\underline{r}^c, \underline{r}^s | M = m, \Theta = \theta) \\ &= p_{\underline{N}^c,\underline{N}^s}(\underline{r}^c - \underline{s}_m\cos(\theta), \underline{r}^s - \underline{s}_m\sin(\theta)) \\ &= \left(\frac{1}{\pi N_0}\right)^N \exp\left(-\frac{\|\underline{r}^c - \underline{s}_m\cos(\theta)\|^2 + \|\underline{r}^s - \underline{s}_m\sin(\theta)\|^2}{N_0}\right). \end{aligned} \quad (12.8)$$

Therefore we investigate

$$
\begin{aligned}
&\|\underline{r}^c - \underline{s}_m \cos(\theta)\|^2 + \|\underline{r}^s - \underline{s}_m \sin(\theta)\|^2 \\
&\quad = \|\underline{r}^c\|^2 - 2(\underline{r}^c \cdot \underline{s}_m)\cos(\theta) + \|\underline{s}_m\|^2 \cos^2(\theta) + \|\underline{r}^s\|^2 - 2(\underline{r}^s \cdot \underline{s}_m)\sin(\theta) + \|\underline{s}_m\|^2 \sin^2(\theta) \\
&\quad = \|\underline{r}^c\|^2 + \|\underline{r}^s\|^2 - 2(\underline{r}^c \cdot \underline{s}_m)\cos(\theta) - 2(\underline{r}^s \cdot \underline{s}_m)\sin(\theta) + \|\underline{s}_m\|^2, \qquad (12.9)
\end{aligned}
$$

and note that both $\|\underline{r}^c\|^2$ and $\|\underline{r}^s\|^2$ do not depend on the message m and can be ignored. Therefore the relevant part of the decision variable is

$$
\int_0^{2\pi} p_\Theta(\theta) \exp\left(\frac{2}{N_0}[(\underline{r}^c \cdot \underline{s}_m)\cos(\theta) + (\underline{r}^s \cdot \underline{s}_m)\sin(\theta)]\right) d\theta \exp\left(-\frac{E_m}{N_0}\right), \qquad (12.10)
$$

where $E_m = \|\underline{s}_m\|^2$. Note that we have to maximize the decision variable in 12.10 over all $m \in \mathcal{M}$.

We next consider $(\underline{r}^c \cdot \underline{s}_m)\cos(\theta) + (\underline{r}^s \cdot \underline{s}_m)\sin(\theta)$. Note that $(\underline{r}^c \cdot \underline{s}_m)$ and $(\underline{r}^s \cdot \underline{s}_m)$ are the outputs of the matched-filter. For each $m \in \mathcal{M}$, we first make a transformation of these matched-filter outputs $(\underline{r}^c \cdot \underline{s}_m)$ and $(\underline{r}^s \cdot \underline{s}_m)$ from rectangular into the polar coordinates (amplitude X_m and phase γ_m). Define (see figure 12.1):

$$
X_m \triangleq \sqrt{(\underline{r}^c \cdot \underline{s}_m)^2 + (\underline{r}^s \cdot \underline{s}_m)^2} \qquad (12.11)
$$

and let the angle γ_m be such that

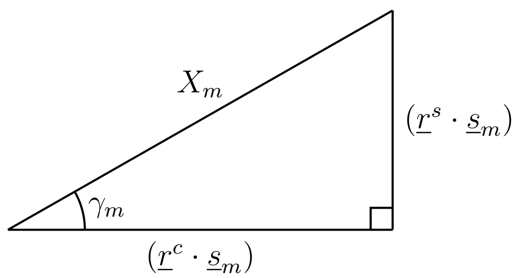

Figure 12.1: Polar transformation of matched-filter outputs.

$$
\begin{aligned}
(\underline{r}^c \cdot \underline{s}_m) &= X_m \cos(\gamma_m), \\
(\underline{r}^s \cdot \underline{s}_m) &= X_m \sin(\gamma_m). \qquad (12.12)
\end{aligned}
$$

Therefore

$$
\begin{aligned}
(\underline{r}^c \cdot \underline{s}_m)\cos(\theta) + (\underline{r}^s \cdot \underline{s}_m)\sin(\theta) &= X_m \cos(\gamma_m)\cos(\theta) + X_m \sin(\gamma_m)\sin(\theta) \\
&= X_m \cos(\theta - \gamma_m), \qquad (12.13)
\end{aligned}
$$

and the integral in (12.10) becomes

$$
\begin{aligned}
&\int_0^{2\pi} p_\Theta(\theta) \exp\left(\frac{2}{N_0}[(\underline{r}^c \cdot \underline{s}_m)\cos(\theta) + (\underline{r}^s \cdot \underline{s}_m)\sin(\theta)]\right) d\theta \\
&\quad = \int_0^{2\pi} \frac{1}{2\pi} \exp\left(\frac{2X_m}{N_0}\cos(\theta - \gamma_m)\right) d\theta \\
&\quad \overset{(a)}{=} \int_0^{2\pi} \frac{1}{2\pi} \exp\left(\frac{2X_m}{N_0}\cos(\theta)\right) d\theta = I_0\left(\frac{2X_m}{N_0}\right). \qquad (12.14)
\end{aligned}
$$

Here (a) follows from the periodicity of the cosine. Note that therefore the angle γ_m is not relevant! The integral denoted by $I_0(\cdot)$ is called the "zero-order modified Bessel function of the first kind". This function is shown in Fig. 12.2.

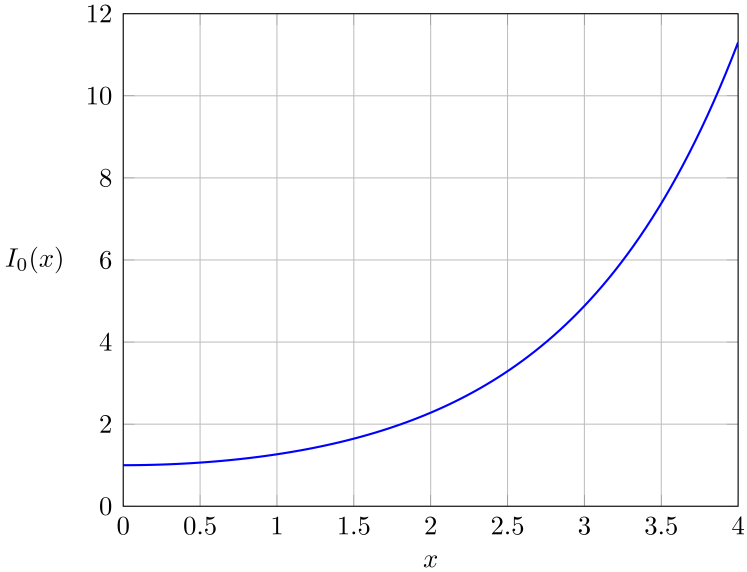

Figure 12.2: A plot of $I_0(x) \triangleq \frac{1}{2\pi}\int_0^{2\pi} \exp(x\cos(\theta))d\theta$ as a function of x.

RESULT 12.1 *Combining everything we obtain, we conclude that the optimum receiver for "random-phase transmission" (incoherent detection) has to choose the message $m \in \mathcal{M}$ that maximizes*

$$I_0\left(\frac{2X_m}{N_0}\right)\exp\left(-\frac{E_m}{N_0}\right) \tag{12.15}$$

where $X_m = \sqrt{(\underline{r}^c \cdot \underline{s}_m)^2 + (\underline{r}^s \cdot \underline{s}_m)^2}$

12.3 Equal energy signals, receiver implementation

If all the signals have the same energy the optimum receiver (see (12.15)) only has to maximize $I_0(2X_m/N_0)$. However, since $I_0(x)$ is a monotonically increasing function of x (see Fig. 12.2), this is equivalent to maximizing X_m, or its square

$$X_m^2 = (\underline{r}^c \cdot \underline{s}_m)^2 + (\underline{r}^s \cdot \underline{s}_m)^2. \tag{12.16}$$

How can we now determine, e.g., $(\underline{r}^c \cdot \underline{s}_m)$? We can use the standard approach as shown in Fig. 11.4 and late $r(t)$ with the bandpass building-block waveforms $\phi_{c,i}(t) = \varphi_i(t)\sqrt{2}\cos(2\pi f_0 t)$ to obtain the components of $\underline{r}^c$ and then form the dot products. However, there is also a more direct way. Note that

$$\begin{aligned}(\underline{r}^c \cdot \underline{s}_m) = \sum_{i=1}^{N} r_i^c s_{mi} &= \sum_{i=1}^{N} \left(\int_{-\infty}^{\infty} r(t)\phi_{c,i}(t)dt \right) s_{mi} \\ &= \sum_{i=1}^{N} \left(\int_{-\infty}^{\infty} r(t)\varphi_i(t)\sqrt{2}\cos(2\pi f_0 t)dt \right) s_{mi} \\ &= \int_{-\infty}^{\infty} r(t)\sqrt{2}\cos(2\pi f_0 t) \sum_{i=1}^{N} s_{mi}\varphi_i(t)dt \\ &= \int_{-\infty}^{\infty} r(t)\sqrt{2}\cos(2\pi f_0 t) s_m^b(t)dt. \qquad (12.17)\end{aligned}$$

A similar result holds for the product $(\underline{r}^s \cdot \underline{s}_m)$. All this suggests the implementation shown in Fig. 12.3. As usual there is also a matched-filter version of this incoherent receiver.

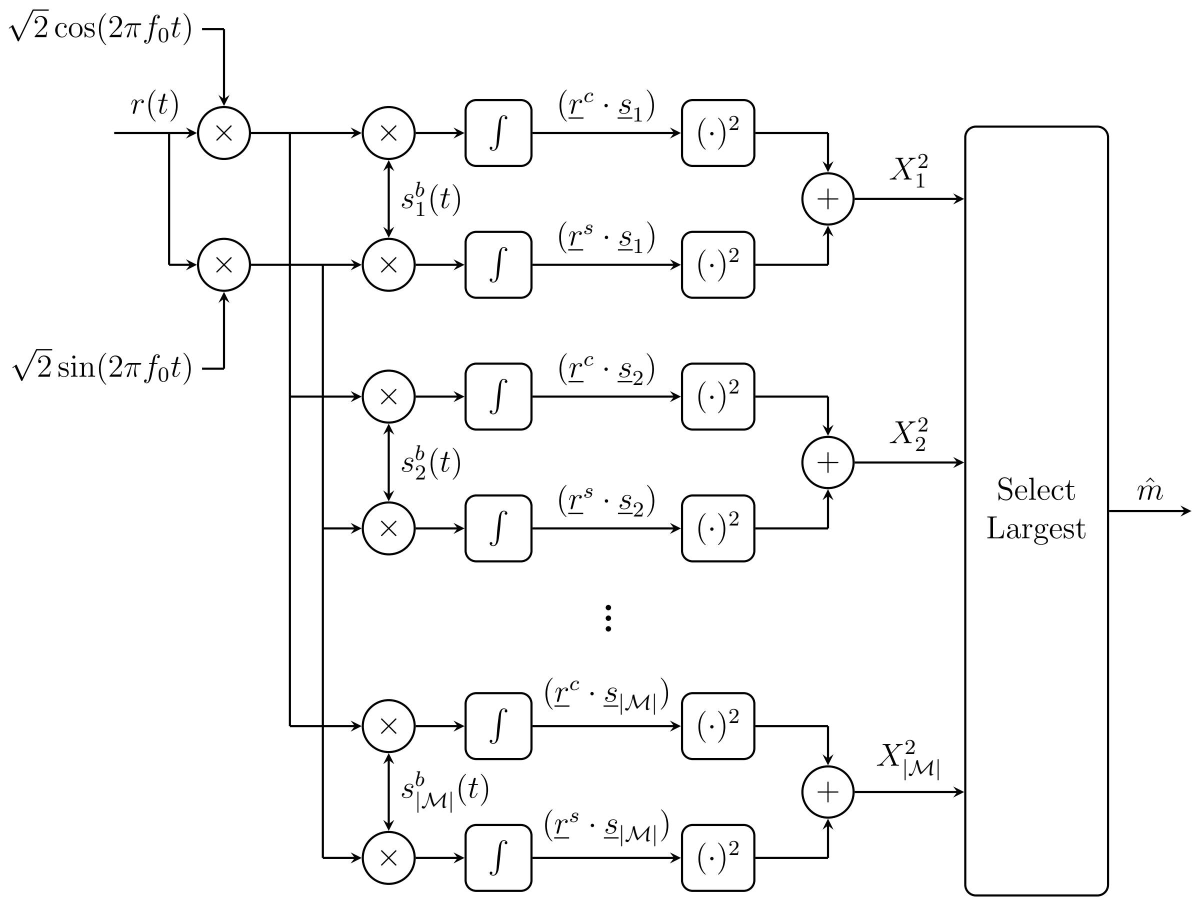

Figure 12.3: Correlation receiver for equal-energy signals with random phase.

12.4 Envelope detection

Fix an $m \in \mathcal{M}$. The matched filter for the (bandpass) signal $s_m(t) = s_m^b(t)\sqrt{2}\cos(2\pi f_0 t - \theta)$ has impulse response $s_m(T-t) = s_m^b(T-t)\sqrt{2}\cos(2\pi f_0(T-t)-\theta)$. Here it is assumed that the signal $s_m(t)$ is zero outside $[0,T]$. Since the phase θ of the transmitted signal is unknown to the receiver, the impulse response

$$h_m(t) = s_m^b(T-t)\sqrt{2}\cos(2\pi f_0 t) \tag{12.18}$$

is probably a good matched filter. Let's investigate this!

The response of this filter on $r(t)$ is

$$\begin{aligned}
u_m(t) &= \int_{-\infty}^{\infty} r(\alpha)h_m(t-\alpha)d\alpha \\
&= \int_{-\infty}^{\infty} r(\alpha)s_m^b(T-t+\alpha)\sqrt{2}\cos(2\pi f_0(t-\alpha))d\alpha \\
&= \int_{-\infty}^{\infty} r(\alpha)s_m^b(T-t+\alpha)\sqrt{2}[\cos(2\pi f_0 t)\cos(2\pi f_0\alpha) + \sin(2\pi f_0 t)\sin(2\pi f_0\alpha)]d\alpha \\
&= \cos(2\pi f_0 t)\int_{-\infty}^{\infty} r(\alpha)s_m^b(T-t+\alpha)\sqrt{2}\cos(2\pi f_0\alpha)d\alpha \\
&\quad + \sin(2\pi f_0 t)\int_{-\infty}^{\infty} r(\alpha)s_m^b(T-t+\alpha)\sqrt{2}\sin(2\pi f_0\alpha)d\alpha \\
&= u_m^c(t)\cos(2\pi f_0 t) + u_m^s(t)\sin(2\pi f_0 t),
\end{aligned} \tag{12.19}$$

with

$$\begin{aligned}
u_m^c(t) &\triangleq \int_{-\infty}^{\infty} r(\alpha)\sqrt{2}\cos(2\pi f_0\alpha)s_m^b(T-t+\alpha)d\alpha, \\
u_m^s(t) &\triangleq \int_{-\infty}^{\infty} r(\alpha)\sqrt{2}\sin(2\pi f_0\alpha)s_m^b(T-t+\alpha)d\alpha.
\end{aligned} \tag{12.20}$$

The signals $u_m^c(t)$ and $u_m^s(t)$ are baseband signals. Why? The reason is that we can regard, e.g., $u_m^c(t)$ as the output of the filter with impulse response $s_m^b(T-t)$ when the excitation is $r(t)\sqrt{2}\cos(2\pi f_0 t)$. It is clear that signal-components outside the frequency band $[-W, W]$ can not pass the filter $s_m^b(T-t)$ since $s_m^b(t)$ is a baseband signal.

We now use the trick of Sec. 12.2 again. Write the matched-filter output as

$$u_m(t) = X_m(t)\cos[2\pi f_0 t - \gamma_m(t)] \tag{12.21}$$

where

$$X_m(t) \triangleq \sqrt{(u_m^c(t))^2 + (u_m^s(t))^2} \tag{12.22}$$

and angle $\gamma_m(t)$ is such that

$$\begin{aligned}
u_m^c(t) &= X_m(t)\cos(\gamma_m(t)), \\
u_m^s(t) &= X_m(t)\sin(\gamma_m(t)).
\end{aligned} \tag{12.23}$$

Now $X_m(t)$ is a slowly-varying "envelope" (amplitude) and $\gamma_m(t)$ a slowly-varying "phase" of the output $u_m(t)$ of the matched filter. By slowly-varying we mean within bandwidth $[-W, W]$.

Next let us consider what happens at $t = T$. Observe from equations (12.17) and (12.20) that

$$\begin{aligned} u_m^c(T) &= (\underline{r}^c \cdot \underline{s}_m), \\ u_m^s(T) &= (\underline{r}^s \cdot \underline{s}_m), \end{aligned} \tag{12.24}$$

hence

$$X_m(T) = \sqrt{(\underline{r}^c \cdot \underline{s}_m)^2 + (\underline{r}^s \cdot \underline{s}_m)^2}. \tag{12.25}$$

The expression in (12.25) coincides with (12.16), and therefore, for equal-energy signals, we can construct an optimum receiver by sampling (see (12.18)) the **envelope** of the outcomes of the matched filters $h_m(t) = s_m^b(T-t)\sqrt{2}\cos(2\pi f_0 t)$ for all $m \in \mathcal{M}$ and comparing the samples. This leads to the implementation shown in Fig. 12.4.

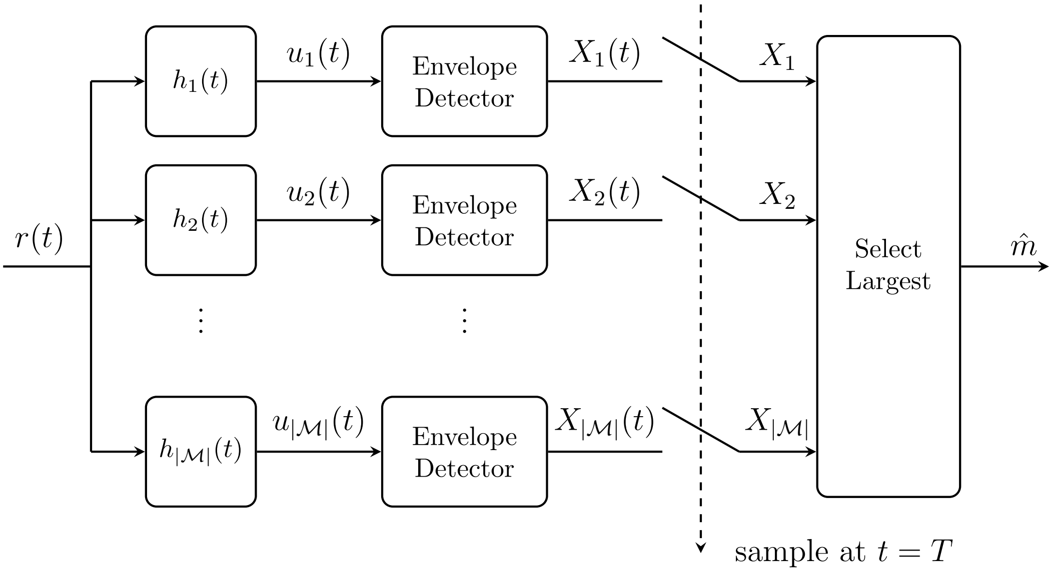

Figure 12.4: Envelope-detector receiver for equal energy signals with random phase.

Example 12.1 For some $m \in \mathcal{M}$ assume that $s_m^b(t) = 1$ for $0 \le t \le 1$ and zero elsewhere. If the random phase turns out to be $\theta = \pi/2$ then

$$s_m(t) = s_m^b(t)\sqrt{2}\cos(2\pi f_0 t - \pi/2) = s_m^b(t)\sqrt{2}\sin(2\pi f_0 t). \tag{12.26}$$

For the matched-filter impulse response, noting that $T = 1$, we can write

$$h_m(t) = s_m^b(1-t)\sqrt{2}\cos(2\pi f_0 t). \tag{12.27}$$

If we assume that there is no noise, hence $r(t) = s_m(t)$, the output $u_m(t)$ of the matched filter will be

$$\begin{aligned} u_m(t) &= \int_{-\infty}^{\infty} r(\alpha)h_m(t-\alpha)d\alpha \\ &= \int_{-\infty}^{\infty} s_m^b(\alpha)\sqrt{2}\sin(2\pi f_0\alpha)s_m^b(1-t+\alpha)\sqrt{2}\cos(2\pi f_0(t-\alpha)d\alpha. \end{aligned} \tag{12.28}$$

All these signals are shown in Fig. 12.5 for $f_0 = 7$ Hz.

Note that the envelope of $u_m(t)$ has the triangular shape which is the output of a matched filter for a rectangular pulse if the input of this matched filter is this rectangular pulse.

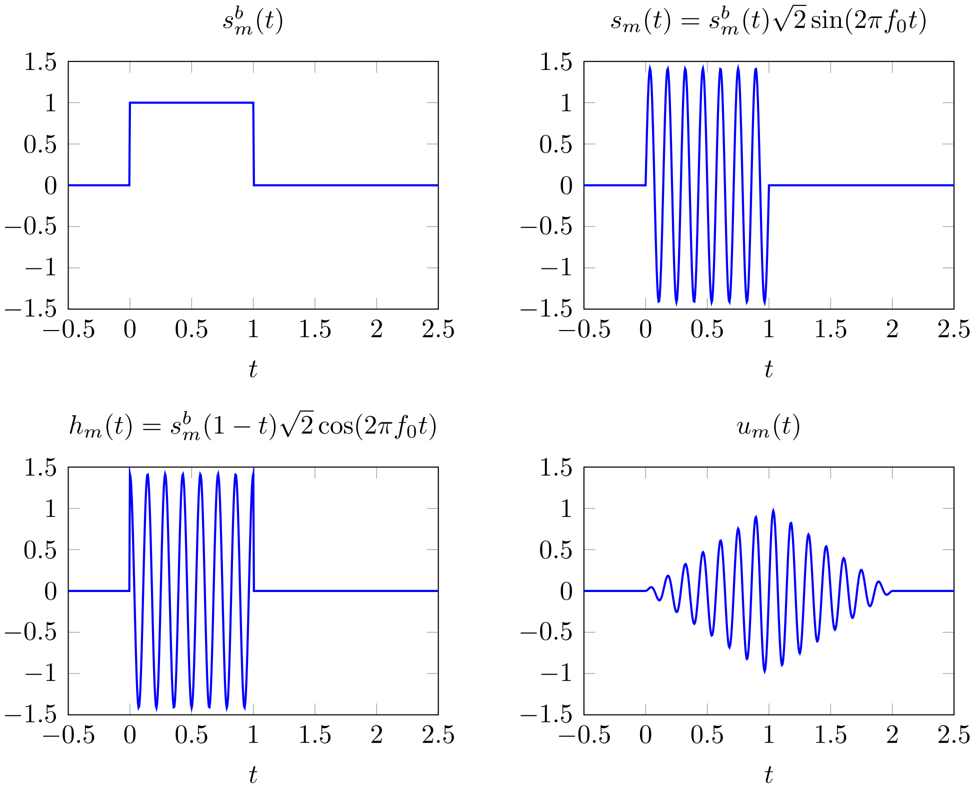

Figure 12.5: Signals $s_m^b(t)$, $s_m(t)$, impulse-response $h_m(t)$, and $u_m(t)$.

The results in Fig. 12.5 ($u_m(t)$) clearly shows that an envelope detector (which can be implemented by squaring the signal and low-pass filtering it) followed by a sampler will indeed return the message encoded in $s_m^b(t)$ (a positive 1). This result, however, also shows a disadvantage of the studied system. Supposed we would have used antipodal signaling, i.e., $s_1^b(t)$ to be a square pulse for message $m = 1$ and $s_2^b(t)$ to be minus that pulse for $m = 2$. In this case, an envelope detector would not be able to differentiate the two messages. This shows that for this detector, antipodal signaling is simply not possible.

12.5 Probability of error for two orthogonal signals

An incoherent receiver does not consider phase information. Therefore it can not yield so small an error probability as a coherent receiver. To illustrate this we will now calculate the probability of error for white Gaussian noise when one of two equally likely messages is communicated over a system utilizing an incoherent receiver and DSB-SC modulated equal-energy orthogonal baseband signals

$$\begin{aligned} s_1^b(t) &= \sqrt{E_s}\varphi_1(t), \text{ hence } \underline{s}_1 = (\sqrt{E_s}, 0), \text{ and} \\ s_2^b(t) &= \sqrt{E_s}\varphi_2(t), \text{ hence } \underline{s}_2 = (0, \sqrt{E_s}). \end{aligned} \tag{12.29}$$

An optimum receiver (see result 12.1) now chooses $\hat{m} = 1$ if and only if

$$(\underline{r}^c \cdot \underline{s}_1)^2 + (\underline{r}^s \cdot \underline{s}_1)^2 > (\underline{r}^c \cdot \underline{s}_2)^2 + (\underline{r}^s \cdot \underline{s}_2)^2. \tag{12.30}$$

Here all vectors are two-dimensional, more precisely

$$\begin{aligned} \underline{r}^c &= \underline{s}_m \cos(\theta) + \underline{n}^c \\ \underline{r}^s &= \underline{s}_m \sin(\theta) + \underline{n}^s. \end{aligned} \tag{12.31}$$

When $M = 1$ then the vector components of $\underline{r}^c = (r_1^c, r_2^c)$ and $\underline{r}^s = (r_1^s, r_2^s)$ are

$$\begin{aligned} r_1^c &= \sqrt{E_s}\cos(\theta) + n_1^c, \\ r_1^s &= \sqrt{E_s}\sin(\theta) + n_1^s, \\ r_2^c &= n_2^c, \\ r_2^s &= n_2^s, \end{aligned} \tag{12.32}$$

where $\underline{n}^c = (n_1^c, n_2^c)$ and $\underline{n}^s = (n_1^s, n_2^s)$. Now by $\underline{s}_1 = (\sqrt{E_s}, 0)$ and $\underline{s}_2 = (0, \sqrt{E_s})$ the optimum receiver decodes $\hat{m} = 1$ if and only if

$$(r_1^c)^2 + (r_1^s)^2 > (r_2^c)^2 + (r_2^s)^2. \tag{12.33}$$

The noise components are all statistically independent Gaussian variables with density function

$$p_N(n) = \frac{1}{\sqrt{\pi N_0}} \exp\left(-\frac{n^2}{N_0}\right). \tag{12.34}$$

Now fix some θ. Assume that $(r_1^c)^2 + (r_1^s)^2 = \rho^2$. What is now the probability of error given that $M = 1$ and $\Theta = \theta$? Therefore consider

$$\begin{aligned}
\Pr\{\hat{M} = 2|\Theta = \theta, M = 1, (R_1^c)^2 + (R_1^s)^2 = \rho^2\} &= \Pr\{(R_2^c)^2 + (R_2^s)^2 \geq \rho^2\} \\
&= \int\int_{\alpha^2+\beta^2 \geq \rho^2} p_N(\alpha) p_N(\beta) d\alpha d\beta \\
&= \int\int_{\alpha^2+\beta^2 \geq \rho^2} \frac{1}{\pi N_0} \exp\left(-\frac{\alpha^2+\beta^2}{N_0}\right) d\alpha d\beta \\
&= \int_\rho^\infty \int_0^{2\pi} \frac{1}{\pi N_0} \exp\left(-\frac{r^2}{N_0}\right) r dr d\theta \\
&= \exp\left(-\frac{\rho^2}{N_0}\right). \qquad (12.35)
\end{aligned}$$

We obtain the error probability for the case where $M = 1$ by averaging over all R_1^c and R_1^s, hence

$$\begin{aligned}
&\Pr\{\hat{M} = 2|\Theta = \theta, M = 1\} \\
&= \int_{-\infty}^\infty \int_{-\infty}^\infty p_{R_1^c, R_1^s}(r_1^c, r_1^s|\Theta = \theta, M = 1) \exp\left(-\frac{(r_1^c)^2 + (r_1^s)^2}{N_0}\right) dr_1^c dr_1^s \\
&= \int_{-\infty}^\infty \int_{-\infty}^\infty p_{R_1^c}(r_1^c|\Theta = \theta, M = 1) p_{R_1^s}(r_1^s|\Theta = \theta, M = 1) \exp\left(-\frac{(r_1^c)^2 + (r_1^s)^2}{N_0}\right) dr_1^c dr_1^s \\
&= \int_{-\infty}^\infty p_{R_1^c}(r_1^c|\Theta = \theta, M = 1) \exp\left(-\frac{(r_1^c)^2}{N_0}\right) dr_1^c \cdot \\
&\qquad \int_{-\infty}^\infty p_{R_1^s}(r_1^s|\Theta = \theta, M = 1) \exp\left(-\frac{(r_1^s)^2}{N_0}\right) dr_1^s. \qquad (12.36)
\end{aligned}$$

Consider the first factor. Note that $r_1^c = \sqrt{E_s}\cos(\theta) + n_1^c$. Therefore

$$\begin{aligned}
&\int_{-\infty}^\infty p_{R_1^c}(r_1^c|\Theta = \theta, M = 1) \exp\left(-\frac{(r_1^c)^2}{N_0}\right) dr_1^c \\
&= \int_{-\infty}^\infty \frac{1}{\sqrt{\pi N_0}} \exp\left(-\frac{(\alpha - \sqrt{E_s}\cos(\theta))^2}{N_0}\right) \exp\left(-\frac{\alpha^2}{N_0}\right) d\alpha. \qquad (12.37)
\end{aligned}$$

With $m = \sqrt{E_s}\cos(\theta)$ this integral becomes

$$\begin{aligned}
&\int_{-\infty}^{\infty} \frac{1}{\sqrt{\pi N_0}} \exp\left(-\frac{(\alpha-m)^2}{N_0}\right) \exp\left(-\frac{\alpha^2}{N_0}\right) d\alpha \\
&= \int_{-\infty}^{\infty} \frac{1}{\sqrt{\pi N_0}} \exp\left(-\frac{2\alpha^2 - 2\alpha m + m^2}{N_0}\right) d\alpha \\
&= \int_{-\infty}^{\infty} \frac{1}{\sqrt{\pi N_0}} \exp\left(-\frac{2(\alpha^2 - \alpha m + m^2/4) + m^2/2}{N_0}\right) d\alpha \\
&= \frac{\exp\left(-\frac{m^2}{2N_0}\right)}{\sqrt{2}} \int_{-\infty}^{\infty} \frac{1}{\sqrt{\pi N_0/2}} \exp\left(-\frac{(\alpha - m/2)^2}{N_0/2}\right) d\alpha = \frac{\exp\left(-\frac{m^2}{2N_0}\right)}{\sqrt{2}} \\
&= \frac{\exp\left(-\frac{E_s\cos^2(\theta)}{2N_0}\right)}{\sqrt{2}}. \qquad (12.38)
\end{aligned}$$

Combining this with a similar result for the second factor we obtain

$$\Pr\{\hat{M} = 2|\Theta = \theta, M = 1\} = \frac{\exp\left(-\frac{E_s\cos^2(\theta)}{2N_0}\right)}{\sqrt{2}} \cdot \frac{\exp\left(-\frac{E_s\sin^2(\theta)}{2N_0}\right)}{\sqrt{2}} = \frac{1}{2}\exp\left(-\frac{E_s}{2N_0}\right). \qquad (12.39)$$

Although we have fixed θ this probability is independent of θ. Averaging over θ yields therefore

$$\Pr\{\hat{M} = 2|M = 1\} = \frac{1}{2}\exp\left(-\frac{E_s}{2N_0}\right). \qquad (12.40)$$

Based on symmetry we can obtain a similar result for $\Pr\{\hat{M} = 1|M = 2\}$.

RESULT 12.2 *The error probability for an incoherent receiver for two equally likely orthogonal signals, both having energy E_s, is*

$$P_e = \frac{1}{2}\exp\left(-\frac{E_s}{2N_0}\right). \qquad (12.41)$$

Note that for coherent reception of two equally likely orthogonal signals we have obtained before that

$$P_e = Q\left(\sqrt{\frac{E_s}{N_0}}\right) \le \frac{1}{2}\exp\left(-\frac{E_s}{2N_0}\right). \qquad (12.42)$$

Here we have used the bound on the Q-function that was derived in Appendix E. Figure 12.6 shows that the error probabilities are comparable however.

Another disadvantage of incoherent transmission of two orthogonal signals is that we loose 3 dB relative to antipodal signaling (see Example 12.1). Also the bandwidth efficiency of random-phase transmission of two-orthogonal signals is a factor of two smaller than that of coherent transmission. A transmitted dimension spreads out over two received dimensions. On the other hand, incoherent transmission is simpler (and cheaper) to implement because no local oscillator is required. Or even if a local oscillator is used, there is no need to track the phase difference between transmitter and receiver.

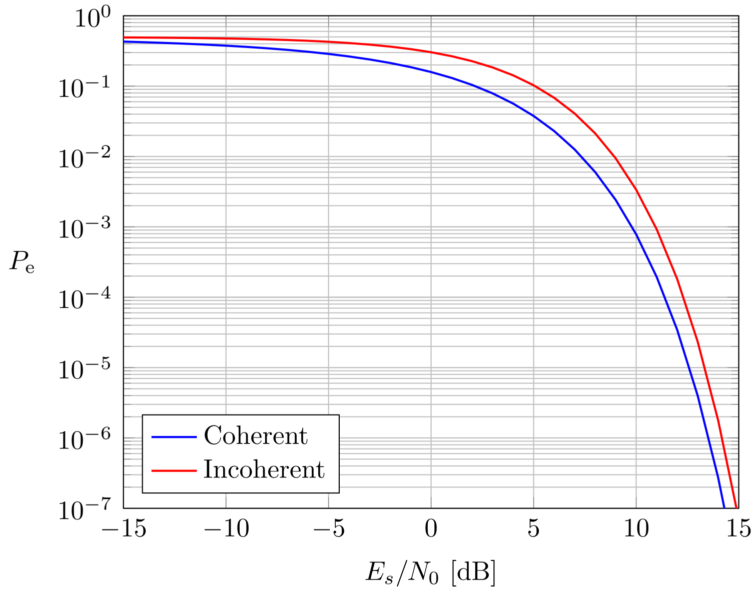

Figure 12.6: Probability of error for coherent and incoherent reception of two equally likely orthogonal signals of energy E_s as a function of E_s/N_0 in dB. Note that probability of error for incoherent reception is largest.

Part IV

Appendices

Appendix A

The Fourier Transform

A.1 Main Result

THEOREM A.1 *If the signal $x(t)$ satisfies the Dirichlet conditions ($x(t)$ is absolutely integrable on the real line, number of maxima and minima of $x(t)$ and number of discontinuities of $x(t)$ in any finite interval on the real line is finite, and when $x(t)$ is discontinuous at t then $x(t) = (x(t^+) + x(t^-))/2$), then the Fourier transform (or Fourier integral) of $x(t)$, defined by*

$$X(f) = \int_{-\infty}^{\infty} x(t) \exp(-j2\pi f t) dt \tag{A.1}$$

exists and the original signal can be obtained from its Fourier transform by

$$x(t) = \int_{-\infty}^{\infty} X(f) \exp(j2\pi f t) df. \tag{A.2}$$

A.2 Properties

A.2.1 Parseval's Relation

RESULT A.2 *If the Fourier transforms of the real signals $f(t)$[1] and $g(t)$ are denoted by $F(f)$ and $G(f)$ respectively, then*

$$\int_{-\infty}^{\infty} f(t)g(t)dt = \int_{-\infty}^{\infty} F(f)G^*(f)df. \tag{A.3}$$

[1]Note that if the signals are complex, Parseval's Relation states that $\int_{-\infty}^{\infty} f(t)g^*(t)dt = \int_{-\infty}^{\infty} F(f)G^*(f)df$.

Proof: Note that for a real signal $g(t)$ we have that $g^*(t) = g(t)$. Then

$$\begin{aligned}\int_{-\infty}^{\infty} f(t)g(t)dt &= \int_{-\infty}^{\infty}\left[\int_{-\infty}^{\infty} F(f)\exp(j2\pi ft)df\right] g(t)dt \\ &= \int_{-\infty}^{\infty} F(f)\left[\int_{-\infty}^{\infty} g(t)\exp(-j2\pi tdt)\right]^* df \\ &= \int_{-\infty}^{\infty} F(f)G^*(f)df. \qquad \text{(A.4)}\end{aligned}$$

□

For the particular case of $f(t) = g(t)$, Parseval's relation gives

$$\int_{-\infty}^{\infty} g^2(t)\,dt = \int_{-\infty}^{\infty} |G(f)|^2\,df, \qquad \text{(A.5)}$$

where

$$E_x \triangleq \int_{-\infty}^{\infty} g^2(t)\,dt \qquad \text{(A.6)}$$

is the energy of the signal.

Appendix B

Correlation Functions, Power Spectra

We will investigate here what the influence is of a filter with impulse response $h(t)$ on the spectrum $S_x(f)$ of the input random process $X(t)$. Then we study the consequences of our findings. Consider figure B.1. The filter produces the random process $Y(t)$ at its output while the input process is $X(t)$.

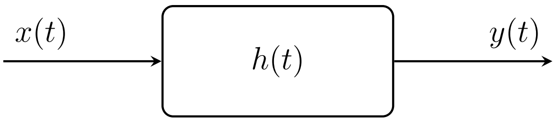

Figure B.1: Filtering the noise process $X(t)$.

B.1 Expectation of an integral

For the expected value of the random process $Y(t)$ we can write[1]

$$\begin{aligned} m_y(t) = E[Y(t)] &= E\left[\int_{-\infty}^{\infty} X(\alpha)h(t-\alpha)d\alpha\right] \\ &= \int_{-\infty}^{\infty} E[X(\alpha)]h(t-\alpha)d\alpha. \end{aligned} \tag{B.1}$$

The autocorrelation function of the random process is

$$\begin{aligned} R_y(t,s) = E[Y(t)Y(s)] &= E\left[\int_{-\infty}^{\infty} X(\alpha)h(t-\alpha)d\alpha \int_{-\infty}^{\infty} X(\beta)h(s-\beta)d\beta\right] \\ &= \int_{-\infty}^{\infty}\int_{-\infty}^{\infty} E[X(\alpha)X(\beta)]h(t-\alpha)h(s-\beta)d\alpha d\beta \\ &= \int_{-\infty}^{\infty}\int_{-\infty}^{\infty} R_x(\alpha,\beta)h(t-\alpha)h(s-\beta)d\alpha d\beta. \end{aligned} \tag{B.2}$$

[1]Note that we do not assume (yet) that the process $X(t)$ is Gaussian.

B.2 Power spectrum

To study the effect of filtering a random process we assume that $R_x(t,s) = R_x(\tau)$ with $\tau = t - s$, i.e., the autocorrelation function $R_x(t,s)$ of the input random process depends only on the difference in time $t - s$ between the sample times t and s. If this condition is satisfied we can investigate the distribution of the mean power of a random process as a function of frequency. Now

$$\begin{aligned} R_y(t,s) &= \int_{-\infty}^{\infty}\int_{-\infty}^{\infty} R_x(\alpha-\beta)h(t-\alpha)h(s-\beta)d\alpha d\beta \\ &= \int_{-\infty}^{\infty}\int_{-\infty}^{\infty} R_x(t-s+\mu-\nu)h(\nu)h(\mu)d\nu d\mu, \end{aligned} \tag{B.3}$$

with $\nu = t - \alpha$ and $\mu = s - \beta$. Observe that now also $R_y(t,s)$ only depends on the time difference $\tau = t - s$ hence $R_y(t,s) = R_y(\tau)$.

Next consider the Fourier transforms $S_x(f)$ and $S_y(f)$ of $R_x(\tau)$ and $R_y(\tau)$ respectively (see Appendix A):

$$\begin{aligned} S_x(f) &\stackrel{\Delta}{=} \int_{-\infty}^{\infty} R_x(\tau)\exp(-j2\pi f\tau)d\tau \quad \text{and } R_x(\tau) = \textstyle\int_{-\infty}^{\infty} S_x(f)\exp(j2\pi f\tau)df \\ S_y(f) &\stackrel{\Delta}{=} \int_{-\infty}^{\infty} R_y(\tau)\exp(-j2\pi f\tau)d\tau \quad \text{and } R_y(\tau) = \textstyle\int_{-\infty}^{\infty} S_y(f)\exp(j2\pi f\tau)df. \end{aligned} \tag{B.4}$$

Note that these Fourier transforms can only be defined if the correlation functions depend only on the time-difference $\tau = t - s$. Next we obtain

$$\begin{aligned} R_y(\tau) &= \int_{-\infty}^{\infty}\int_{-\infty}^{\infty} R_x(\tau+\mu-\nu)h(\nu)h(\mu)d\nu d\mu \\ &= \int_{-\infty}^{\infty}\int_{-\infty}^{\infty}\left[\int_{-\infty}^{\infty} S_x(f)\exp(j2\pi f(\tau+\mu-\nu))df\right] h(\nu)h(\mu)d\nu d\mu \\ &= \int_{-\infty}^{\infty} S_x(f)\left[\int_{-\infty}^{\infty} h(\nu)\exp(-j2\pi f\nu)d\nu\right]\left[\int_{-\infty}^{\infty} h(\mu)\exp(-j2\pi f\mu)d\mu\right]\exp(j2\pi f\tau)df \\ &= \int_{-\infty}^{\infty} S_x(f)H(f)H^*(f)\exp(j2\pi f\tau)df, \end{aligned} \tag{B.5}$$

hence

$$S_y(f) = S_x(f)H(f)H^*(f) = S_x(f)|H(f)|^2. \tag{B.6}$$

B.3 Interpretation

First note that the mean square value of the filter output process $Y(t)$ is time-independent if $R_x(t,s) = R_x(t-s)$. This follows from

$$E[Y^2(t)] = R_y(t,t) = R_y(t-t) = R_y(0). \tag{B.7}$$

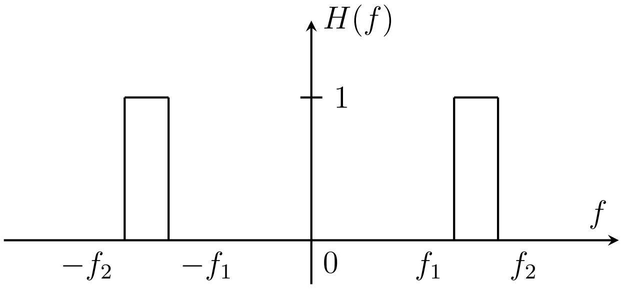

Figure B.2: An ideal bandpass filter.

Therefore $R_y(0)$ is the expected value of the power that is dissipated in a resistor of 1Ω connected to the output of the filter, at any time instant. Next note that

$$R_y(0) = \int_{-\infty}^{\infty} S_y(f)df = \int_{-\infty}^{\infty} S_x(f)|H(f)|^2 df. \tag{B.8}$$

Consider a filter with transfer function $H(f)$ shown in figure B.2. This is a bandpass filter and

$$H(f) = \begin{cases} 1 & \text{for } f_1 \leq |f| \leq f_2, \\ 0 & \text{elsewhere.} \end{cases} \tag{B.9}$$

Then we obtain

$$R_y(0) = \int_{-f_2}^{-f_1} S_y(f)df + \int_{f_1}^{f_2} S_y(f)df. \tag{B.10}$$

Now let $f_1 = f$ and $f_2 = f + \Delta f$. The filter $H(f)$ now only transfers components of $X(t)$ in the frequency band $(f, f + \Delta f)$ and stops all other components. Since a power spectrum is always even, see Sec. B.6, the expected power at the output of the filter is approximately $2S_x(f)\Delta f$. This implies that $S_x(f)$ is the distribution of average power in the process $X(t)$ over the frequencies. Therefore we call $S_x(f)$ the power spectral density function of $X(t)$.

B.4 Wide-sense stationarity

Definition B.1 *A random process $Z(t)$ is called* wide-sense stationary (WSS) *if and only if*

$$\begin{aligned} m_z(t) &= \textit{constant} \\ \text{and } R_z(t, s) &= R_z(t - s). \end{aligned} \tag{B.11}$$

For a WSS process $Z(t)$ it is meaningful to consider its power spectral density $S_z(f)$. For a WSS process $Y(t)$ the expected power can be expressed as in equation (B.7). When a WSS process $X(t)$ is the input of a filter then the filter output process $Y(t)$ is also WSS and its power spectral density $S_y(f)$ is related to the input power spectral density $S_x(f)$ as given by (B.8). These consequences already justify the concept wide-sense stationarity.

B.5 Gaussian processes

Recall that a Gaussian process $Z(t)$ is completely specified by its mean $m_z(t)$ and autocorrelation function $R_z(t,s)$ for all t and s. Therefore a WSS (wide-sense stationary) Gaussian process $Z(t)$ is also (strict-sense) stationary.

Furthermore note that when a Gaussian process $X(t)$ is the input of a filter then the filter output process $Y(t)$ is also Gaussian. Remember that the output process is WSS when input process is WSS.

B.6 Properties of $S_x(f)$ and $R_x(\tau)$

Let $X(t)$ be a WSS random process again.

a) First observe that $R_x(\tau)$ is a (real) even function of τ. This follows from

$$R_x(-\tau) = E[X(t-\tau)X(t)] = E[X(t)X(t-\tau)] = R_x(\tau). \tag{B.12}$$

b) Next we show that $S_x(f)$ is a real even function of f. Since $R_x(\tau)$ is an even funtion and $\sin(2\pi f\tau)$ an odd function of τ

$$\int_{-\infty}^{\infty} R_x(\tau)\sin(2\pi f\tau)d\tau = 0. \tag{B.13}$$

Therefore

$$\begin{aligned} S_x(f) &= \int_{-\infty}^{\infty} R_x(\tau)\exp(-2\pi f\tau)d\tau \\ &= \int_{-\infty}^{\infty} R_x(\tau)[\cos(2\pi f\tau) - j\sin(2\pi f\tau)]d\tau \\ &= \int_{-\infty}^{\infty} R_x(\tau)\cos(2\pi f\tau)d\tau, \end{aligned} \tag{B.14}$$

which is even and real.

c) The power spectral density $S_x(f)$ is a non-negative function of the frequency f. To see why this statement is true suppose that $S_x(f)$ is negative for $f_1 < |f| < f_2$. Then consider an ideal bandpass filter $H(f)$ as given by (B.9). The expected power of the output $Y(t)$ of this filter when the input is the random process $X(t)$ is given by

$$E[Y^2(t)] = R_y(0) = 2\int_{f_1}^{f_2} S_x(f)df < 0, \tag{B.15}$$

which yields a contradiction.

d) Without proof we give another property of $R_x(\tau)$. It can be shown that

$$|R_x(\tau)| \leq R_x(0). \tag{B.16}$$

Appendix C

Impulse signal, filters

C.1 The impulse or delta signal

In mathematical sense (see, e.g., [11]) the delta signal $\delta(t)$ is not a funtion but a *distribution* or a *generalized function*. A distribution is defined in terms of its effect on another function (usually called "test function"). The impulse distribution can be defined by its effect on the test function $f(t)$, which is supposed to be continuous at the origin, by the relation

$$\int_{-\infty}^{\infty} f(t)\delta(t)dt = f(0). \tag{C.1}$$

We call this property the *sifting property* of the impulse signal. Note that we defined the impulse signal $\delta(t)$ by desribing its action on the test function $f(t)$ and not by specifying its value for different values of t.

C.2 Linear time-invariant systems, filters

Definition C.1 *A system $\mathcal{L}$ is* **linear** *if and only if for any two legitimate input signals $x_1(t)$ and $x_2(t)$ and any two scalars α_1 and α_2, the linear combination $\alpha_1 x_1(t) + \alpha_2 x_2(t)$ is again a legitimate input, and*

$$\mathcal{L}[\alpha_1 x_1(t) + \alpha_2 x_2(t)] = \alpha_1 \mathcal{L}[x_1(t)] + \alpha_2 \mathcal{L}[x_2(t)]. \tag{C.2}$$

A system that does not satisfy this relation is **nonlinear**.

Definition C.2 *The* **impulse response** *$h(t)$ of a system $\mathcal{L}$ is the response of the system to an impulse input $\delta(t)$, thus*

$$h(t) = \mathcal{L}[\delta(t)]. \tag{C.3}$$

The response of the **time-invariant system** *time-invariant system to a unit response applied at time τ, i.e., $\delta(t-\tau)$ is obviously $h(t-\tau)$.*

Now we can determine the response of a **linear time-invariant** system $\mathcal{L}$ to an input signal $x(t)$ as follows:

$$\begin{aligned} y(t) &= \mathcal{L}\left[x(t)\right] \\ &= \mathcal{L}\left[\int_{-\infty}^{\infty} x(\tau)\delta(t-\tau)d\tau\right] \\ &= \int_{-\infty}^{\infty} x(\tau)\mathcal{L}\left[\delta(t-\tau)\right]d\tau \\ &= \int_{-\infty}^{\infty} x(\tau)h(t-\tau)d\tau. \end{aligned} \tag{C.4}$$

The final integral is called the *convolution* of the signal $x(t)$ and the impulse response $h(t)$.

A linear time-invariant system is often called a **filter**.

Appendix D

Schwarz inequality

LEMMA D.1 (Schwarz inequality) *For two finite-energy waveforms $a(t)$ and $b(t)$ the inequality*

$$\left(\int_{-\infty}^{\infty} a(t)b(t)dt\right)^2 \leq \int_{-\infty}^{\infty} a^2(t)dt \int_{-\infty}^{\infty} b^2(t)dt \tag{D.1}$$

holds. Equality is obtained only if $b(t) \equiv Ca(t)$ for some constant C.

Proof: Form an orthonormal expansion for $a(t)$ and $b(t)$, i.e.,

$$\begin{aligned} a(t) &= a_1\phi_1(t) + a_2\phi_2(t), \\ b(t) &= b_1\phi_1(t) + b_2\phi_2(t), \end{aligned} \tag{D.2}$$

with $\int_{-\infty}^{\infty} \phi_i(t)\phi_j(t)dt = \delta_{ij}$ for $i = 1, 2$ and $j = 1, 2$.

Then with $\underline{a} = (a_1, a_2)$ and $\underline{b} = (b_1, b_2)$ and the Parseval results $(\underline{a} \cdot \underline{b}) = \int_{-\infty}^{\infty} a(t)b(t)dt$, $(\underline{a} \cdot \underline{a}) = \int_{-\infty}^{\infty} a^2(t)dt$, and $(\underline{b} \cdot \underline{b}) = \int_{-\infty}^{\infty} b^2(t)dt$, we find for the vectors $\underline{a}$ and $\underline{b}$ that

$$\frac{(\underline{a} \cdot \underline{b})}{\|\underline{a}\|\|\underline{b}\|} = \frac{\int_{-\infty}^{\infty} a(t)b(t)dt}{\sqrt{\int_{-\infty}^{\infty} a^2(t)dt}\sqrt{\int_{-\infty}^{\infty} b^2(t)dt}}. \tag{D.3}$$

If we now can prove that $(\underline{a} \cdot \underline{b})^2 \leq \|\underline{a}\|^2\|\underline{b}\|^2$ we get Schwarz inequality.

We start by stating the triangle inequality for $\underline{a}$ and $\underline{b}$:

$$\|\underline{a} + \underline{b}\| \leq \|\underline{a}\| + \|\underline{b}\|. \tag{D.4}$$

Moreover

$$\|\underline{a} + \underline{b}\|^2 = (\underline{a} + \underline{b})^2 = \|\underline{a}\|^2 + \|\underline{b}\|^2 + 2(\underline{a} \cdot \underline{b}) \tag{D.5}$$

hence

$$\|\underline{a}\|^2 + \|\underline{b}\|^2 + 2(\underline{a} \cdot \underline{b}) \leq \|\underline{a}\|^2 + \|\underline{b}\|^2 + 2\|\underline{a}\|\|\underline{b}\|, \tag{D.6}$$

and therefore

$$(\underline{a} \cdot \underline{b}) \leq \|\underline{a}\|\|\underline{b}\|. \tag{D.7}$$

From this it also follows that

$$-(\underline{a} \cdot \underline{b}) = (\underline{a} \cdot (-\underline{b})) \leq \|\underline{a}\|\| - \underline{b}\| = \|\underline{a}\|\|\underline{b}\| \tag{D.8}$$

or

$$(\underline{a} \cdot \underline{b}) \geq -\|\underline{a}\|\|\underline{b}\|. \tag{D.9}$$

We therefore may conclude that $-\|\underline{a}\|\|\underline{b}\| \leq (\underline{a} \cdot \underline{b}) \leq \|\underline{a}\|\|\underline{b}\|$ or $(\underline{a} \cdot \underline{b})^2 \leq \|\underline{a}\|^2\|\underline{b}\|^2$ and this proves Schwarz inequality.

Equality in Schwarz inequality is achieved only when equality in the triangle inequality is obtained. This the case when (first part of proof) $\underline{b} = C\underline{a}$ or (second part) $-\underline{b} = (-\underline{b}) = C\underline{a}$ for some non-negative C. $\square$

Appendix E

An upper bound for the Q-function

Note that the Q-function is defined as

$$Q(x) \triangleq \int_x^\infty \frac{1}{\sqrt{2\pi}} \exp\left(-\frac{\alpha^2}{2}\right) d\alpha. \tag{E.1}$$

The lemma below gives a useful upper bound for $Q(x)$. In figure E.1 the Q-function and the derived upper bound are plotted.

LEMMA E.1 *For $x \geq 0$ the Q-function is bounded as*

$$Q(x) \leq \frac{1}{2} \exp\left(-\frac{x^2}{2}\right). \tag{E.2}$$

Proof: Note that for $\alpha \geq x$, and since $x \geq 0$,

$$\begin{aligned} \alpha^2 &= (\alpha - x)^2 + 2\alpha x - x^2 \\ &\geq (\alpha - x)^2 + 2x^2 - x^2 \\ &= (\alpha - x)^2 + x^2. \end{aligned} \tag{E.3}$$

Therefore

$$\begin{aligned} Q(x) &= \int_x^\infty \frac{1}{\sqrt{2\pi}} \exp\left(-\frac{\alpha^2}{2}\right) d\alpha \\ &\leq \int_x^\infty \frac{1}{\sqrt{2\pi}} \exp\left(-\frac{(\alpha - x)^2 + x^2}{2}\right) d\alpha \\ &= \exp\left(-\frac{x^2}{2}\right) \int_x^\infty \frac{1}{\sqrt{2\pi}} \exp\left(-\frac{(\alpha - x)^2}{2}\right) d\alpha \\ &= \frac{1}{2} \exp\left(-\frac{x^2}{2}\right). \end{aligned} \tag{E.4}$$

□

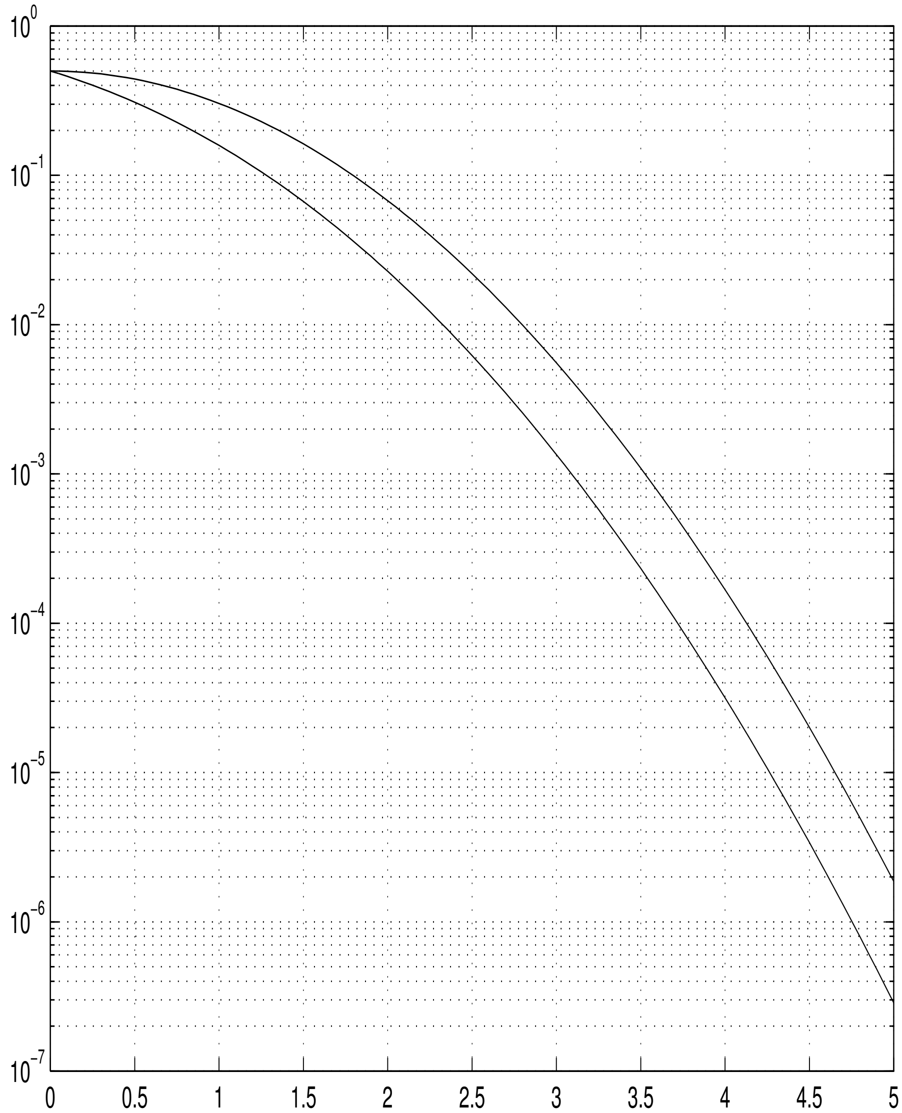

Figure E.1: The Q-function and the derived upper bound.

Appendix F

Bound error probability orthogonal signaling

Note that the correct probability satisfies

$$P_{\mathrm{c}} = \int_{-\infty}^{\infty} p(\mu - b)(1 - Q(\mu))^{|\mathcal{M}|-1} d\mu \tag{F.1}$$

where $b = \sqrt{2E_s/N_0}$, hence

$$P_{\mathrm{e}} = 1 - P_{\mathrm{c}} = \int_{-\infty}^{\infty} p(\mu - b)[1 - (1 - Q(\mu))^{|\mathcal{M}|-1}] d\mu. \tag{F.2}$$

The term in square brackets is the probability that at least one of $|\mathcal{M}| - 1$ noise components exceeds μ. By the union bound this probability is not larger than the sum of the probabilities that individual components exceed μ, thus

$$1 - (1 - Q(\mu))^{|\mathcal{M}|-1} \leq (|\mathcal{M}| - 1)Q(\mu) \leq |\mathcal{M}|Q(\mu). \tag{F.3}$$

Moreover, since this term is a probability we can also write

$$1 - (1 - Q(\mu))^{|\mathcal{M}|-1} \leq 1. \tag{F.4}$$

When μ is small $Q(\mu)$ is large and then the unity bound is tight. On the other hand for large μ the bound $|\mathcal{M}|Q(\mu)$ is tighter. Therefore we split the integration range into two parts, $(-\infty, a)$ and (a, ∞):

$$P_{\mathrm{e}} \leq \int_{-\infty}^{a} p(\mu - b) d\mu + |\mathcal{M}| \int_{a}^{\infty} p(\mu - b) Q(\mu) d\mu. \tag{F.5}$$

If we take $a \geq 0$ we can use the upper bound $Q(\mu) \leq \exp(-\mu^2/2)$, see the proof in appendix E, and we obtain

$$P_{\mathrm{e}} \leq \int_{-\infty}^{a} p(\mu - b) d\mu + |\mathcal{M}| \int_{a}^{\infty} p(\mu - b) \exp\left(-\frac{\mu^2}{2}\right) d\mu. \tag{F.6}$$

If we denote the first integral by P_1 and the second by P_2, we get

$$P_e \leq P_1 + |\mathcal{M}|P_2. \tag{F.7}$$

To minimize the bound we choose a such that the derivative of (F.6) with respect to a is equal to 0, i.e.,

$$\begin{aligned} 0 &= \frac{d}{da}[P_1 + |\mathcal{M}|P_2] \\ &= p(a-b) - |\mathcal{M}|p(a-b)\exp(-\frac{a^2}{2}). \end{aligned} \tag{F.8}$$

This results in

$$\exp\left(\frac{a^2}{2}\right) = M. \tag{F.9}$$

Therefore the value $a = \sqrt{2\ln|\mathcal{M}|}$ achieves a (at least a local) minimum in P_e. Note that $a \geq 0$ as was required. Now we can consider the separate terms. For the first term we can write

$$\begin{aligned} P_1 &= \int_{-\infty}^{a} \frac{1}{\sqrt{2\pi}} \exp\left(-\frac{(\mu-b)^2}{2}\right) d\mu \\ &= \int_{-\infty}^{a-b} \frac{1}{\sqrt{2\pi}} \exp\left(-\frac{\gamma^2}{2}\right) d\gamma \\ &= Q(b-a) \\ &\overset{(*)}{\leq} \exp\left(-\frac{(b-a)^2}{2}\right) \text{ if } 0 \leq a \leq b. \end{aligned} \tag{F.10}$$

Here the inequality $(*)$ follows from appendix E. For the second term we get

$$\begin{aligned} P_2 &= \int_{a}^{\infty} \frac{1}{\sqrt{2\pi}} \exp\left(-\frac{(\mu-b)^2}{2}\right) \exp\left(-\frac{\mu^2}{2}\right) d\mu \\ &\overset{(**)}{=} \exp\left(-\frac{b^2}{4}\right) \int_{a}^{\infty} \frac{1}{\sqrt{2\pi}} \exp\left(-(\mu-b/2)^2\right) d\mu \\ &= \exp\left(-\frac{b^2}{4}\right) \frac{1}{\sqrt{2}} \int_{a}^{\infty} \frac{1}{\sqrt{2\pi}} \exp\left(-\frac{\left(\mu\sqrt{2}-(b/2)\sqrt{2}\right)^2}{2}\right) d\mu\sqrt{2} \\ &= \exp\left(-\frac{b^2}{4}\right) \frac{1}{\sqrt{2}} \int_{a\sqrt{2}}^{\infty} \frac{1}{\sqrt{2\pi}} \exp\left(-\frac{\left(\gamma-(b/2)\sqrt{2}\right)^2}{2}\right) d\gamma \\ &= \exp\left(-\frac{b^2}{4}\right) \frac{1}{\sqrt{2}} Q(a\sqrt{2}-(b/2)\sqrt{2}). \end{aligned} \tag{F.11}$$

Here the equality $(**)$ follows from

$$\begin{aligned}\frac{1}{2}(\mu-b)^2+\frac{\mu^2}{2} &= \frac{\mu^2}{2}-\mu b+\frac{b^2}{2}+\frac{\mu^2}{2}\\ &= \mu^2-\mu b+\frac{b^2}{4}+\frac{b^2}{4}\\ &= (\mu-\frac{b}{2})^2+\frac{b^2}{4}.\end{aligned} \tag{F.12}$$

From (F.11) we get

$$P_2 \leq \begin{cases} \exp(-b^2/4) & 0 \leq a \leq b/2 \\ \exp(-b^2/4-(a-b/2)^2) & a \geq b/2. \end{cases} \tag{F.13}$$

If we now collect the bounds (F.10) and (F.13) and substitute the optimal value of a found in (F.9) we get

$$P_{\text{e}} \leq \begin{cases} \exp(-(b-a)^2/2)+\exp(a^2/2)\exp(-b^2/4) & 0 \leq a < b/2 \\ \exp(-(b-a)^2/2)+\exp(a^2/2)\exp(-b^2/4-(a-b/2)^2) & b/2 \leq a \leq b. \end{cases} \tag{F.14}$$

Now we note that

$$\frac{(a-b)^2}{2}-\left(\frac{b^2}{4}-\frac{a^2}{2}\right)=\left(a-\frac{b}{2}\right)^2 \geq 0. \tag{F.15}$$

Therefore for $0 \leq a < b/2$ the first term is not larger than the second one while for $b/2 \leq a \leq b$ both terms are equal. This leads to

$$P_{\text{e}} \leq \begin{cases} 2\exp(-b^2/4+a^2/2) & 0 \leq a < b/2 \\ 2\exp(-(b-a)^2/2) & b/2 \leq a \leq b. \end{cases} \tag{F.16}$$

Now we rewrite both a an b as

$$\begin{aligned} a &= \sqrt{2\ln|\mathcal{M}|}=\sqrt{2\ln 2}\cdot\sqrt{\log_2|\mathcal{M}|}\\ b &= \sqrt{2E_s/N_0}=\sqrt{2E_b/N_0}\cdot\sqrt{\log_2|\mathcal{M}|}, \end{aligned} \tag{F.17}$$

where we used the following definition for E_b i.e., the energy per transmitted bit of information

$$E_b \triangleq \frac{E_s}{\log_2|\mathcal{M}|}. \tag{F.18}$$

This finally leads to

$$P_{\text{e}} \leq \begin{cases} 2\exp(-\log_2|\mathcal{M}|[E_b/(2N_0)-\ln 2]) & E_b/N_0 \geq 4\ln 2 \\ 2\exp(-\log_2|\mathcal{M}|[\sqrt{E_b/N_0}-\sqrt{\ln 2}]^2) & \ln 2 \leq E_b/N_0 \leq 4\ln 2. \end{cases} \tag{F.19}$$

Bibliography

[1] G.A. Campbell, U.S. Patent 1,227,113, May 22, 1917, "Basic Types of Electric Wave Filters."

[2] J.R. Carson, "Notes on the Theory of Modulation," *Proc. IRE,* vol. 10, pp. 57-64, February 1922. Reprinted in *Proc. IEEE,* Vol. 51, pp. 893-896, June 1963.

[3] G.D. Forney, Jr., and G. Ungerboeck, "Modulation and Coding for Linear Gaussian Channels," *IEEE Trans. Inform. Theory,* vol. 44, pp. 2384-2415, October 1998.

[4] R.G. Gallager, *Principles of Digital Communication,* Cambridge, 2008.

[5] R.V.L. Hartley, "Transmission of Information," *Bell Syst. Tech. J.*, vol. 7, pp. 535-563, July 1928.

[6] V.A. Kotelnikov, *The Theory of Optimum Noise Immunity.* Dover Publications, 1960.

[7] S.P. Lloyd, "Least Squares Quantization in PCM," *IEEE Trans. Inform. Theory,* vol. IT-28, pp. 129-137, March 1982.

[8] D.O. North, Analysis of the Factors which determine Signal/Noise Discrimination in Radar. RCA Laboratories, Princeton, Technical Report, PTR-6C, June 1943. Reprinted in *Proc. IEEE,* vol. 51, July 1963.

[9] H. Nyquist, "Certain factors affecting telegraph speed," *Bell Syst. Tech. J.*, vol. 3, pp. 324-346, April 1924.

[10] B.M. Oliver, J.R. Pierce, and C.E. Shannon, "The Philosophy of PCM," Proc. IRE, vol. 36, pp. 1324-1331, Nov. 1948.

[11] J.G. Proakis and M. Salehi, *Communication Systems Engineering.* Prentice Hall, 1994.

[12] C.E. Shannon, "A Mathematical Theory of Communication," *Bell Syst. Tech. J.,* vol. 27, pp. 379-423 and 623 - 656, July and October 1948. Reprinted in the Key Papers on Information Theory.

[13] C.E. Shannon, "Communication in the Presence of Noise," *Proc. IRE,* vol. 37, pp. 10-21, January 1949. Reprinted in the Key Papers on Information Theory.

[14] J.H. Van Vleck and D. Middleton, "A Theoretical Comparison of Visual, Aural, and Meter Reception of Pulsed Signals in the Presence of Noise," *Journal of Applied Physics,* vol. 17, pp. 940-971, November 1946.

[15] J.M. Wozencraft and I.M. Jacobs, *Principles of Communication Engineering*, Wiley, New York, 1965.

[16] S.T.M. Ackermans and J.H. van Lint, *Algebra en Analyse,* Academic Service, Den Haag, 1976.

Index